FOLLOW-UP PHOTOMETRY OF A NEW ECLIPSING BINARY FROM THE SLOAN DIGITAL SKY SURVEY: SDSS J214140.43 +050730.0

Kittipong   Wangnok

A Thesis Submitted in Partial Fullfillment of the Requirements for the

Degree of Master in Physics

Suranaree University of Technology

Academic Year 2016

การติดตามผลโฟโตเมทรีของดาวคู่อุปราคาระบบใหม่จาก THE SLOAN DIGITAL SKY SURVEY: SDSS J214140.43 +050730.0
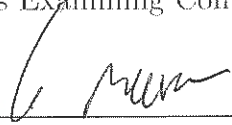
นายกิตติพงษ์ หวังนอก

วิทยานิพนธ์นี้เป็นส่วนหนึ่งของการศึกษาตามหลักสูตรปริญญาวิทยาศาสตรมหาบัณฑิต
สาขาวิชาฟิสิกส์
มหาวิทยาลัยเทคโนโลยีสุรนารี
ปีการศึกษา 2559

FOLLOW-UP PHOTOMETRY OF A NEW ECLIPSING BINARY FROM THE SLOAN DIGITAL SKY SURVEY: SDSS J214140.43 +050730.0

Suranaree University of Technology has approved this thesis submitted in partial fulfillment of the requirements for a Master's Degree.

Thesis Examining Committee

_____

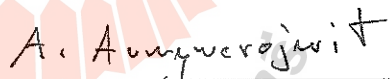(Asst. Prof. Dr. Worawat Meevasana)

Chairperson

_____

(Dr. Nuanwan Sanguansak)

Member (Thesis Advisor)

_____

(Dr. Puji Irawati)

Member

_____

(Asst. Prof. Dr. Amornrat Aungwerojwit)

Member

_____   _____

(Prof. Dr. Sukit Limpijumnong)   (Prof. Dr. Santi Maensiri)

Vice Rector for Academic Affairs   Dean of Institute of Science

and Innovation

กิตติพงษ์ หวังนอก : การติดตามผลโฟโตเมทรีของดาวคู่อุปราคาระบบใหม่จาก THE SLOAN DIGITAL SKY SURVEY: SDSS J214140.43 +050730.0 (FOLLOW-UP PHOTOMETRY OF A NEW ECLIPSING BINARY FROM THE SLOAN DIGITAL SKY SURVEY: SDSS J214140.43 +050730.0) อาจารย์ที่ปรึกษา : อาจารย์ ดร.นวลวรรณ สงวนศักดิ์, 105 หน้า .

ระบบดาวคู่อุปราคา SDSS J2141 +0507 ถูกรายงานครั้งแรกว่าเป็นดาวคู่อุปราคาแบบเปลี่ยนแปลงที่รุนแรง (Cataclysmic Variable; CV) ระบบใหม่จาก the Sloan Digital Sky Survey Data Release 10 โดย Szkody et al. (2014) ในงานวิจัยนี้ เราได้ทำการสังเกตการณ์ และเก็บข้อมูลผ่านกล้องโทรทรรศน์แบบสะท้อนแสง (Reflecting Telescope) ขนาดเส้นผ่านศูนย์กลาง 2.4 เมตร ณ หอดูดาวเฉลิมพระเกียรติ 7 รอบพระชนมพรรษา อุทยานแห่งชาติดอยอินทนนท์ จ.เชียงใหม่ ร่วมกับอุปกรณ์ ULTRASPEC โดยใช้ฟิลเตอร์ SDSS g' KG5 r' และ i' ตามลำดับ และใช้โปรแกรม Binary Maker 3.0 และ JKTEBOP code ในการสร้างแบบจำลองและคำนวณหาค่าพารามิเตอร์ของระบบดาวคู่อุปราคานี้ ซึ่งจากการวิเคราะห์พบว่าอัตราส่วนระหว่างมวล (M2/M1) เท่ากับ 0.058 อุณหภูมิยังผลของดาวแคระขาว และดาวในแถบลำดับหลักเท่ากับ 31200 ± 300 K และ 3540 ± 40 K ตามลำดับ ความเอียงของระนาบการโคจรนี้คือ (86 ± 1)° และรัศมีของดาวแคระขาว และดาวในแถบลำดับหลัก เท่ากับ (0.030 ± 0.003)$R_\odot$ และ (0.20 ± 0.01)$R_\odot$ ตามลำดับ ค่า The mid-eclipse timing (ในหน่วย HJD) และค่าคาบการโคจรของระบบมีค่าเท่ากับ 2456215.45338 ± 0.00005 และ 0.05469 ± 0.00004 วัน เราสามารถเขียนสมการ Linear ephemeris ใหม่ คือ T_0 (HJD) = 2456215.45338 + 0.05469 × E

สาขาวิชาฟิสิกส์   ลายมือชื่อนักศึกษา_____
ปีการศึกษา 2559   ลายมือชื่ออาจารย์ที่ปรึกษา_____
                               ลายมือชื่ออาจารย์ที่ปรึกษาร่วม_____

KITTIPONG WANGNOK : FOLLOW-UP PHOTOMETRY OF A NEW ECLIPSING BINARY FROM THE SLOAN DIGITAL SKY SURVEY: SDSS J214140.43 +050730.0. THESIS ADVISOR : NAUNWAN SANGUANSAK, Ph.D. 105 P.

PHOTOMETRY/ECLIPSING BINARY/CV/ULTRASPEC

SDSS J2141 +0507 was first identified as a new eclipsing cataclysmic variable (CV) from the Sloan Digital Sky Survey Data Release 10 by Szkody et al. (2014). In this research, the observational data was obtained by using the 2.4m Thai National Telescope (TNT) at Thai National Observatory (TNO), Doi Inthanon National park, Chiang Mai, Thailand with ULTRASPEC instrument using filter SDSS g', KG5, r' and i'. The Binary Maker 3.0 and JKTEBOP code softwares were used for obtaining the stellar and binary parameters of this system. The estimated mass ratio (M2/M1) is 0.058 with white dwarf and main sequence stars effective temperatures of 31200 ± 300 K and 3540 ± 40 K. The orbital inclination of this system is $(86 \pm 1)°$ and the radius of the white dwarf and the main sequence stars are $(0.030 \pm 0.003)R_\odot$ and $(0.20 \pm 0.01)R_\odot$, respectively. The mid eclipse timing (in HJD) and an orbital period are $2456215.45338 \pm 0.00005$ and 0.05469 ± 0.00004 days, respectively. The new ephemeris for SDSS J2141 +0507 can be written as T_0 (HJD) $= 2456215.45338 + 0.05469 \times E$.

School of Physics

Academic Year 2016

Student's Signature _Kittipong Wangnok_

Advisor's Signature _N. Sanguansak_

Co-advisor's Signature _____

ACKNOWLEDGEMENTS

<div align="right">Kittipong Wangnok</div>

CONTENTS

CONTENTS (Continued)

CONTENTS (Continued)

CONTENTS (Continued)

LIST OF TABLES

LIST OF TABLES (Continued)

LIST OF FIGURES

LIST OF FIGURES (Continued)

LIST OF FIGURES (Continued)

LIST OF FIGURES (Continued)

LIST OF FIGURES (Continued)

LIST OF FIGURES (Continued)

LIST OF ABBREVIATIONS

AURA	Association of Universities for Research in Astronomy
BM	Binary Maker
CCD	Charge-Coupled Device
CE	Common Envelope
CV	Cataclysmic Variable
EMCCD	Electron-Multiplying Charge-Coupled Device
FWHM	Full-Width at Half Maximum
GMT	Greenwich Mean Time
HJD	Heliocentric Julian Date
IRAF	Image Reduction and Analysis Facility
ISYA	International School for Young Astronomers
JD	Julian Date
MJD	Modified Julian Date
MS	Main Sequence
NOAO	National Optical Astronomy Observatories
PCEB	Post Common Envelope Binary
ROC	Radius of Curvature
SDSS	Sloan Digital Sky survey
TFP	Telescope Focal Plane
TNO	Thai National Observatory
TNT	Thai National Telescope
WD	White Dwarf

CHAPTER I

INTRODUCTION

1.1 Introduction

A binary star is a system consisting of two stars that are orbiting around
their common center of mass. The first binary system was discovered by Sir
William Herschel in 1802 (Herschel, 1802). We can classify binary systems into
four types, according to the method of detection. These four types are visual
binaries, spectroscopic binaries, astrometric binaries and eclipsing binaries.

1.1.1 Visual Binary

A visual binary consists of two stars with different brightness. The brighter
star and the fainter one are called the primary and the companion, respectively. If
the primary is too bright relative to the companion, this can cause a glare making
it difficult to resolve the two components through a telescope.

1.1.2 Spectroscopic Binary

The spectroscopic binary consists of a pair of stars with distinct spectral
lines emitted from each star. This system is detected by Doppler shift in their
spectrum line. The shift towards the blue is called blue shift and the one towards
the red is called red shift.

1.1.3 Astrometric Binary

Astrometric binary is relatively nearby stars which can be observed due to the oscillation of the star in space. We cannot distinguish the two stars visually because the companion is so much fainter than the other one. If only one component is visible and the other one is too faint or is too close to its brighter companion, we cannot observe both components of the double system with telescope.

1.1.4 Eclipsing Binary

An eclipsing binary is a binary star in which the orbital planes oriented along the line of sight of the observer. When the smaller star passes in front of the brighter star, there will be dropped in the light curve which called primary eclipse. Also, when the smaller star passes behind the bright star, giving a more-shallow drop in the light curve which called secondary eclipse.

1.2 Motivation

Szkody et al. (2014) reported that SDSS J2141 +0507 is a new cataclysmic variable (CV) from the Sloan Digital Sky survey (SDSS) data release 10 which need to be confirmed. The system was reported to have an orbital period of 76 ± 2 minutes, based on their photometric data which was obtained during two nights of observation. However, the eclipse was not well-resolved due to the long exposure time (194 seconds) as seen in Figure 1.1. From the spectrum of SDSS J2141 +0507, they can confirm that the system is a CV from the deep absorption in the Balmers lines. Also, the emission line is indicated that SDSS J2141 +0507 have the high inclination with the low mass transfer rate (Szkody et al., 2014).

In this work, we perform follow up photometry of SDSS J2141 +0507 in
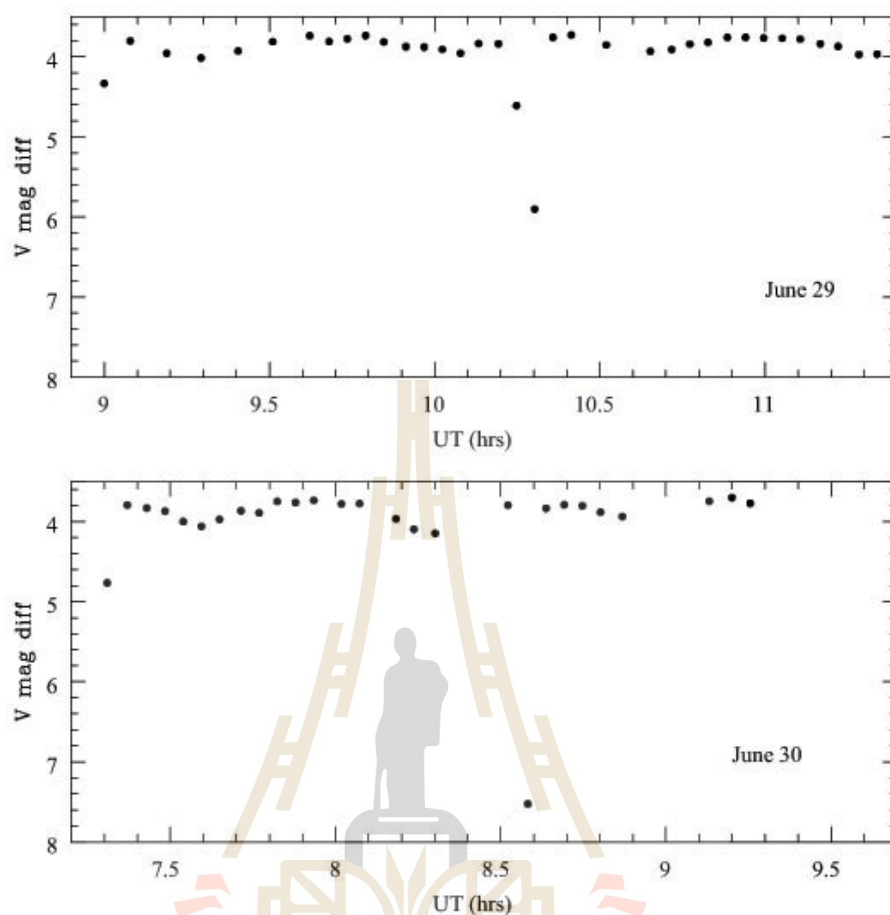
Figure 1.1 The light curves of J2141 +0507 by Szkody et al. (2014), revealing a possible orbital period of 76 minutes (Szkody et al., 2014).

which the orbital and stellar parameters are not known giving a perfect opportunity for us to study this binary and to confirm whether this system is a cataclysmic variable. Figure 1.2 shows the spectrum of SDSS J2141 +0507 which consists of the deep absorption and the double peak of emission lines. This phenomena is indicated that the absorption line occurred from the White Dwarf star (WD) when the hot gas on WD emits the light through atmosphere then the light of hot gas on WD will be absorbed. The emission line was produced by hot gas surrounding the WD star which in this case is accretion disc of system.
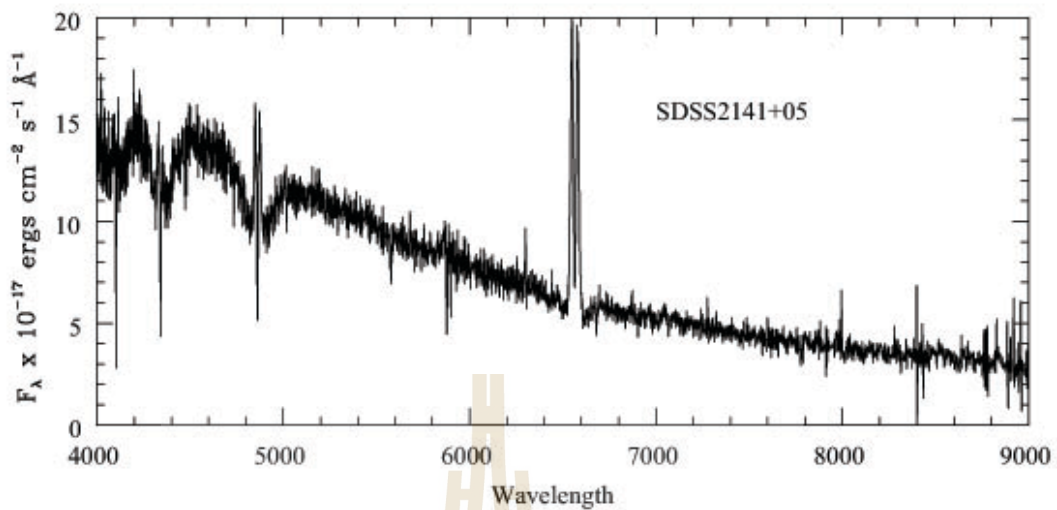
Figure 1.2 The spectrum of SDSS J2141 +0507 (Szkody et al., 2014).

We obtained the light curve of SDSS J2141 +0507 by using ULTRASPEC and IRAF. Then, the mid-eclipse timing (T_0) was estimated in order to have more accurate orbital period. After that, the 3D model of this system was constructed using Binary Maker 3.0 and JKTEBOP code which was used for getting the precise stellar and orbital parameters.

1.3 Research Objectives

1.3.1 To study a new eclipsing binary system and to perform light curve analysis to estimate the mid-eclipse timing (T_0) and the accurate orbital period of SDSS J2141 +0507.

1.3.2 To obtain the precise stellar and orbital parameters (e.g. masses, temperature, radii of WD and MS stars) of the eclipsing binary system using JKTEBOP code and to analyze the light curve outside the eclipse to study and to confirm the type of this new eclipsing binary. Furthermore, the 3D model of the system will be made using Binary Maker 3.0.

1.4   Scope and Limitation of the Study

In this work, we focus on studying the newly discovered binary system SDSS J2141 +0507, using the 2.4m Thai National Telescope (TNT) with the ULTRASPEC instrument (in SDSS g', KG5, r' and i' filters) at the Thai National Observatory (TNO), Doi Inthanon, Chiang Mai, Thailand. Then, the 3D model will be constructed using Binary Maker 3.0 and the parameters of the system will be obtained using JKTEBOP code.

CHAPTER II

THEORY

2.1 Eclipsing Binary

An eclipsing binary system is a binary star in which the orbital planes oriented along the line of sight of the observer. When the fainter star passes in front of the brighter star, the light from the system will be decreased which called primary eclipse. Also, when the fainter star passes behind the bright star, giving a more- shallow drop in the light curve which called secondary eclipse. The observational data can provide the information about the relative effective temperatures, the radii of each star based on the depths of the light curve and lengths of the eclipses.
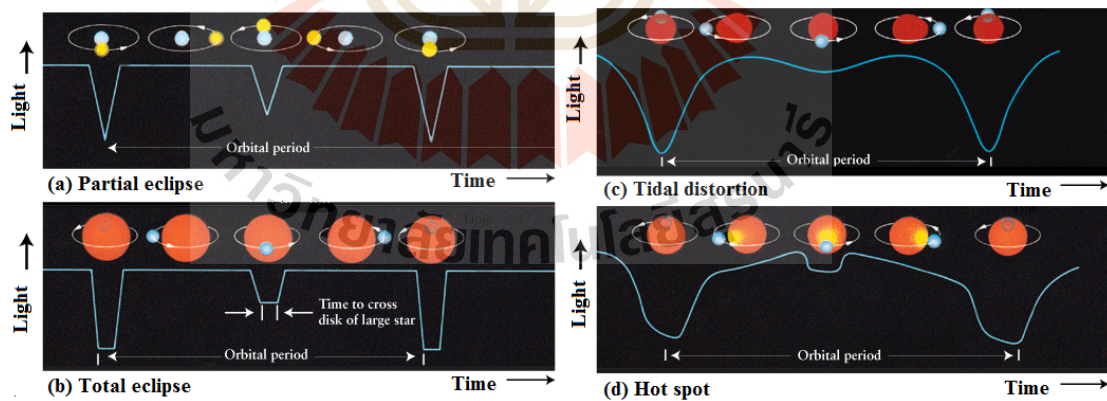
Figure 2.1 Examples light curves of eclipsing binaries (Bogan, 1997).

The orbital component and the physical properties of the eclipsing binaries can be analyzed from their light curves. The ratio of the radii can be estimated from the duration of the eclipse. Figure 2.2 shows an eclipsing binaries system

with the inclination (i) from the line of sight of the observer is close to 90°. When
the smaller and hotter stars is not completely eclipse by companion star then
eclipse shape will differ from the first case as shown in Figure 2.3. In this case,
the inclination angle will be less than 90°.
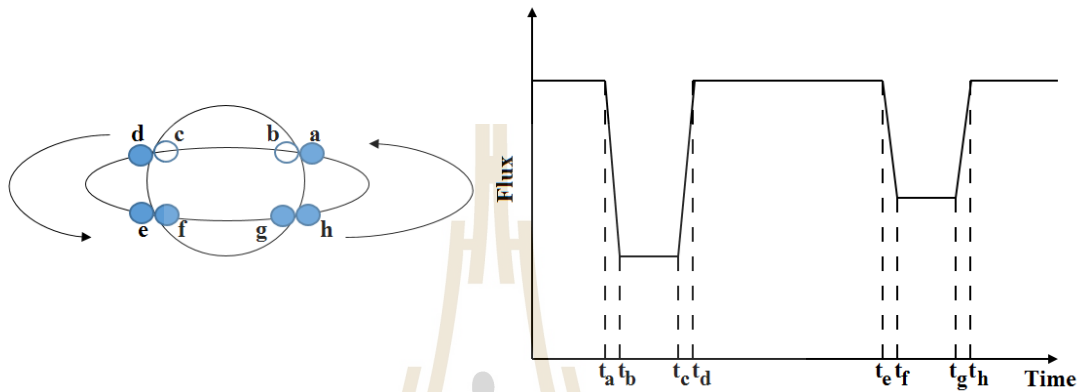
Figure 2.2 Light curve of an eclipsing binary for where i = 90°. The primary
component is the one with smaller radius (Carroll and Ostlie, 2007).
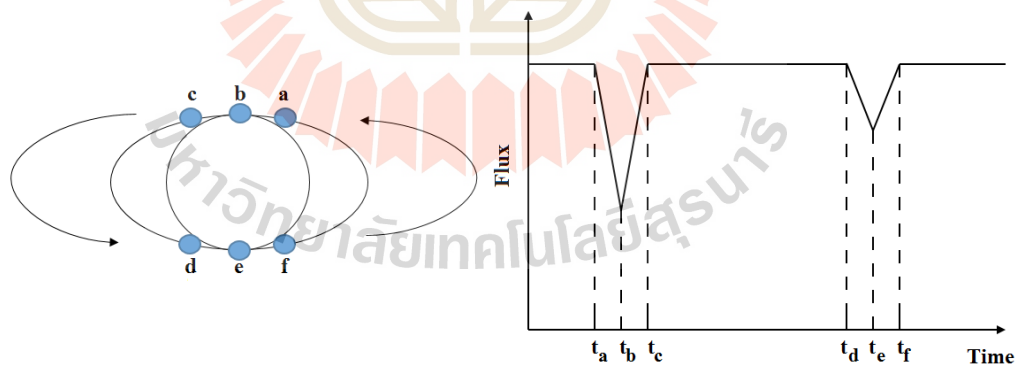
Figure 2.3 The light curve of a partial eclipsing binary. Same as before, we
assume that the smaller star is hotter (Carroll and Ostlie, 2007).

2.2 Roche Geometry

In binary star, it is useful to describe the system in a coordinate system which is rotating along with the objects. We called the region where the gravitational force and the centrifugal force are equals as the equipotential surface. The position where the gravitational force is equal to the centrifugal force or, where the potential is equal to zero is called Lagrangian point. The Lagrangian point consists of L_1, L_2, L_3, L_4 and L_5 where L_1 is called the inner Lagrangian or the gravitational equilibrium point. The critical equipotential intersects itself at the Lagrangian point L_1, forming a two lobed figure of eight between both of the primary and companion star from the center of each lobe. L_2 and L_3 are the gravitational perturbation equilibrium points while L_4 and L_5 are the maximum potential points in the system. Figure 2.4 shows the representation of a three dimensional of Roche potential in binary star system.
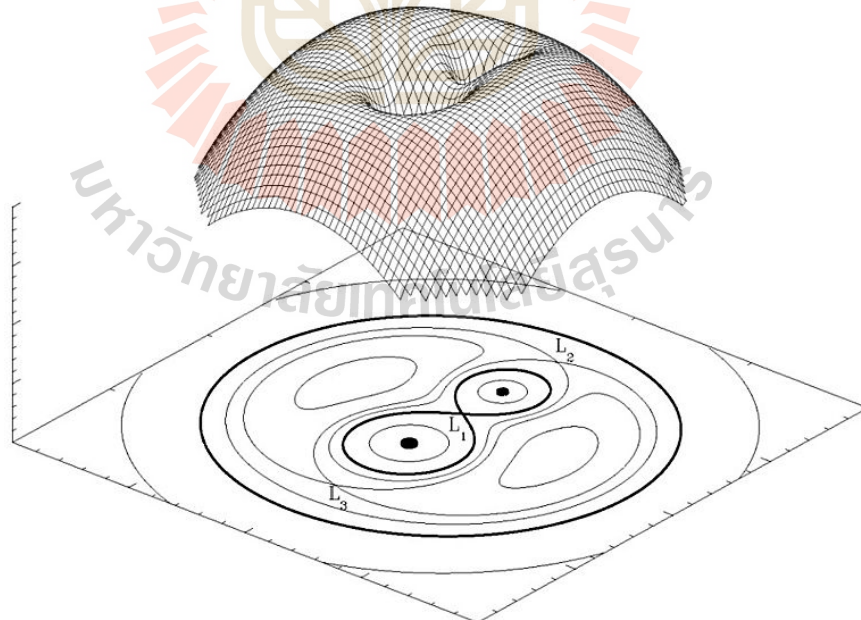
Figure 2.4 The representation of a three dimensional of Roche potential in binary star system with mass ratio (q) of 2 in the co-rotating frame (Van der Sluys, 2006).

The eclipsing binary star system are classified into three types, according to their Roche models in Figure 2.5:

2.2.1 Detached Binary

There is no physical contact between both stars. They are both spherical in shape because they do not fill in the Roche lobe.

2.2.2 Semi-detached Binary

One of the stars fills its Roche lobe and forms a shape which resembles an egg due to the gravitational distortion. The gas from the secondary star often has a too high angular momentum while moving towards the compact object that the gas slowly forms an accretion disc.

2.2.3 Contact Binary

Both of stars have filled their Roche lobes, and may have egg shaped.

2.3 Evolution of Binary Star System

2.3.1 Common Envelope

A common envelope (CE) is formed in a binary system when the orbital separation decreased rapidly or where one of the star expands rapidly. The mass transfer from the donor star occurs when it overfill its Roche lobe as the consequence the orbit will shrink further causing it to overflow the Roche lobe even more, which accelerates the mass transfer, causing the orbit to shrink even faster and the donor to expand more. This process is leading to dynamically unstable
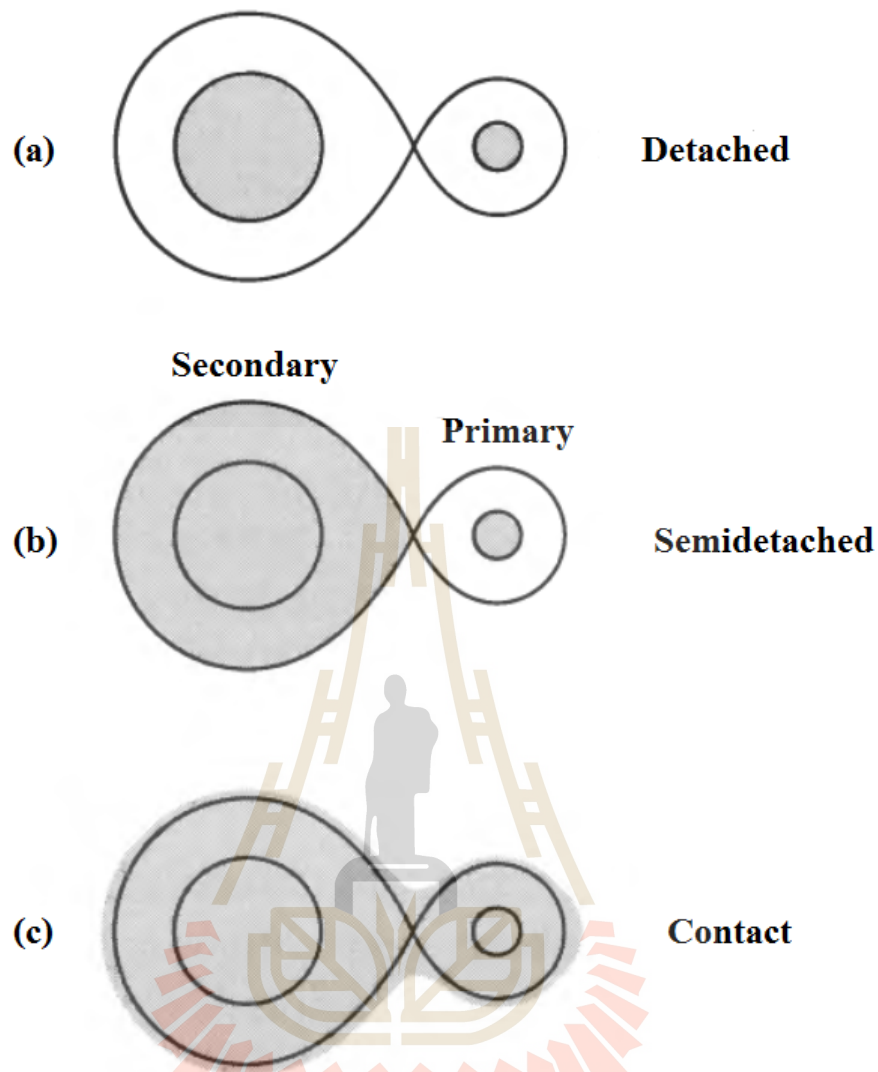
Figure 2.5 The schematic of Binary Star Evolution (Carroll and Ostlie, 2007).

mass transfer and in some cases the receiving star is unable to accept all material, which indicated the formation of a common envelope where the primary is engulfing the companion star. The common-envelope evolution was proposed by Paczynski (1976) to explain the formation of PCEBs, cataclysmic variables, and similar systems. In this evolutionary scenario, the secondary will fall into the envelope of the primaries and slowly expelling the primary's envelope as it moves inside (Paczynski, 1976).

During a CE phase, the embedded binary system is subject to drag forces

from the envelope which cause the separation of the two stars to decrease. The phase ends either when the envelope is ejected to leave the binary system with much smaller orbital separation, or when the two stars become sufficiently close to merge and form a single star. A CE phase is short-lived.

Figure 2.6 shows the life of a binary star before mass transfer and during its CE evolution. The binary has a mass ratio M1/M2=3 and the black line is the Roche equipotential surface. The CoM is the center of mass of the binary system (Izzard et al., 2012). Figure 2.6(a) shows the two stars with the relatively unevolved primary star on the left (M1) and the secondary star on the right (M2). Figure 2.6(b) shows that the primary star evolves it grows in size. Figure 2.6(c) shows the primary star fills its Roche lobe. Figure 2.6(d) shows the primary star transfer mass to the secondary star. Figure 2.6(e) shows the secondary star cannot accept the mass from the primary star which called the unstable mass transfer. Therefore, the material cannot be accreted onto the secondary so it swells to fill the both Roche lobes then the CE forms around both stars.

2.3.2 Post Common Envelope Binaries

This process occurred after the CE evolution, Angular Momentum Loss (AML) will be loss because the magnetic braking or gravitational radiation. The binary separation is decreased enough to bring the secondary star into contact with its Roche lobe (Aungwerojwit, 2007; Rebassa-Mansergas, 2008). The end outcome of the CE evolution is a naked core of the primaries accompanied by a low mass M dwarf star. One of the most common products of the CE phase is the detached white dwarf plus main-sequence close binaries, known as PCEBs (Kepler et al., 2007; Rebassa-Mansergas et al., 2009; Parsons et al., 2013). Typically, PCEBs have short orbital period of a few hours, although some systems were found to be
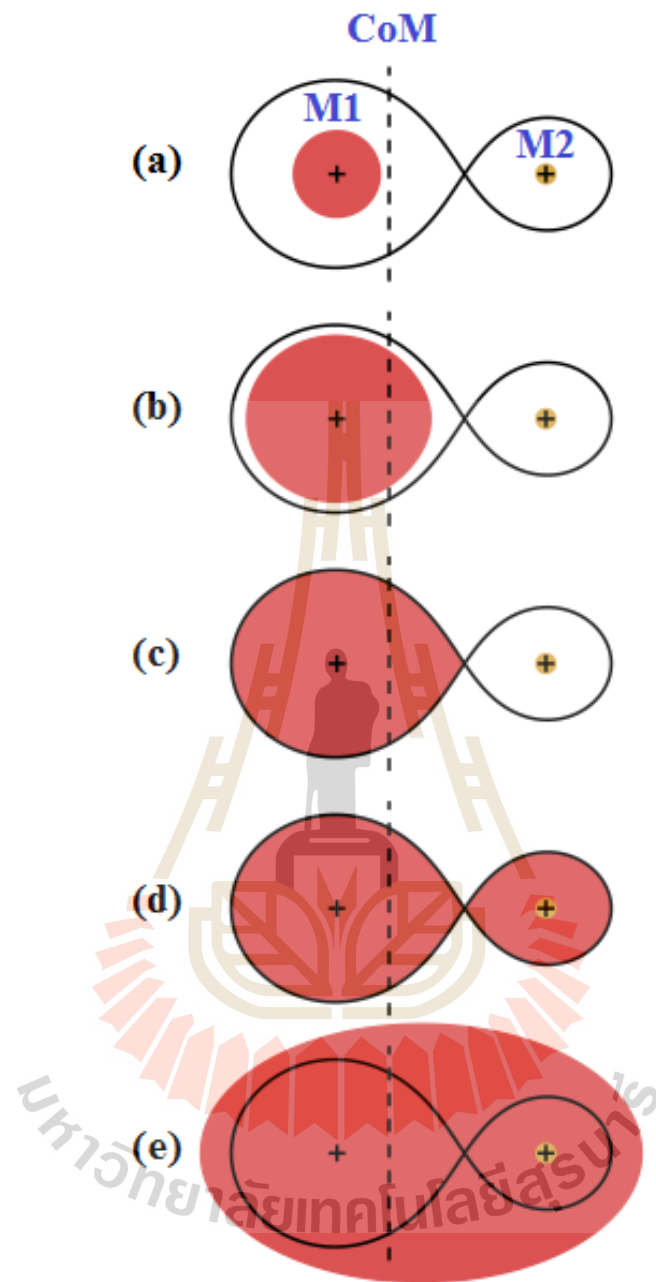
Figure 2.6 The schematic of the life of a binary star before mass transfer and during its CE evolution (Izzard et al., 2012).

in a longer (>1 day) period.
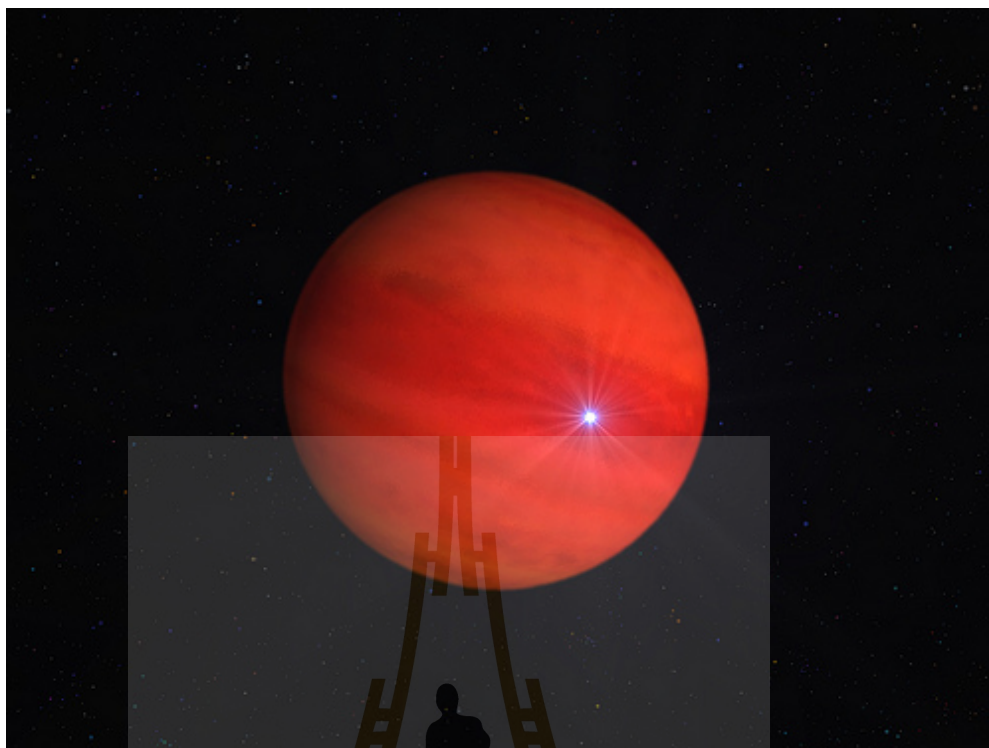
Figure 2.7 Example of PCEB WD 0137-349 (Digital-Drew-Space-Art's-Photostream, 2013).

2.3.3 Cataclysmic Variables

Cataclysmic Variables (CVs) are short period semi-detached binaries consisting of an accreting white dwarf primary star and (typically) a low-mass Main Sequence star. The orbital period of CVs typically range from approximately 65 minutes to 1 days. CVs are the connected from the Post Common Envelope Binaries (PCEBs). These systems were occurred from the lost angular momentum through a CE phase. The binary separation will be decreased because the angular momentum loss by the magnetic braking and/or gravitational radiation then the systems will be evolved into CV. The CV configuration time to evolve is 2 Gyr (Aungwerojwit, 2007).

The white dwarfs and its magnetic fields have important role in the mass accretion process in CVs. The amount of the accreted mass in the disk will depend
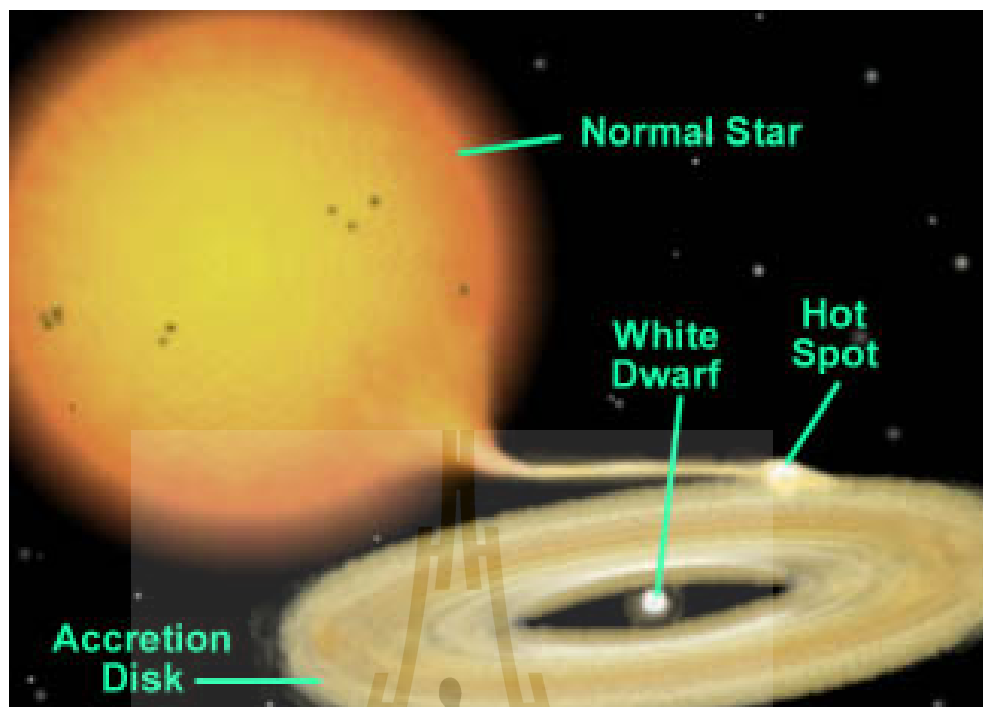
Figure 2.8 The Schematic of CV (Smale, 2004).

on the WD's magnetic strength, but the accretion are often found within the range of $10^{-11} - 10^{-8} \mathrm{M}_\odot \mathrm{yr}^{-1}$. Figure 2.9 shows the stars is rotating around the center of mass of the system G. In the weak/non-magnetic system, there is an accretion disc which the gas stream hits at the bright spot. In the strong magnetic system, the gas stream is channeled along field lines onto the white dwarf.

The accretion disc configurations are shown in the two drawings in Figure 2.9, where the WD has low or weak magnetic field allowing the system to develop a disc (Figure 2.9(a)) and where there is no disc (Figure 2.9(b)) due to the magnetic field of the WD. In this case, the accreted mass will follow the magnetic field lines and will fall on the poles region of the WD (Aungwerojwit, 2007).
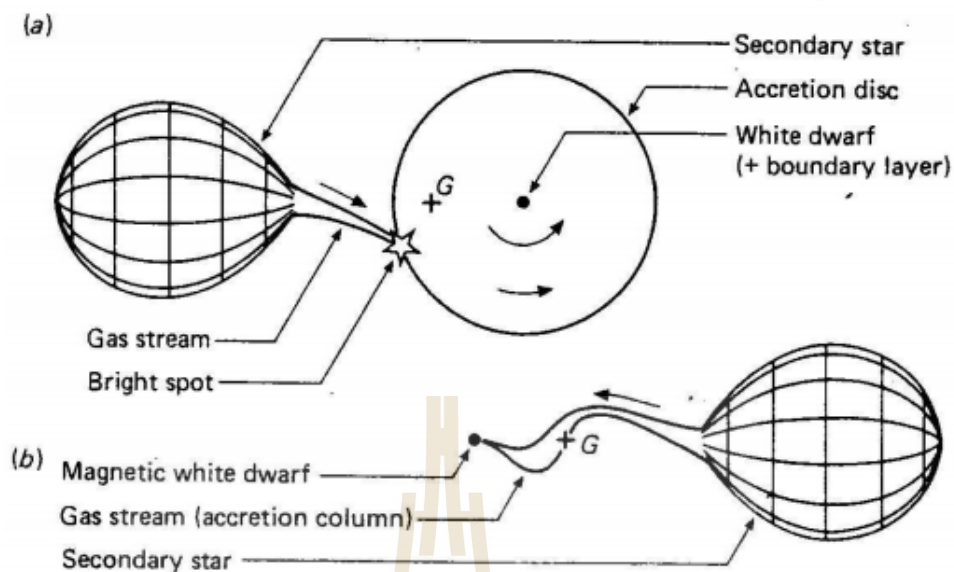
Figure 2.9 The Schematic of the components (a) a weak or non-magnetic CV and (b) a strong magnetic CV (Pringle and Wade, 1985).

2.4 Julian Date, Modified Julian Date and Heliocentric Julian Date

The Julian Date (JD) is the integer number which assigned to a whole solar day. The Julian Day can be counted which starting from noon Greenwich Mean Time (GMT). The number of Julian Day is zero which assigned to the day starting at noon on 1st January 4713 B.C.

The Modified Julian Date (MJD) is the modification of the original Julian Date which have been used for astronomer, geophysicists and others who have to use the accurate of dating system which based on the continued of day counting (Ray, 2000). In 1973, the International Astronomical Union (IAU) recommended that a Modified Julian Date be adopted which neglected the first two digits that were rarely of interest (McCarthy, 1998). The MJD has been started point of midnight on 17th November 1858 which can be computed as

$$MJD = JD - 2400000.5 \tag{2.1}$$

In 1958, the Smithsonian Astrophysics Observatory used the Modified Julian Date to record the orbit of Sputnik. If we assumed that we are observing the star from the center of the Sun which called the Heliocentric Julian Date (HJD) because we need to correct for the differences in the Earth's position with respect to the sun. The HJD can be calculated as

$$HJD = JD - \frac{r}{c}[\sin(\delta)\sin(\delta_\odot) + \cos(\delta)\cos(\delta_\odot)cos(\alpha - \alpha_\odot)] \tag{2.2}$$

Where JD is Julian Date, r is the distance between Sun and observer, c is the speed of light, α, δ are Right Ascention and Declination of our target and $\alpha_\odot$, $\delta_\odot$ are Right Ascention and Declination of our target of the Sun. Figure 2.10 shows the light time effect occurs because the Earth's orbiting around the Sun. The distance between the Sun to the Earth is 1 AU or 149,597,871 km which means that the Sun's light is travelling to the Earth is 8.3 minutes. Therefore, to correct the differences between the coordinate of the Earth to the Sun, we will assume that we observed the star from the Sun which called Heliocentric Julian Date (HJD).
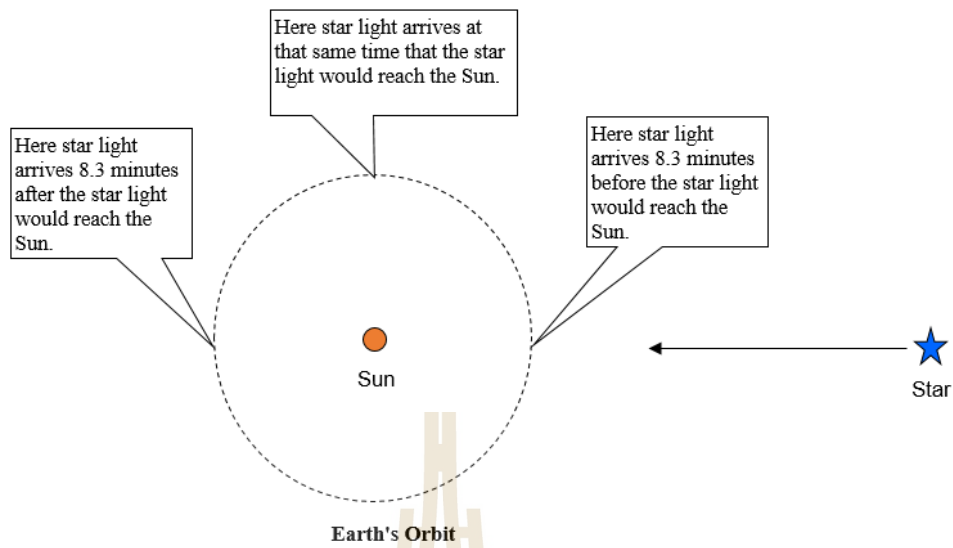
Figure 2.10 The light time effect occurs when the Earth's orbiting around the Sun (Bradstreet, 2011).

2.5 Kepler's law

In astronomy, Kepler's law of motion are describing the motion of the planets around the sun.

The 1ˢᵗ Kepler's Law: Law of Ellipses

The orbit of a planet is an ellipse where one focus of the ellipse is the Sun.
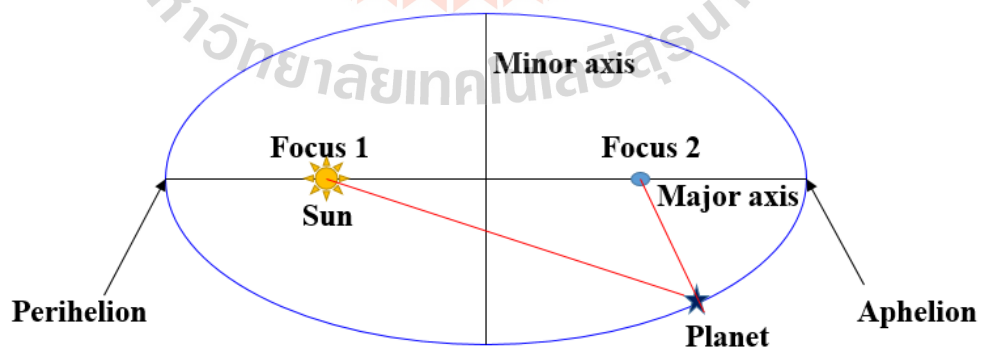
Figure 2.11 Illustration of the Kepler's 1ˢᵗ law, the orbit of planet is an ellipse with the Sun at one of two foci.

The 2ⁿᵈ Kepler's Law: Law of Equal Areas

A line segment from the planet to the Sun sweeps out equal area during intervals of time.
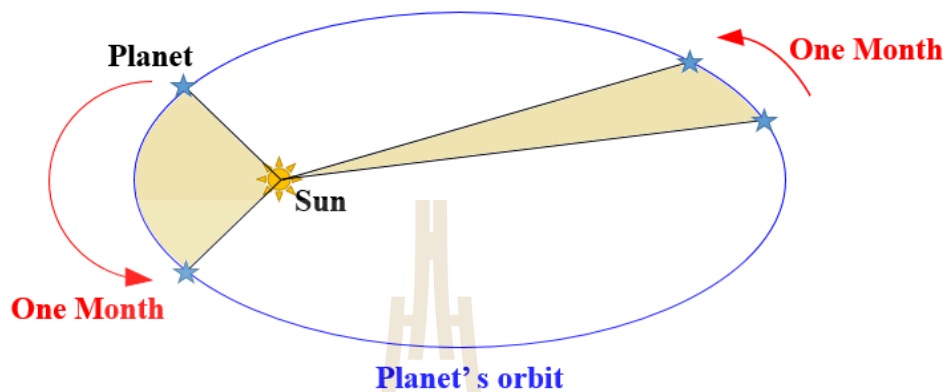
Figure 2.12 Illustration of the Kepler's 2ⁿᵈ law, a line from the planet to the sun sweeps out equal areas in equal amounts of time.

The 3ʳᵈ Kepler's Law: Law of Period

The square of orbital period of a planet is proportional to the cube of the semi-major axis of the orbit, then the Kepler's 3ʳᵈ law can be written:

$$P^2 = a^3 \tag{2.3}$$

Where P is period which was measured in years and a is the semi-major axis which was given in astronomical units (the distance between the Earth and the Sun is 1 AU).

If we consider a planet with mass (M_p) to orbit in nearly circular motion around the Sun with the mass $(M_\odot)$ with the distance a. The centripetal force acting upon this orbiting planet is given by

$$F_\text{cent} = M_\text{p} \frac{v^2}{a} \tag{2.4}$$

The centripetal force is the result of the gravitational force that attracts the planet towards the Sun, and can be represented as

$$F_{\text{grav}} = \frac{GM_{\text{p}}M_{\odot}}{a^2} \tag{2.5}$$

Since $F_{\text{cent}} = F_{\text{grav}}$, the above expressions for centripetal force and gravitational are equal, thus

$$v^2 = \frac{GM_{\odot}}{a} \tag{2.6}$$

We know that, the velocity of an object in nearly circular motion can be approximated as

$$v = \frac{2\pi a}{P} \tag{2.7}$$

Substitute equation (2.7) in equation (2.6), then

$$P^2 = \frac{4\pi^2}{GM_{\odot}}a^3 \tag{2.8}$$

Equation (2.8) is called the Kepler's 3$^{\text{rd}}$ law in term of an approximation that serves well for the orbits of the planets because the Sun's mass is so dominant. But more precisely the law should be written

$$P^2 = \frac{4\pi^2}{G(M_1 + M_2)}a^3 \tag{2.9}$$

Where P is an orbital period (years), G is the universal gravitational constant is $6.67 \times 10^{-11} \text{m}^3\text{kg}^{-1}\text{s}^{-2}$, both of M_1 and M_2 are the mass of primary and companion stars, respectively and a is the separation distance between the star (AU).

CHAPTER III

OBSERVATION, DATA REDUCTION AND

DATA ANALYSIS

To observe the observational data, we used the 2.4m Thai National Telescope (TNT) with ULTRASPEC instrument in several filters (SDSS g', KG, r', and i' filters) at Thai National Observatory (TNO), Doi Inthanon National Park, Chiang Mai, Thailand. The data reduction and data analysis have been done using the ULTRASPEC pipeline and IRAF to obtain light curve for SDSS J2141 +0507. Binary Maker 3.0 (BM3) and JKTEBOP code were used to obtain the stellar and binary parameters of this system which we will discuss in the next section.

3.1　Photometric Observations

The data were collected at the Thai National Observatory (TNO) using the 2.4 m Thai National Telescope(TNT) with the ULTRASPEC instrument on 9th Dec, 22nd Dec, 24th Dec, 25th Dec 2014, 20th Oct 2015, 4th Nov and 2nd Dec 2016 using SDSS g', KG5, r' and i' filters, respectively. The details of the log of the observation were shown in Table 3.1.

Table 3.1 Observation log.

Date of observation	Filter SDSS	Exposure time	Phase of observation (UT)	Phase coverage	Observer(s)	Observing condition (seeing)
9th Dec 2014	g'	7.0 s	13:03:58 – 14:48:17	0.0 to 1.2	Zhang Haojing,	1.8-3.0
					Han Zhongtao,	
					Shruthi S Bhat,	
					Dr. Puji Irawati	
22nd Dec 2014	KG5	7.0 s	11:45:04 – 14:12:35	1.0 to 1.5	Dr.Nuanwan Sanguansak,	2.0-6.0
					Dr. Puji Irawati,	
					Niwat Hemha,	
					Kittipong Wangnok,	
					Khunagorn Chanthorn	
24th Dec 2014	r'	7.0 s	11:56:33 – 13:01:24	0.3 to 1.2	Dr. David Mkrtichian	2.0-5.0
25th Dec 2014	i'	7.0 s	11:55:59 – 13:19:03	0.6 to 1.7	Dr. David Mkrtichian	1.4-6.0

Continued on next page

Table 3.1 Observation log. (Continued).

Date of observation	Filter SDSS	Exposure time	Phase of observation (UT)	Phase coverage	Observer(s)	Observing condition (seeing)
20$^{\text{th}}$ Oct 2015	g'	0.7 ms	13:23:09 – 14:35:56	0.9 to 1.75	Dr. Puji Irawati	1.4-2.8
4$^{\text{th}}$ Nov 2016	g'	7.0 s	12:57:12 – 16:42:54	0.8 to 3.3	Kittipong Wangnok,	2.0-2.8
					Khunagorn Chanthorn,	
					Dr. Puji Irawati	
2$^{\text{nd}}$ Dec 2016	r'	7.0 s	11:25:45 – 13:56:48	0.6 to 2.4	Kittipong Wangnok,	1.0-2.0
					Khunagorn Chanthorn,	
					Dr. Puji Irawati	

An example of the visibility chart from the night of 20th Oct 2015 shows in Figure 3.1. The Figure 3.2 shows the finding chart of target and the comparison stars.
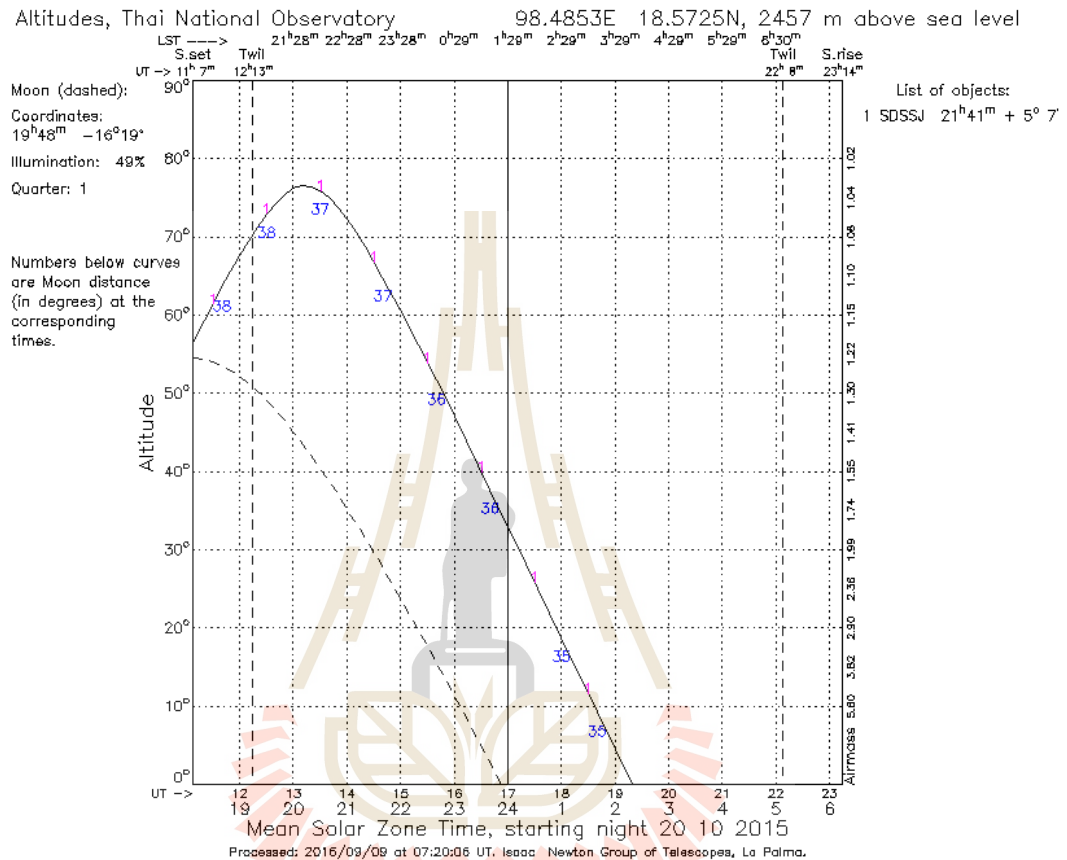
Figure 3.1 The target visibility of SDSS J2141 +0507 was obtained on 20th Oct 2015.

The vertical dash lines on the left and the right hand side of Figure 3.1 are the time of evening and morning twilights. The solid line represents the altitude of SDSS J2141 +0507, showing that our target has been observed during 13:00 UT – 17:00 UT before it becomes too low to be observed from TNO (less than 25 degree at 17:30 UT). We know that the predicted orbital period of SDSS J2141 +0507 is $\approx$ 76 minutes then, we are quite confident that we will be able to get at least 3 eclipse, if we can observe 4 hours observing window. The dash line on the

Figure 3.1 means the position of the Moon and the numbers of 36-38 on the solid line are the distance between the target and the Moon.
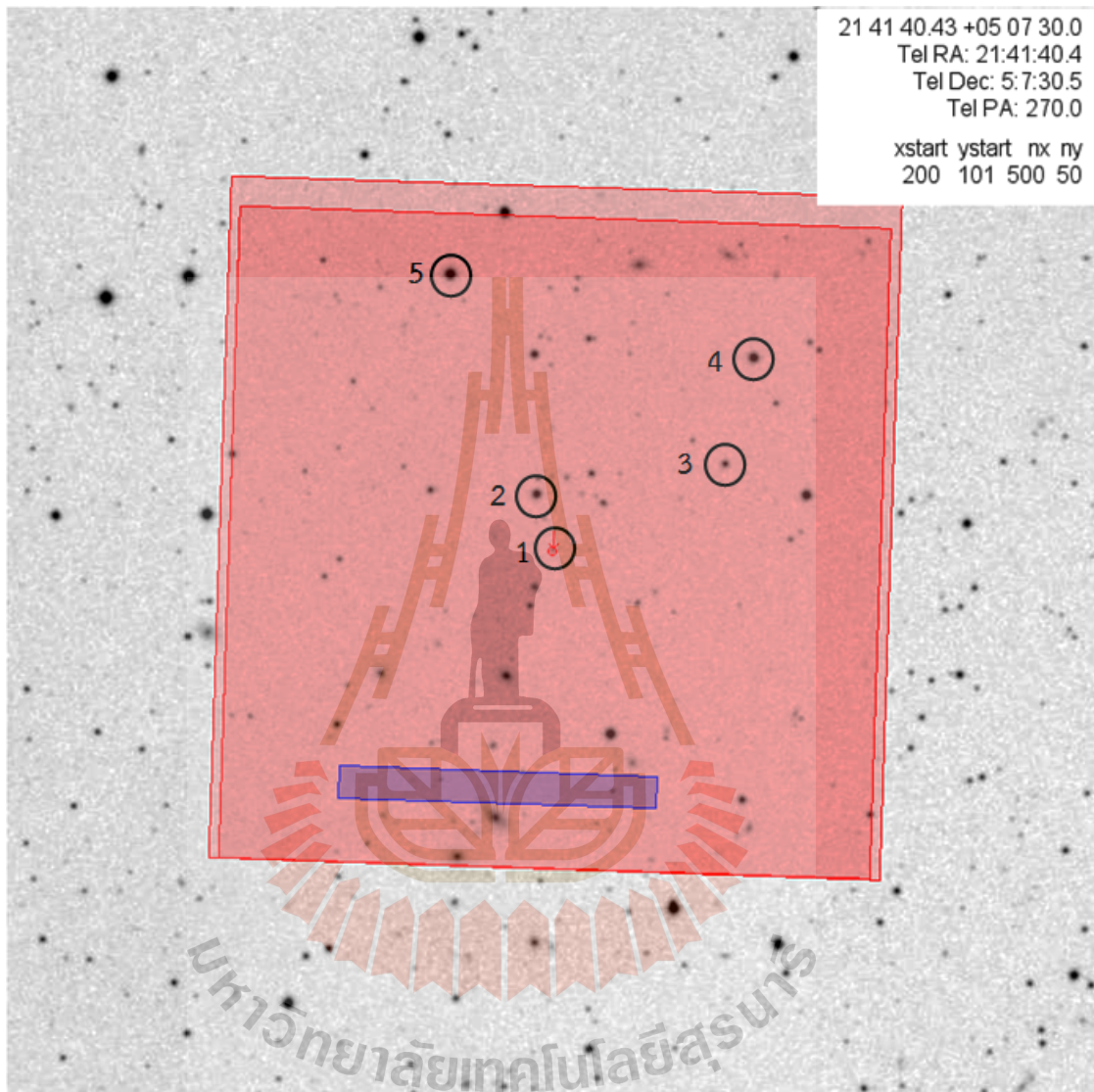
Figure 3.2 The finding chart of SDSS J2141 +0507.

In Figure 3.2, we marked the position of our target and several comparison stars which we are going to use for photometric analysis. Star 1 and 2 are our target star and reference stars, respectively. Star 3-5 are the check stars which are known to be non-variable star. Figure 3.3 shows the light curve of target, reference, and check stars which are not variable star.
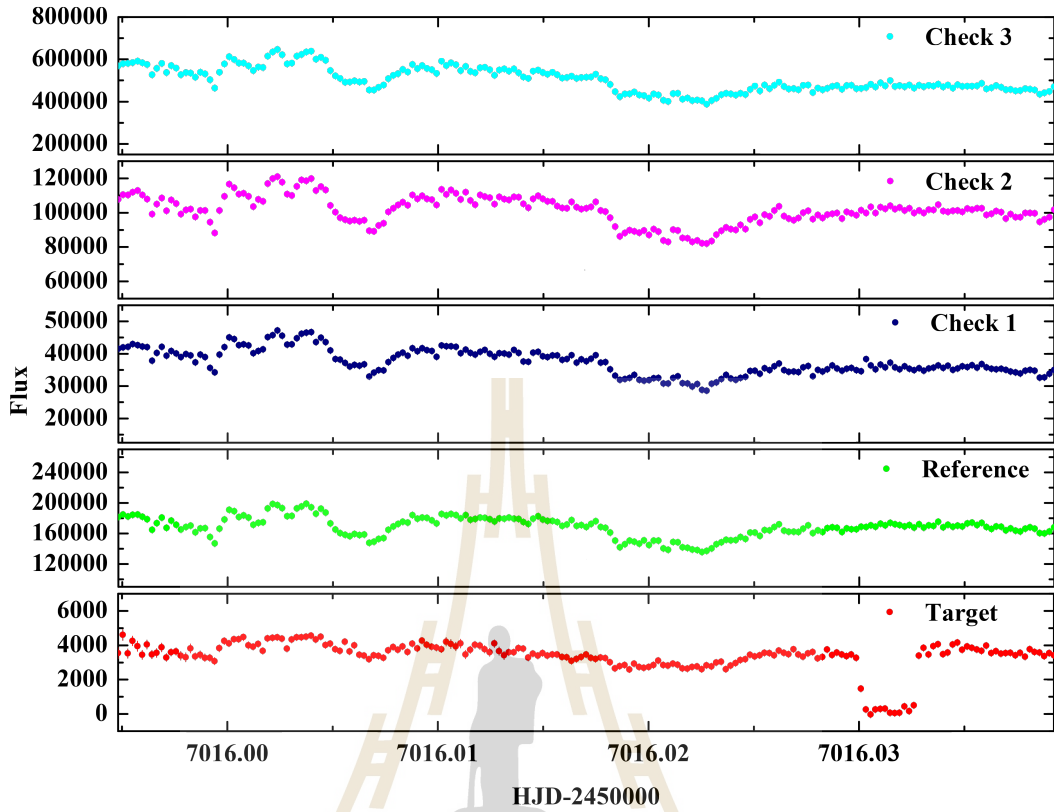
Figure 3.3 The light curve of target, reference and check stars which using UL-
TRASPEC pipeline.

3.2   Data Reduction

3.2.1   Photometric Data Reduction with the ULTRASPEC pipeline

SDSS J2141 +0507 was observed on 7 nights of observation with the high-
speed photometric camera ULTRASPEC in SDSS g', KG5, r', and i' filters. To
obtain the light curve using ULTRASPEC pipeline, we will follow the step to
obtain the light curve:

The first step in reducing raw data is subtract the bias frame. Bias frame are
used to remove the readout signal from camera sensor. This background level can

be easily accounted by taking some zero-second exposures, and subtracting a mean bias frame from the science data. Flat fielding frames are used for solving problem in the optical path which included dust, dirt, vignette and internal reflection. The flat-field frame are uniform, blank images and can be taken either of twilight sky or the lamp-illuminated inside of telescope dome. Generally, one aims for a large number of photon counts, while ensuring that the signal stays well within the linear range of CCD, because the CCD is illuminated uniformly, the number of counts in the pixel of flat-field frame accurately represent the sensitivity of the pixels. Note that a corresponding bias should first be subtracted from the flat-field frames, before creating the final master flat-field. The science data can then be divided by the flat-field to normalize the response of the pixels (Dhillon et al., 2014). Before we do the follow up photometric observations, we marked the position of target, reference and check stars which was shown in Figure 3.2. After we selected the star then we can obtain the light curves of the star using ULTRASPEC. ULTRASPEC will give a display of the flux of target which is divided reference/comparison stars, the position of reference star (in X and Y), the percentage of transmission, and the Full Width at Half Maximum (FWHM) which was shown in Figure 3.4.

3.2.2 Photometric Data Reduction with IRAF

IRAF is the Image Reduction and analysis facility which is used for reduction and analysis of astronomical data. IRAF is written and supported by the National Optical Astronomy Observatories (NOAO) in Tucson, Arisona. NOAO is operated by the Association of Universities for research in Astronomy (AURA), Inc. under cooperative agreement with the National Science Foundation (NOAO, 2015).The process of IRAF for doing the data reduction and data analysis is similar to ULTRASPEC pipeline. We need to do data reduction then we will get
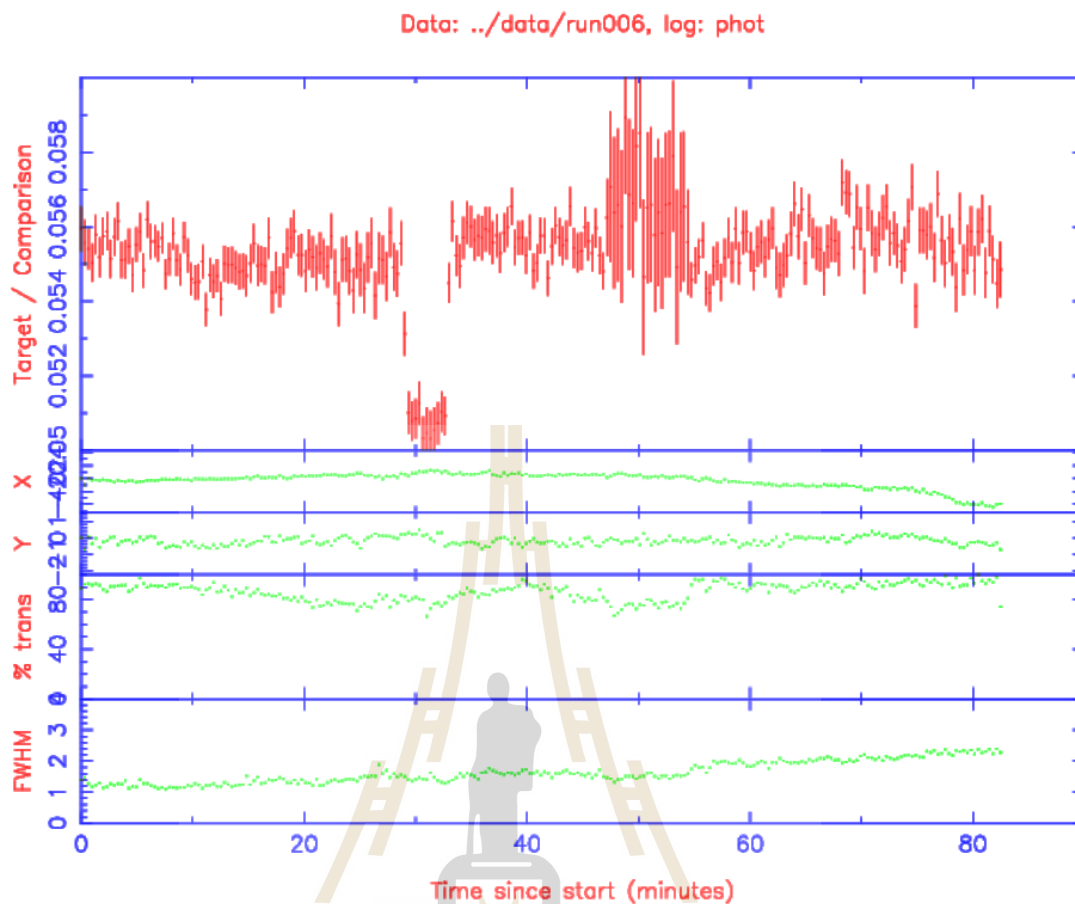
Figure 3.4 The real time light curve of SDSS J2141 +0507 from ULTRASPEC which was taken on 25th Dec 2014 in SDSS i' filter (the observational data taken by Mkrtichian D.).

the reduced image in order to do data analysis. There are two ways to do the extraction of the fluxes from the CCD images. In this work, the photometric data are reduced using relative aperture photometry, in which the target's flux is divided by the flux of a comparison star in order to remove flux variations caused by variable atmospheric conditions. The schematic of IRAF process and the frames of image are shown in Figure 3.5 and Figure 3.6, respectively. The data reduction and data analysis have been done using ULTRASPEC pipeline and IRAF.

This observational data was observed on 24th Dec 2014 in SDSS r' filter. Due to the ULTRAPEC pipeline used automatically alignment to measure the
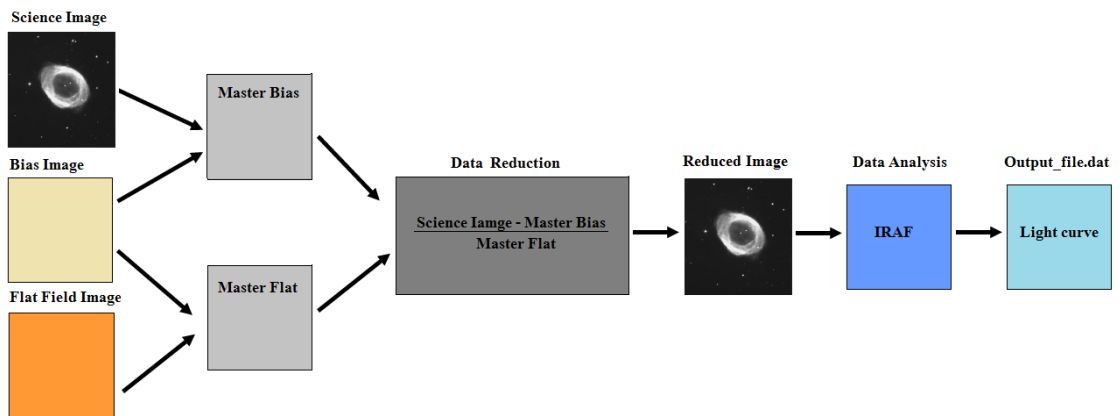
Figure 3.5 Example of the schematic of IRAF Processing. We start with data reduction and then data analysis in order to obtain light curve.
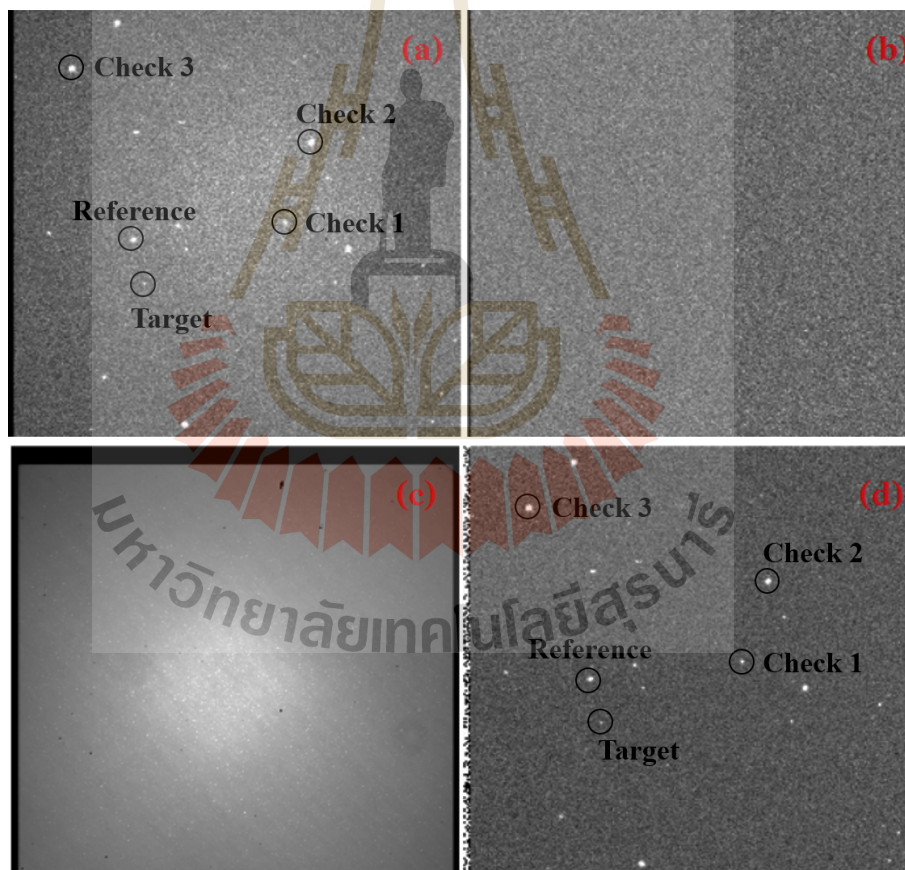
Figure 3.6 The frame of (a) Science Image, (b) Master Bias, (c) Master Flat and (d) Reduced Image.
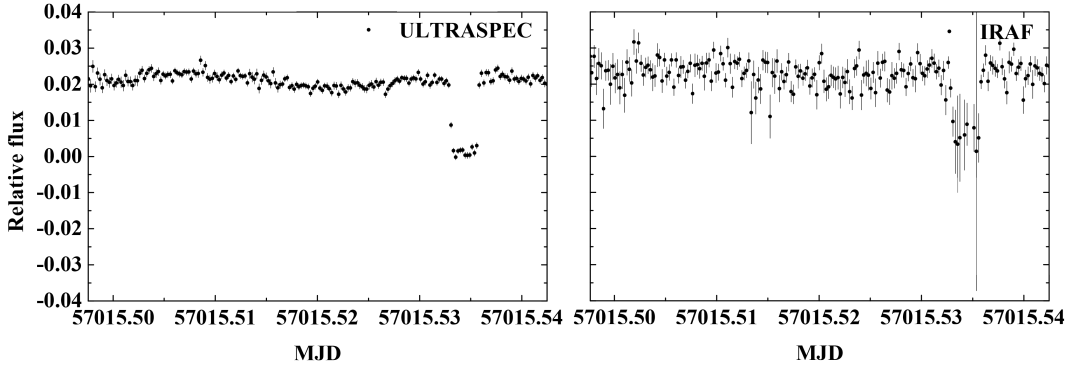
Figure 3.7 The light curves of SDSS J2141 +0507 were obtained on 24$^{\text{th}}$ Dec 2014 using (a) ULTRASPEC pipeline and (b) IRAF.

flux of the star while IRAF software used manually alignment to measure the flux of the star therefore the scattering of the data was using ULTRASPEC is very small compared with IRAF. Therefore, ULTRASPEC pipeline will give the result of light curve better than the result from IRAF. We used the light curve using ULTRASPEC pipeline to model and obtain the stellar and binary parameters. The example of light curves were obtained using ULTRASPEC pipeline and IRAF are shown in Figure 3.7.

3.3 Light Curve Analysis

To perform the light curve for each observational data, the light curve have been plotted between the normalized flux versus orbital phase. First step, we have to calculate HJD from MJD and MJD using equation (2.1) and (2.2) and we can calculate normalized flux using the normalization condition which can be writing as

$$\text{Normalized} \quad \text{flux} = \frac{flux - flux_{\min}}{flux_{\max} - flux_{\min}} \tag{3.1}$$

Where is the $flux$ of star from observation. $flux_{\max}$ is the average maximum

of flux between phase 0.95 to 0.97 and $flux_{\min}$ is the average minimum of flux between phase 0.98 to 1.00.

The observational data was observed on 9th Dec, 22nd Dec, 24th Dec, 25th Dec 2014, 20th Oct 2015, 4th Nov and 2nd Dec 2016 in SDSS g', KG5, r', and i' filters, respectively which the light curves shown in Figure 3.8. To obtain a plot between the normalized flux versus orbital phase, we used the ephemeris of T_0 (HJD) and the orbital period as 2457001.04619 and 0.05467 days (ISYA school 2014, private communication). The light curves were shown in Figure 3.9 and 3.10 where the mid-eclipse is only located at orbital phase 1.0 on the data from 9th Dec 2014 and the primary eclipse was shift to the right toward that means the ephemeris is still incorrect.

In Figure 3.11 and 3.12, we show the light curve with the orbital phase calculated using the ephemeris of T_0(HJD) and an orbital period are 2456215.45334 and 0.05469 days, respectively which calculated by Bours (2015). Both of T_0(HJD) and an orbital period are more precise than the previous one.

Although Bours got the ephemeris of T_0 (HJD) and an orbital period which made the position of an eclipse closed to 1.0 but the result is still incorrect. The primary eclipse are slightly shifted to the left. Therefore, in this work we will determine the ephemeris of the system and after that, we will model the binary system using Binary Maker 3 (BM3) and JKTEBOP code to obtain the stellar and binary parameters.
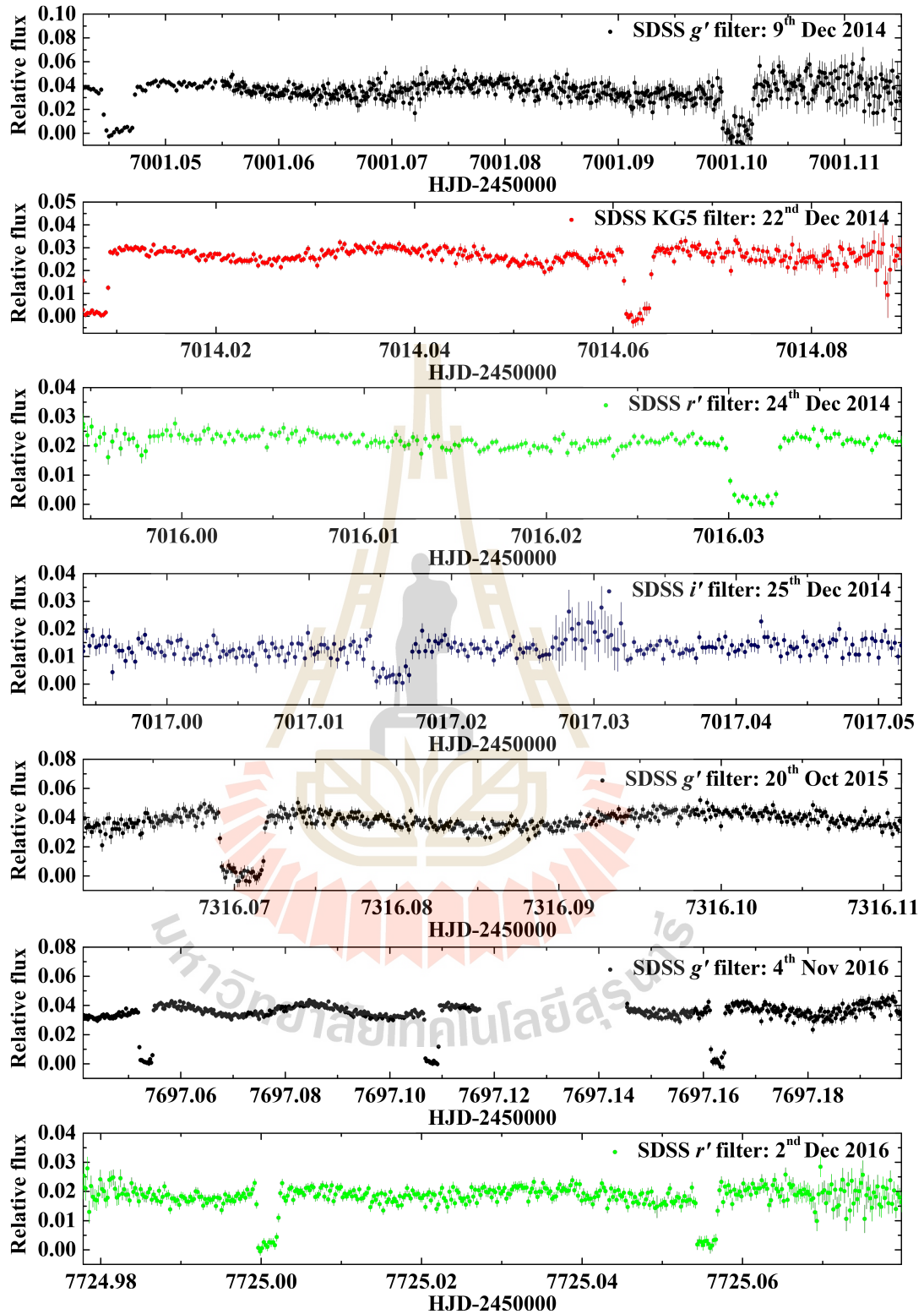
Figure 3.8 From top to bottom: The light curve of SDSS J2141 +0507 in SDSS g', KG5, r', and i' filters which was observed on 9th Dec, 22nd Dec, 24th Dec, 25th Dec 2014, 20th Oct 2015, 4th Nov and 2nd Dec 2016, respectively.
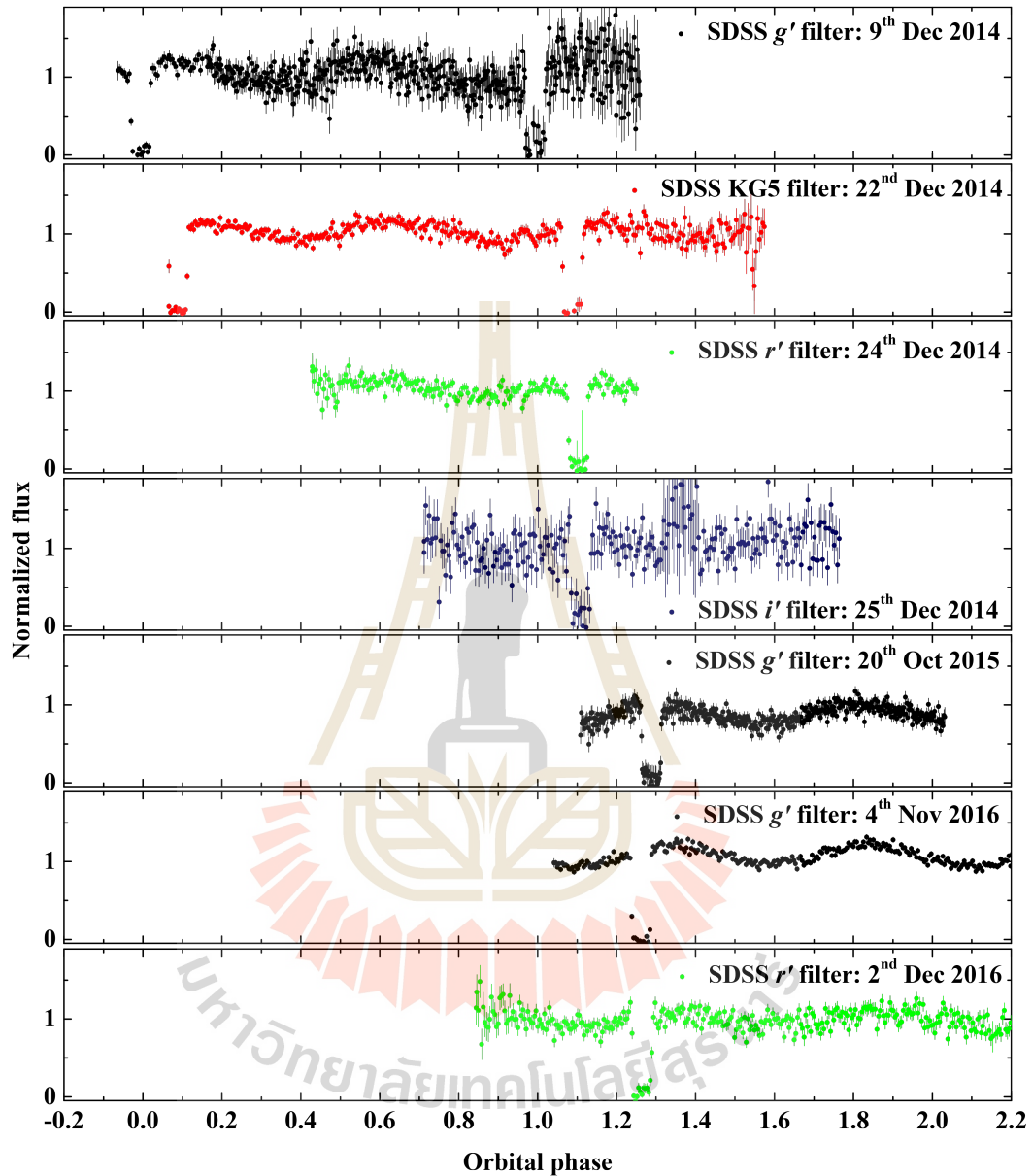
Figure 3.9 From top to bottom: Light curve of SDSS J2141 +0507 in SDSS g', KG5, r', and i' filters which was observed on 9$^{\text{th}}$ Dec, 22$^{\text{nd}}$ Dec, 24$^{\text{th}}$ Dec, 25$^{\text{th}}$ Dec 2014, 20$^{\text{th}}$ Oct 2015, 4$^{\text{th}}$ Nov and 2$^{\text{nd}}$ Dec 2016 using the ephemeris of T_0 (HJD) and the orbital period are 2457001.04619 and 0.05467 days (ISYA school 2014, private communication).
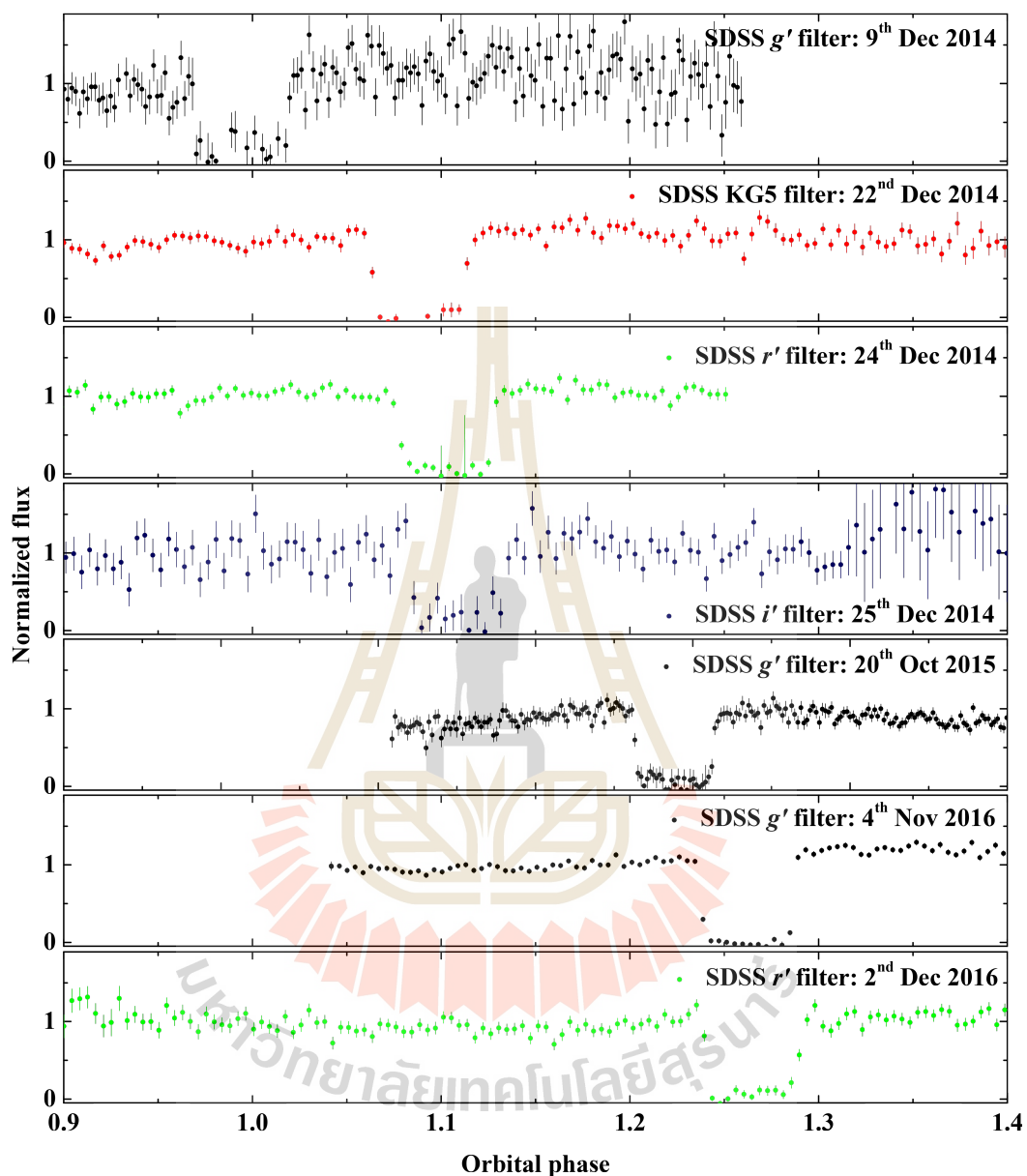
Figure 3.10 Zooming in the range of eclipse. From top to bottom: Light curve of SDSS J2141 +0507 in SDSS g', KG5, r', and i' filters which was observed on 9th Dec, 22nd Dec, 24th Dec, 25th Dec 2014, 20th Oct 2015, 4th Nov and 2nd Dec 2016 using the ephemeris of T_0 (HJD) and the orbital period are 2457001.04619 and 0.05467 days (ISYA school 2014, private communication).
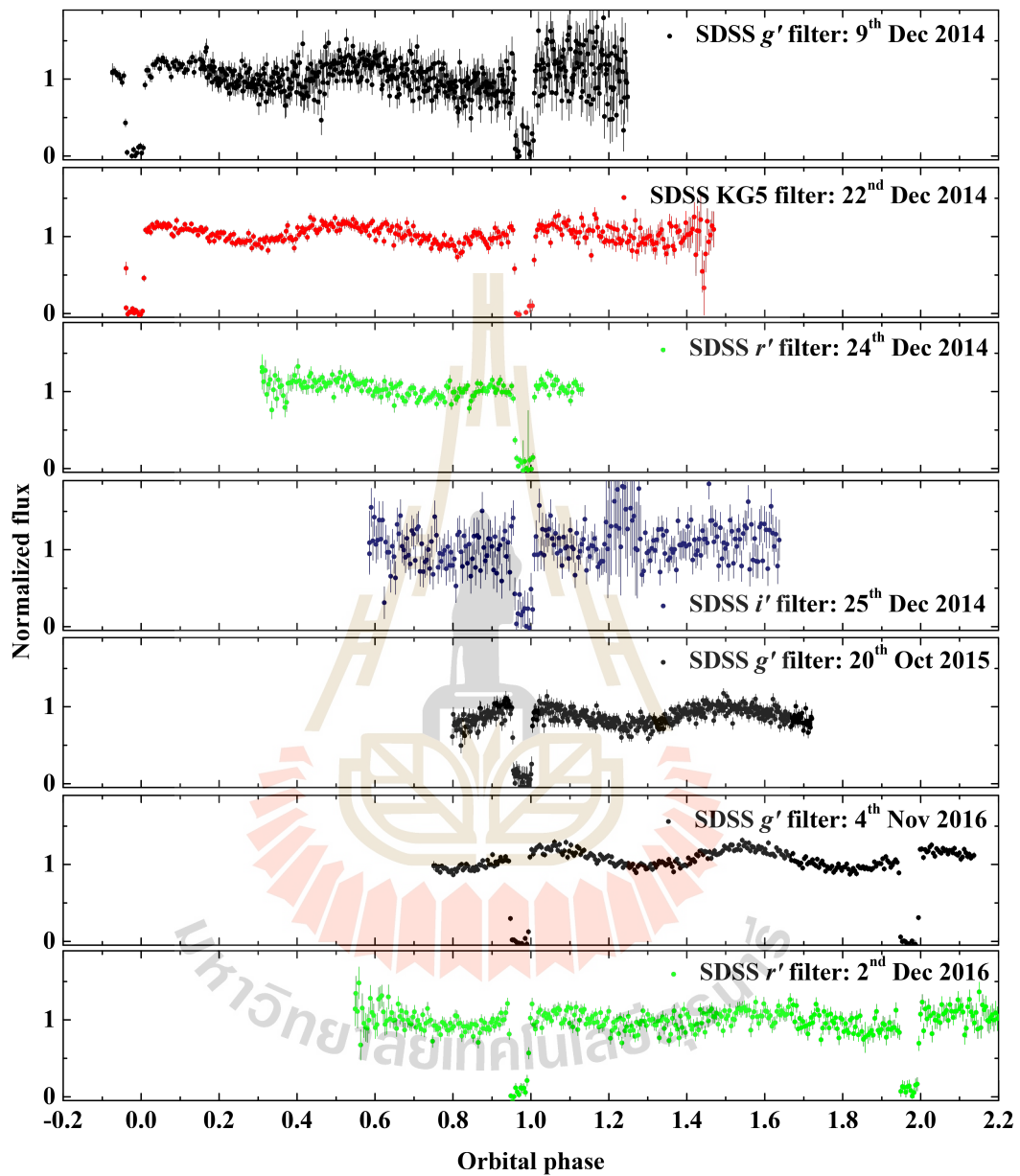
Figure 3.11 From top to bottom: Light curve of SDSS J2141 +0507 in SDSS g', KG5, r', and i' filters which was observed on 9th Dec, 22nd Dec, 24th Dec, 25th Dec 2014, 20th Oct 2015, 4th Nov and 2nd Dec 2016 using the ephemeris of T_0 (HJD) and an orbital period are 2456215.45334 and 0.05469 days (Bours, 2015).
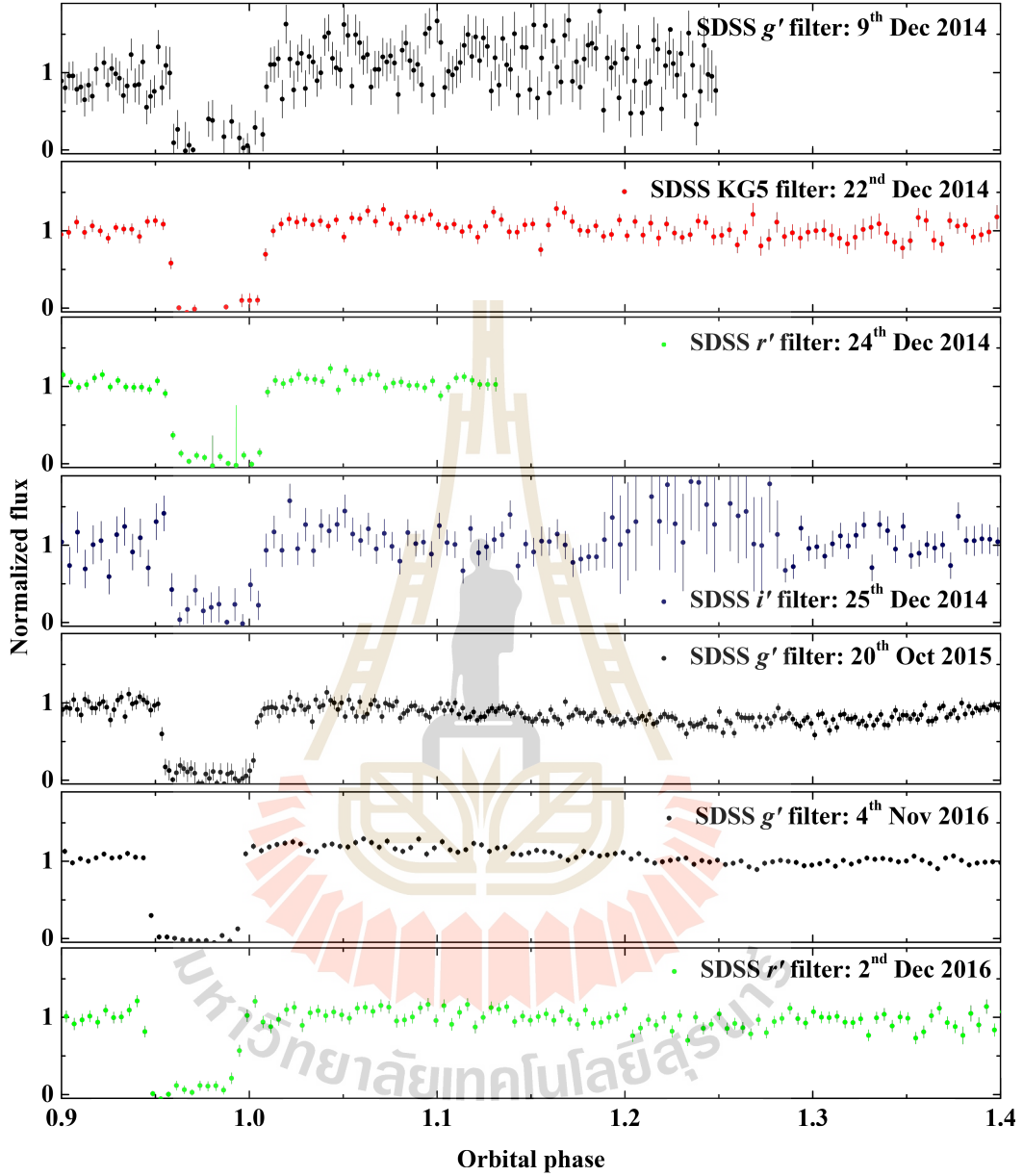
Figure 3.12 Zooming in the range of eclipse. From top to bottom: Light curve of SDSS J2141 +0507 in SDSS g', KG5, r', and i' filters which was observed on 9th Dec, 22nd Dec, 24th Dec, 25th Dec 2014, 20th Oct 2015, 4th Nov and 2nd Dec 2016 using the ephemeris of T_0 (HJD) and an orbital period are 2456215.45334 and 0.05469 days (Bours, 2015).

3.4   Mid-Eclipse Timing Determination (T_0)

To calculate the new ephemeris of SDSS J2141 +0507, we need to use JK-TEBOP code to determine the mid-eclipse timing (T_0) and the orbital period. The first step to calculate the ephemeris of T_0 (HJD) and the orbital period, we need to input the initial parameters for the ephemeris of T_0 (HJD) and the orbital period. We used the ephemeris of T_0 (HJD) and the orbital period are 2456215.45334 and 0.05469 days which calculated by Bours (2015). JKTEBOP code will be iterated until found a good fit of the ephemeris. From our estimation using JKTEBOP code, we get the ephemeris of T_0 (HJD) and the orbital period from our estimation can be determined as 2456215.45338 $\pm$ 0.00005 and 0.05469 $\pm$ 0.00004 days, respectively which made it more accurate than the previous calculation, giving the primary eclipses located at 1.0 as shown in Figure 3.13 and 3.14.

To explain a good fit of the ephemeris using JKTEBOP code, we will use the O-C diagram for obtaining the mid-eclipse (T_0) and the orbital period. The ephemeris of an eclipsing binary star can be estimated using the formula:

$$T_{\mathrm{E}} = T_0 + P_0 E \tag{3.2}$$

Where T_{E} is the mid-eclipse timing of a given orbital cycle E, T_0 is the mid-eclipse timing at which the cycle number E = 0, P_0 is the orbital period in days, and E is the number of cycle.

The O-C diagram have been used to analyze a reliable ephemeris of the periodic variation which can be written as

$$C = T_0 + P_0 E \tag{3.3}$$

$$O = T_0 + PE \qquad (3.4)$$

Where C is the mid-eclipse timing from the calculation, O is the mid-eclipse timing from observation and P is an orbital period from observation.
Then

$$O - C = (P - P_0)E \qquad (3.5)$$

From equation (3.5), if the orbital period of the star from measurement did not change then the points on the O-C diagram will be scattered on a straight horizontal line across the graph.

Table 3.2 shows Orbital period (P_0), observed date, the mid-eclipse timing at any cycle (T_n) and the number of cycle (E) from each observation using the ephemeris of T_0(HJD) and the orbital period as 2456215.45338 $\pm$ 0.00005 and 0.05469 $\pm$ 0.00004 days. Table 3.3 shows the difference between the observed and calculated period with the Cycle (E) using the ephemeris from ISYA School (ISYA Project 2014, private communication) while Table 3.4 shows the difference between the observed and calculated period with the Cycle (E) using the ephemeris from Bours (2015) and our calculation. The diagram of the difference between the observed and calculated orbital period (O-C diagram) using the ephemeris from ISYA, Bours and our calculation were shown in Figure 3.15 and 3.16.
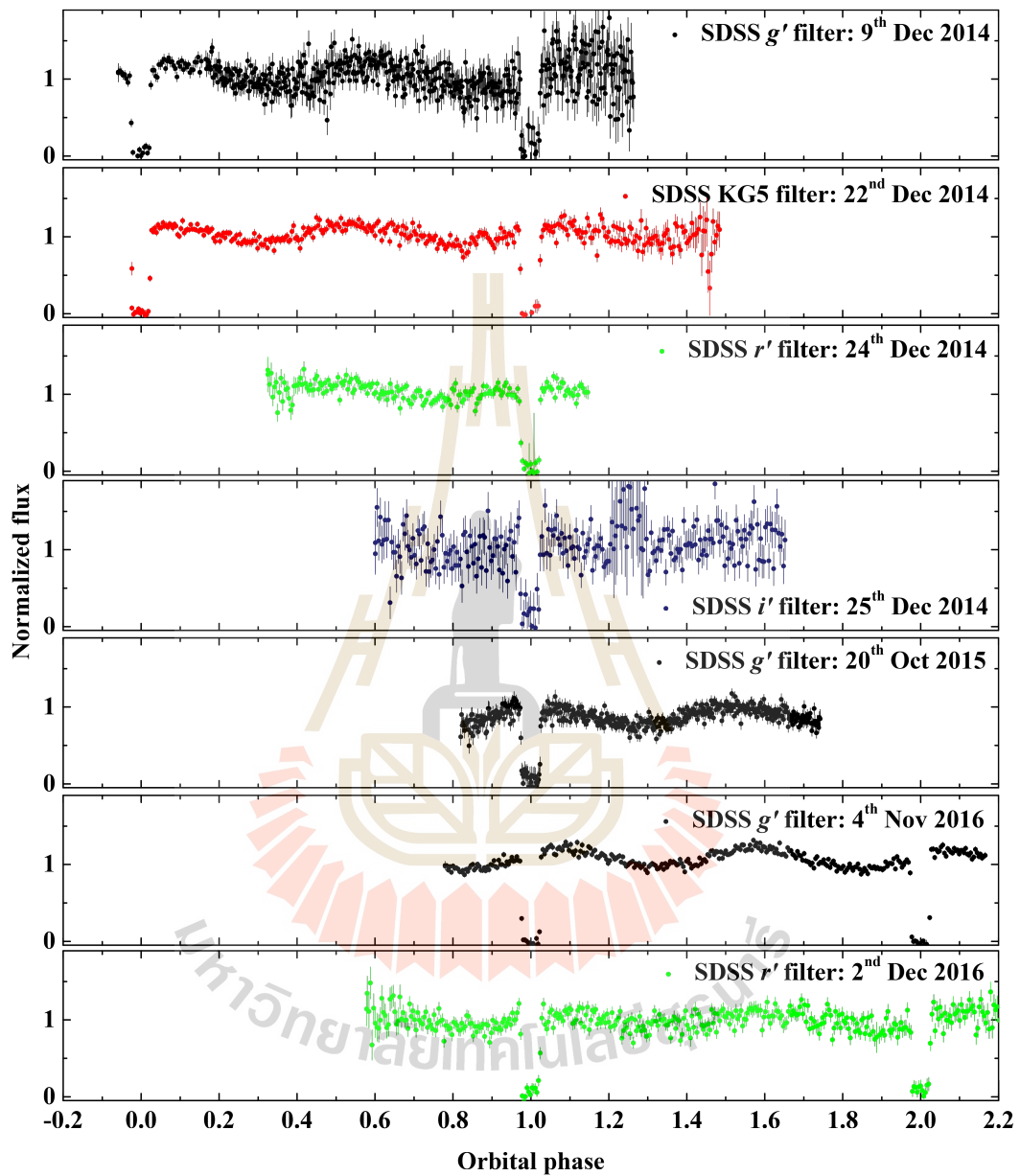
Figure 3.13 From top to bottom: Light curve of SDSS J2141 +0507 in SDSS g', KG5, r', and i' filters which was observed on 9th Dec, 22nd Dec, 24th Dec, 25th Dec 2014, 20th Oct 2015, 4th Nov and 2nd Dec 2016 using the ephemeris of T_0 (HJD) and an orbital period are 2456215.45338 ± 0.00005 and 0.05469 ± 0.00004 days.
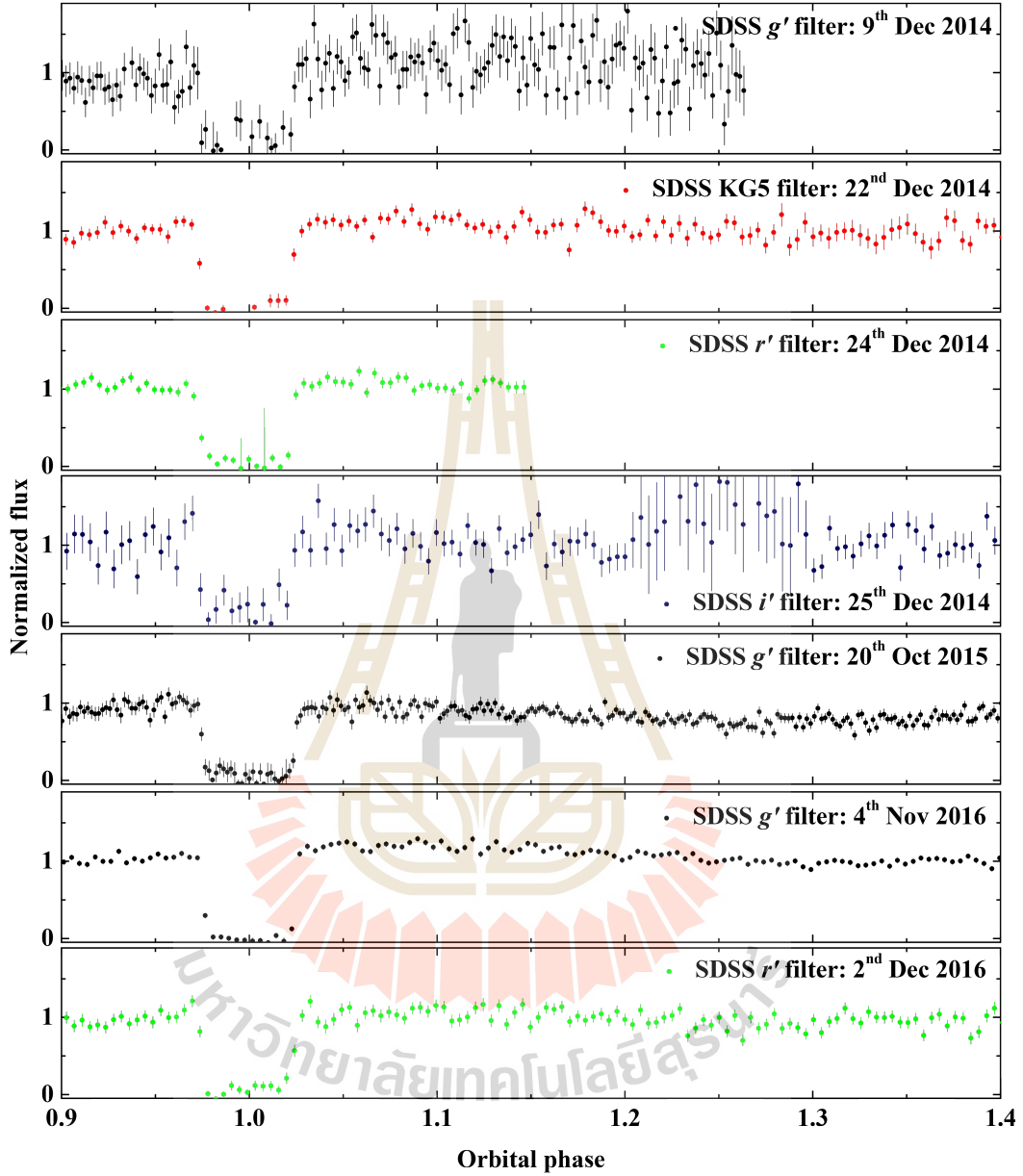
Figure 3.14 Zooming in the range of eclipse. From top to bottom: Light curve of SDSS J2141 +0507 in SDSS g', KG5, r', and i' filters which was observed on 9th Dec, 22nd Dec, 24th Dec, 25th Dec 2014, 20th Oct 2015, 4th Nov and 2nd Dec 2016 using the ephemeris of T_0 (HJD) and an orbital period are 2456215.45338 ± 0.00005 and 0.05469 ± 0.00004 days.

Table 3.2 Orbital period (P_0), observed date, the mid-eclipse timing at any cycle (T_n) and the number of cycle (E) from each observation.

P_0 (days)	Observed date	T_n(HJD)	E	Note
0.05469 ± 0.00004	14th Oct 2012	$2456215.39869 \pm 0.00004$	-1	Bours, 2015
	14th Oct 2012	$2456215.45338 \pm 0.00005$	0	Bours, 2015
	6th Dec 2012	$2456268.34032 \pm 0.00004$	967	Bours, 2015
	9th Dec 2014	$2457001.04586 \pm 0.00008$	14364	ISYA School
	9th Dec 2014	$2457001.10062 \pm 0.00002$	14365	ISYA School
	22nd Dec 2014	$2457014.00782 \pm 0.00009$	14601	TNO WDMS proposal
	22ndDec 2014	$2457014.06257 \pm 0.00001$	14602	TNO WDMS proposal
	24th Dec 2014	$2457016.03133 \pm 0.00005$	14638	Taken during the run of Dr. D. Mkrtichian
	24th Dec 2014	$2457017.01580 \pm 0.00004$	14656	Taken during the run of Dr. D. Mkrtichian

Continued on next page

Table 3.2 Orbital period (P_0), observed date, the mid-eclipse timing at any cycle (T_n) and the number of cycle (E) from each observation. (Continued).

P_0 (days)	Observed date	T_n(HJD)	E	Note
	20th Oct 2015	2457316.07040 $\pm$ 0.00006	20124	Taken during the run of Dr. P. Irawati
	4th Nov 2016	2457697.05332 $\pm$ 0.00003	27090	TNO proposal Cycle 4
	4th Nov 2016	2457697.10819 $\pm$ 0.00008	27091	TNO proposal Cycle 4
	4th Nov 2016	2457697.16284 $\pm$ 0.00008	27092	TNO proposal Cycle 4
	2nd Dec 2016	2457725.00077 $\pm$ 0.00005	27601	TNO proposal Cycle 4
	2nd Dec 2016	2457725.05659 $\pm$ 0.00005	27602	TNO proposal Cycle 4

Table 3.3 The difference between the observed and calculated period with the Cycle (*E*) using the ephemeris from ISYA School (ISYA Project 2014, private communication).

Observed date	*E*	O-C (seconds)
14th Oct 2012	-1	-1.8807
14th Oct 2012	0	0.0000
6th Dec 2012	967	1822.3893
9th Dec 2014	14370	3396.9987
22nd Dec 2014	14607	3841.9487
24th Dec 2014	14644	3903.8112
25th Dec 2014	14662	3939.1488
20th Oct 2015	20132	3160.3391
4th Nov 2016	27101	3713.5584
	27102	3731.5584
	27103	3729.5423
2nd Dec 2016	27612	4671.0432
	27613	4691.5215

Table 3.4 The difference between the observed and calculated period with the Cycle (E) using the ephemeris from Bours(2015) and our calculation.

Observed date	E	O-C (seconds) (Bours, 2015)	O-C (seconds) (Our calculation)
14th Oct 2012	-1	3.7644	0.0000
14th Oct 2012	0	0.0000	0.0000
6th Dec 2012	967	-1.2302	0.0000
9th Dec 2014	14364	-73.9608	-5.4406
22nd Dec 2014	14601	-75.9479	-4.3282
24th Dec 2014	14638	-83.8621	-12.0316
25th Dec 2014	14656	-82.4698	-10.5905
20th Oct 2015	20124	-109.0789	-9.0022
4th Nov 2016	27090	-127.8737	-3.2249
	27091	-139.3139	-6.8433
	27092	-141.5129	-3.2249
2nd Dec 2016	27601	-143.6172	-4.9606
	27602	-145.4999	-6.8200

Table 3.4 The difference between the observed and calculated period with the Cycle (E) using the ephemeris from Bours(2015) and our calculation.

Observed date	E	O-C (seconds) (Bours, 2015)	O-C (seconds) (Our calculation)
14th Oct 2012	-1	3.7644	0.0000
14th Oct 2012	0	0.0000	0.0000
6th Dec 2012	967	-1.2302	0.0000
9th Dec 2014	14364	-73.9608	-5.4406
22nd Dec 2014	14601	-75.9479	-4.3282
24th Dec 2014	14638	-83.8621	-12.0316
25th Dec 2014	14656	-82.4698	-10.5905
20th Oct 2015	20124	-109.0789	-9.0022
4th Nov 2016	27090	-127.8737	-3.2249
	27091	-139.3139	-6.8433
	27092	-141.5129	-3.2249
2nd Dec 2016	27601	-143.6172	-4.9606
	27602	-145.4999	-6.8200

Figure 3.15 The O-C diagram of SDSS J2141 +0507. Top: using the ephemeris of IYSA School (ISYA Project 2014, private communication). Bottom: using the ephemeris of Bours (2015) and our calculation.
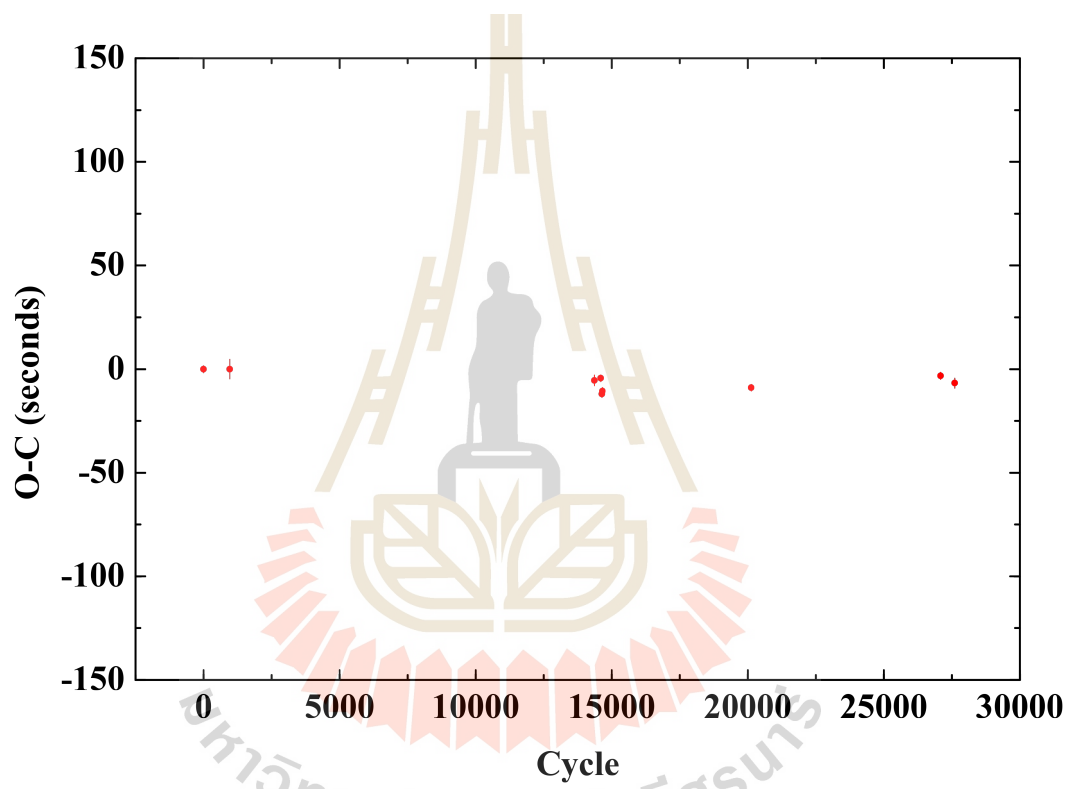
Figure 3.16 The zooming in the O-C diagram of SDSS J2141 +0507, using the ephemeris from our calculation.

3.5 Stellar and Orbital Parameters Determination

To model SDSS J2141 +0507, we determined the stellar and binary parameters for inputting in JKTEBOP code and Binary Maker.

3.5.1 The Binary Separation (a)

According to the Kepler's 3rd law, we can determine the binary separation by assuming that

$$P_{\oplus}^3 = ka_{\oplus}^3 \tag{3.6}$$

Similarly,

$$P_{\star}^3 = ka_{\star}^3 \tag{3.7}$$

Where $P_{\oplus}$ is the orbital period of the Earth orbiting around the Sun which is equal to 1 years. $a_{\oplus}$ is the binary separation between the Earth to the Sun is equal to 1 AU. $P_{\star}$ is the orbital period of the star and $a_{\star}$ is the binary separation of the star. Therefore, we can calculate the binary separation of the star using equation (3.7) divided by equation (3.6), then

$$\frac{P_{\star}^3}{P_{\oplus}^3} = \frac{ka_{\star}^3}{ka_{\oplus}^3} \tag{3.8}$$

$$a_{\star}^3 = a_{\oplus}^3 \left(\frac{P_{\star}}{P_{\oplus}}\right)^2 \tag{3.9}$$

$$a_{\star} = P_{\star}^{2/3} \tag{3.10}$$

For SDSS J2141 +0507, we known that an orbital of system is 0.05469 days or 1.4974×10^{-4} years. Therefore, the binary separation (a) can be calculated as

$$a_\star = (1.4974 \times 10^{-4})^{2/3} = 2.81981 \times 10^{-3} \text{AU} \qquad (3.11)$$

3.5.2 The Radii of White Dwarf (R_s) and Main Sequence (R_l) Stars

Duration of eclipses and shape of light curve can be used to determine the radii of White Dwarf (WD) and Main Sequence (MS) stars.
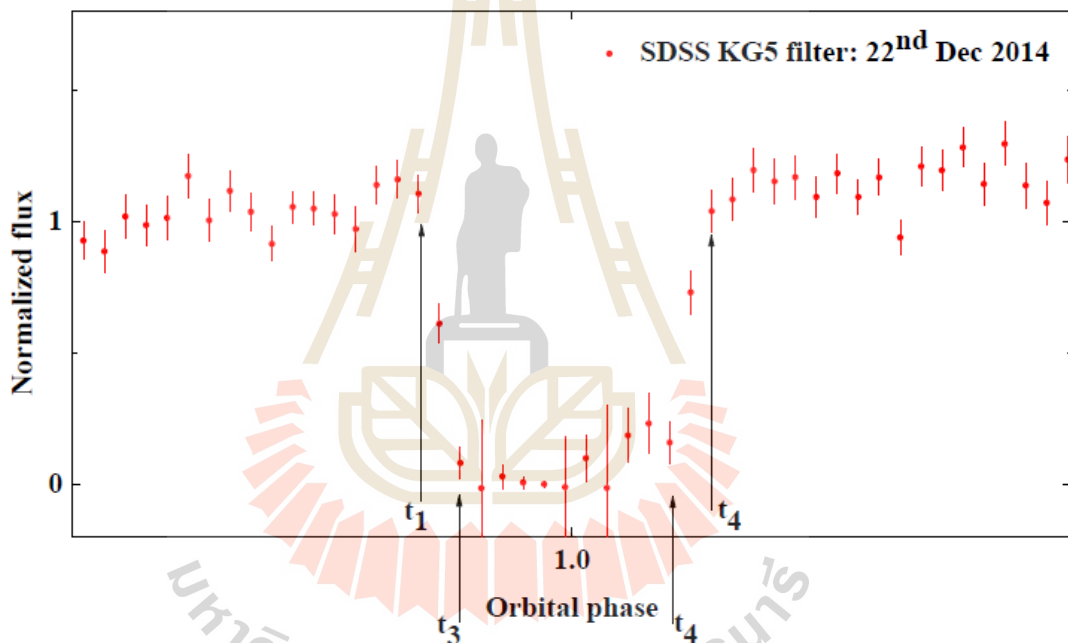
Figure 3.17 Radii determination using light curve observed on 22$^\mathrm{nd}$ Dec 2014 in SDSS KG5 filter.

Figure 3.17 shows light curve of SDSS J2141 +0507 was observed on 22$^\mathrm{nd}$ Dec 2014 in SDSS KG5 filter. We used the light curve of SDSS J2141 +0507 which was obtained on 22$^\mathrm{nd}$ Dec 2014 for calculating the radii of WD and MS stars. Referring the light curve, we can write the time (in HJD) for each phase in Table 3.5

Table 3.5 Time (HJD) for each phase of the observational data which was obtained on 22$^{\text{nd}}$ Dec 2014 in SDSS KG5 filter.

	Phase	Time (HJD)
t_1	0.96932	$2457014.06089 \pm 0.00005$
t_2	0.98188	$2457014.06158 \pm 0.00005$
t_3	1.01538	$2457014.06341 \pm 0.00005$
t_4	1.03214	$2457014.06432 \pm 0.00005$

We can determine the radii of WD and MS as

$$R_{\text{s}} = \frac{v}{2}(t_2 - t_1) \tag{3.12}$$

$$R_{\text{l}} = \frac{v}{2}(t_3 - t_1) \tag{3.13}$$

Where v is the radial velocity which can be written as

$$v = \frac{2\pi a}{P} \tag{3.14}$$

Substitute equation (3.14) into equation (3.12) and (3.13), then we got

$$R_{\text{s}} = \frac{1}{2} . \frac{2\pi a}{P}(t_2 - t_1) \tag{3.15}$$

$$R_{\text{s}} = \frac{\pi a}{P}(t_2 - t_1) \tag{3.16}$$

Also, the radius of MS can be written as

$$R_{\text{l}} = \frac{1}{2} . \frac{2\pi a}{P}(t_3 - t_1) \tag{3.17}$$

$$R_{\text{l}} = \frac{\pi a}{P}(t_3 - t_1) \tag{3.18}$$

According to equation (3.16) and (3.18), the radii of WD and MS can be calculated as

$$R_\text{s} = \frac{\pi(2.81981 \times 10^{-3}\text{AU})(2457014.06158 - 2457014.06089)}{0.05469} \tag{3.19a}$$

$$R_\text{s} = 1.113 \times 10^{-4}\text{AU} \tag{3.19b}$$

Similarly,

$$R_\text{l} = \frac{\pi(2.81981 \times 10^{-3}\text{AU})(2457014.06341 - 2457014.06089)}{0.05469} \tag{3.20a}$$

$$R_\text{l} = 4.081 \times 10^{-4}\text{AU} \tag{3.20b}$$

Hence, JKTEBOP code have to use the scaled radii for modeling the binary system. Therefore, we will calculate the scaled radii of WD and MS which can be written as

$$\frac{R_\text{s}}{a} = \frac{1.113 \times 10^{-4}\text{AU}}{2.81981 \times 10^{-3}\text{AU}} \tag{3.21a}$$

$$\frac{R_\text{s}}{a} = 0.039 \tag{3.21b}$$

$$\frac{R_\text{l}}{a} = \frac{4.081 \times 10^{-4}\text{AU}}{2.81981 \times 10^{-3}\text{AU}} \tag{3.22a}$$

$$\frac{R_\text{l}}{a} = 0.145 \tag{3.22b}$$

3.5.3 Sum of the Radii

We can calculate the sum of the radii from the summation of the scaled radii of WD and MS stars which can be determined as

$$\text{Sum of the radii} = \frac{(R_s + R_s)}{a} = 0.039 + 0.14 \tag{3.23a}$$

$$\text{Sum of the radii} = 0.184 \tag{3.23b}$$

3.5.4 Ratio of the Radii

The ratio of the radii can be written as

$$\text{Ratio of the radii} = \frac{R_s}{R_l} = \frac{0.039}{0.145} \tag{3.24a}$$

$$\text{Ratio of the radii} = 0.269 \tag{3.24b}$$

3.5.5 The Total of Masses

The total of masses can be calculated using the Kepler's 3$^{\text{rd}}$ law which can be written as

$$M_{tot} = \frac{4\pi^2}{G} \cdot \frac{a^3}{P^2} \tag{3.25}$$

Where a is the binary separation $= 2.81981 \times 10^{-3}$ AU or 4.2184×10^8 m. G is the gravitational constant $= 6.67384 \times 10^{-11} \text{m}^{-3} \text{ kg}^{-1}\text{s}^{-2}$ and P is an orbital period $= 0.05469$ days $= 1.4947 \times 10^{-4}$ years $= 4725.36869$ s. Therefore, we can calculate M_{tot} as

$$M_{tot} = \frac{4\pi^2(4.2184 \times 10^8\text{m})^3}{(6.67384 \times 10^{-11}\text{m}^{-3}\text{kg}^{-1}\text{s}^{-2})(4725.36869\text{s})^2} \tag{3.26a}$$

$$M_{tot} = 1.98863 \times 10^{30}\text{kg} \tag{3.26b}$$

We know that

$$M_\odot = 1.9891 \times 10^{30} \text{kg} \tag{3.27}$$

Then equation (3.26b) becomes,

$$M_{tot} = \frac{1.98863 \times 10^{30} \text{kg}.1 M_\odot}{1.9891 \times 10^{30} \text{kg}} \tag{3.28a}$$

$$M_{tot} = 0.99976 M_\odot \tag{3.28b}$$

3.5.6 Mass Ratio

The mass ratio (q) of the system can be written as

$$q = \frac{M_2}{M_1} \tag{3.29}$$

Where M_1 and M_2 are the masses of the WD and MS stars, respectively.

To determine the mass ratio of SDSS J2141 +0507, we have to know the mass for each star but we just known the total of mass. Therefore, we will assume the mass ratio of the system for the initial parameter. According to categories of binary system in case of semidetached binary star, we can assume the mass ratio of the system as 0.1 (Hilditch, 2001) then using the Wilson-Devinney code 2003 (WD 2003) on cluster to determine the accurate of mass ratio. WD 2003 code have been modified by Dr. Utane Sawangwit. The mass ratio from determination is 0.06 and we used the values for using as the initial parameter in JKTEBOP code to get the final parameters.

3.5.7 Orbital Inclination

According to equation (3.25), the orbital inclination(i) can be determined using the Kepler's 3rd law which can be written as

$$P^2 = \frac{4\pi^2}{GM_{tot}}a^3 \tag{3.30}$$

Where a is the binary separation which can be obtained as

$$a = a_1 + a_2 \tag{3.31}$$

Where a_1 and a_2 are the binary separation of WD and MS stars which measured from the center of mass of the system. Therefore, we substituted equation (3.31) into (3.30) then,

$$P^2 = \frac{4\pi^2}{GM_{tot}}(a_1 + a_2)^3 \tag{3.32}$$

Referring equation (3.14), the binary separation can be determined from the radial velocity. Therefore We can write the radial velocity of WD and MS stars as

$$v_1 = \frac{2\pi a_1}{P} \tag{3.33a}$$

$$a_1 = \frac{Pv_1}{2\pi} \tag{3.33b}$$

Similarly,

$$v_2 = \frac{2\pi a_2}{P} \tag{3.34a}$$

$$a_2 = \frac{Pv_2}{2\pi} \tag{3.34b}$$

Substitute equation (3.33b) and (3.34b) in (3.32) then,

$$P^2 = \frac{4\pi^2}{GM_{tot}}[\frac{Pv_1}{2\pi} + \frac{Pv_2}{2\pi}]^3 \qquad (3.35a)$$

$$P^2 = \frac{4\pi^2}{GM_{tot}}[\frac{P}{2\pi}(v_1 + v_2)]^3 \qquad (3.35b)$$

We already known that, the radial velocity of WD and MS stars are also, can be written as

$$v_1 = v_{1r}\sin i \qquad (3.36a)$$

$$v_2 = v_{2r}\sin i \qquad (3.36b)$$

Therefore, we can write equation as

$$v = v_1 + v_2 = (v_{1r} + v_{2r})\sin i \qquad (3.37)$$

Substitute equation (3.37) into (3.35b), then we get

$$P^2 = \frac{4\pi^2}{GM_{tot}}[\frac{P}{2\pi}(v_{1r} + v_{2r})\sin i]^3 \qquad (3.38a)$$

$$P^2 = \frac{4\pi^2}{GM_{tot}}[\frac{P}{2\pi}\cdot\frac{v}{\sin i}]^3 \qquad (3.38b)$$

We substituted equation (3.14) in (3.38b), then equation becomes

$$P^2 = \frac{4\pi^2}{GM_{tot}}[\frac{P}{2\pi}\cdot\frac{2\pi a}{P}\cdot\frac{1}{\sin i}]^3 \qquad (3.39a)$$

$$P^2 = \frac{4\pi^2}{GM_{tot}}\cdot\frac{a^3}{\sin^3 i} \qquad (3.39b)$$

In finally,

$$\sin^3 i = \frac{4\pi^2}{GM_{tot}}\cdot\frac{a^3}{P^2} \qquad (3.40)$$

Where $a = 2.81981 \times 10^{-3}$ AU or 4.2184×10^8 m, G = $6.67384 \times 10^{-11}\text{m}^{-3}, P =$

0.05469 days = 1.4947×10^{-4} years = 4725.36869 s and $M_{tot} = 0.99976 M_\odot = 0.99976 \times 1.9891 \times 10^{30} = 1.98863 \times 10^{30}$kg

Then equation (3.40) becomes,

$$\sin^3 i = \frac{4\pi^2}{(6.67384 \times 10^{-11} \text{m}^{-3}\text{kg}^{-1}\text{s}^{-2})(1.98863 \times 10^{30}\text{kg})} \cdot \frac{(4.2184 \times 10^8 \text{m})^3}{(4725.36869\text{s})^2}$$

(3.41a)

$$\sin^3 i = 1 \tag{3.41b}$$

$$i = \sin^{-1}(1) = 90° \tag{3.41c}$$

Equation (3.41c) is the initial parameter of the orbital inclination for inputting in JKTEBOP code.

3.5.8 Orbital Period of Eclipsing Binary System and Reference Time of Primary Minimum

We used the orbital period and the time of primary minimum or the mid-eclipse timing T_0 from Bours (2015) who determined the ephemeris of T_0 (HJD) and the orbital period as 2456215.45334 and 0.05469 days, respectively.

3.5.9 Surface Brightness Ratio

The surface brightness ratio can be calculated as

$$J = \left[\frac{T_{\text{eff}}(\text{MS})}{T_{\text{eff}}(\text{WD})}\right]^4 \tag{3.42}$$

Due to the effective temperature of WD and MS stars have not been known. From the spectrum of SDSS J2141 +0507 (Szkody et al., 2014), we assumed the surface brightness ratio as 0.7 for inputting in JKTEBOP code and also, we as-

sumed the effective temperature of WD star to input in WD2003 as 30000 K. JKTEBOP and WD code will determine the best fit parameters of the surface brightness ratio and the effective temperature of WD star. In finally, we obtained the surface brightness ratio and the effective temperature of WD as 0.0027 and 32000 K, respectively. Therefore, we can estimate the effective temperature of MS star for inputting in Binary Maker as

$$0.0027 = [\frac{T_{\text{eff}}(\text{MS})}{32000}]^4 \tag{3.43a}$$

$$[T_{\text{eff}}(\text{MS})]^4 = 0.0027[32000]^4 \tag{3.43b}$$

$$T_{\text{eff}}(\text{MS}) = [0.0027]^{1/4}[32000] \tag{3.43c}$$

$$T_{\text{eff}}(\text{MS}) = 7294 \quad \text{K} \tag{3.43d}$$

3.5.10 Gravity Darkening Exponent

Gravity darkening was occurred when star is rotating that the regions are close to the pole are brighter than the regions are far to the pole. Due to the regions which close to the pole have an effective temperature higher than the regions which close to the equator (White and Thomas W. Baumgarte, 2012). In 1924, Von Zeipel solved that the surface flux was directly proportional to the value of the gravitational acceleration at the stellar surface for the totally radiative stars. In 1967, Lucy found that the gravity darkening exponent α is 1.0 and 0.32 for the radiative and convective stars, respectively (Zeipel, 1924; Lucy, 1976; Bradstreet, 2015).

3.5.11 Limb Darkening

Limb darkening is an optical effect in stars which included the Sun. This phenomenon occurred if we are looking at the surface of star from an angle rather than from directly above then the surface brightness is lower. Therefore, if we observed a star at the edge (or limb) of star then the surface brightness of star is fainter more than the center of star (Southworth, 2013).

3.5.12 Spot

The specific parameters for describing a spot region are colatitude, longitude, spot radius and temperature factor.

3.5.12.1 Colatitude

Colatitude is defined as the angle from 0° to 180° which we measured along a meridian from the upper pole (the pole observable from Earth) to the lower pole.

3.5.12.2 Longitude

Longitude is defined as the angle from 0° to 360°] which measured counterclockwise from the meridian along the line connecting the mass centers as seen from the upper poles (positive end of the angular momentum vector).

3.5.12.3 Spot Radius

Spot radius is defined as the approximately circular radius in degree of the spot region centered at the colatitude and longitude coordinates described elsewhere.

3.5.12.4 Temperature Factor

The spot temperature factor is defined as the percentage hotter or cooler that the spot temperature is relative to the local temperature. For example, a spot temperature factor of 0.70 means a spot which is 70% of the tem-

perature of its surrounding photosphere, and a factor of 1.35 means a spot with the temperature 35% hotter that its surrounding. Table 3.7 shown the example of initial stellar and binary parameters for BM3 in SDSS r' filter.

3.5.13 Reflection Effect

Reflection effect or bolometric albedo is the percentage of incident radiation that is re-radiated by the companion star. In 1969, Rucinki found that for radiative stars, the coefficient is assumed to be 1.00 and for convective stars, the reflection effect will be approximated as 0.5 because the surface convection will carry away some of the energy to re-radiate it from regions other than where it was incident. Thus, for stars wholes temperatures are less than 7200 K, this coefficient should be set to 0.50 (Bradstreet, 2015).

3.6 Light Curve Fitting

3.6.1 JKTEBOP Code

JKTEBOP Code is a FORTRAN based code made for analyzing and modelling of the light curves of detached eclipsing binaries and transiting planets. We can derive some stellar parameters such as the radii of the primary and secondary stars, the mass ratio of the system and the surface brightness ratio etc. JKTEBOP Code includes extensive Monte Carlo or bootstrapping error analysis algorithm which is useful to analyze light curve of eclipsing binaries (Southworth, 2014). To obtain the stellar and binary parameters for SDSS J2141 +0507, we need the initial of the stellar and binary parameters such as the mass ratio of the system, orbital inclination, surface brightness ratio, reflection effect etc. JKTEBOP code will give the best-fitting model of the light curve and their residual. The

specific stellar and binary parameters for inputting on JKTEBOP code are: mass ratio of the system, sum of the radii, ratio of the radii, the total of masses, orbital inclination, the orbital period of eclipsing binary system and reference time of primary minimum, surface brightness ratio, gravity brightening, limb darkening and reflection effect. Table 3.6 shows the initial of the stellar and binary parameters for SDSS J2141+0507 using JKTEBOP code.

Table 3.6 The initial parameters for SDSS J2141 +0507 using JKTEBOP code.

Inital values of the parameters			
3	1	Task to do (from 2 to 9)	Integ. ring size (deg)
0.39	1.8	Sum of the radii	Ratio of the radii
87	0.058	Orbital inclination (deg)	Mass ratio of system
0.0	0.0	ecosw or eccentricity	esinw or periastron long
0.3	0.3	Gravity darkening (star A)	Grav darkening (star B)
0.7	0.0	Surface brightness ratio	Amount of third light
sqrt	lin	LD law type for star A	LD law type for star B
0.3	0.3	LD star A (linear coeff)	LD star B (linear coeff)
0.0	0.0	LD star A (nonlin coeff)	LD star B (nonlin coeff)
0.0	0.35	Reflection effect star A	Reflection effect star B
0.0	3.9	Phase of primary eclipse	Light scale factor (mag)
0.054691767280		Orbital period of eclipsing binary system (days)	
2457016.031474960		Reference time of primary minimum (HJD)	
1	1	Adjust RADII SUM or RADII RATIO (0, 1, 2, 3)	
0	0	Adjust INCLINATION or MASSRATIO (0, 1, 2, 3)	

Continued on next page

Table 3.6 The initial parameters for SDSS J2141 +0507 using JKTEBOP code. (Continued).

Inital values of the parameters		
0.0	0.35	Reflection effect star A Reflection effect star B
0.0	3.9	Phase of primary eclipse Light scale factor (mag)
0.054691767280		Orbital period of eclipsing binary system (days)
2457016.031474960		Reference time of primary minimum (HJD)
1	1	Adjust RADII SUM or RADII RATIO (0, 1, 2, 3)
0	0	Adjust INCLINATION or MASSRATIO (0, 1, 2, 3)
0	0	Adjust ECOSW-or-E or ESINW-or-OMEGA (0, 1, 2, 3)
0	0	Adjust GRAVDARK1 or GRAVDARK2 (0, 1, 2, 3)
1	0	Adjust SURFBRIGHT2 or THIRDLIGHT (0, 1, 2, 3)
0	0	Adjust LD-LIN starA or LD-LIN starB (0, 1, 2, 3)
0	0	Adjust LD-NONLIN A or LD-NONLIN B (0, 1, 2, 3)
1	1	Adjust REFLECTION A or REFLECTION B (-1,0,1,2,3)
0	1	Adjust PHASESHIFT or SCALE FACTOR
1	0	Adjust PERIOD or T(pri.ecl.) (0, 1, 2, 3)
jkt_20141224.dat		Name of file containing light curve
jkt_20141224.par		Name of output parameter file
jkt_20141224.out		Name of output light curve file
jkt_20141224.fit		Name of output model light curve fit file

We can obtain some stellar parameters using JKTEBOP by inputting the initial parameter values of mass ratio, orbital inclination, surface brightness ratio, reflection effect etc. The code will give the best-fitting model of the light curve and their residual are shown in Figure 3.18 and the final of the stellar and binary

parameters for SDSS J2141 +0507 using JKTEBOP code was shown in Table 3.7.
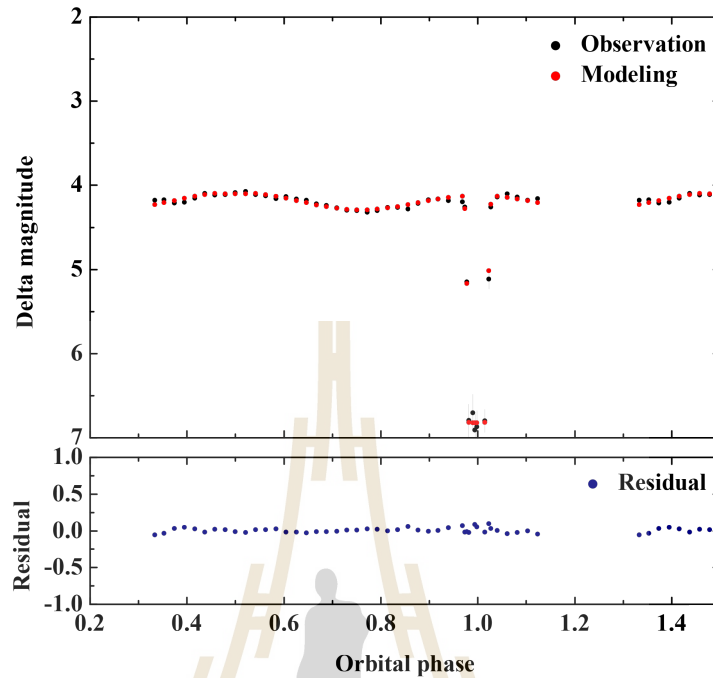
Figure 3.18 The graph fitting with the residual using JKTEBOP Code.

Table 3.7 The final parameters for SDSS J2141 +0507 using JKTEBOP code.

Final values of the parameters	
1 Surf. bright. ratio	$0.0032809803 \pm 0.0004240898$
2 Sum of frac radii	$0.1744601322 \pm 0.0020760606$
3 Ratio of the radii	$7.2585237724 \pm 0.4059096124$
4 Limb darkening A1	0.3000000000 (fixed)
5 Limb darkening B1	0.3000000000 (fixed)
6 Orbit inclination	87.0000000000 (fixed)
7 ecc * cos(omega)	0.0000000000 (fixed)

Table 3.7 The final parameters for SDSS J2141 +0507 using JKTEBOP code. (Continued).

Final values of the parameters	
8 ecc * sin(omega)	0.0000000000 (fixed)
9 Grav darkening A	0.3000000000 (fixed)
10 Grav darkening B	0.3000000000 (fixed)
11 Reflected light A	$0.1931101200 \pm 0.0106720369$
12 Reflected light B	$0.2284911173 \pm 0.0108889881$
13 Phot mass ratio	0.0580000000 (fixed)
15 Third light (L_3)	0.0000000000 (fixed)
16 Phase correction	0.0000000000 (fixed)
17 Light scale factor	$4.4536862553 \pm 0.0136371121$
18 Integration ring	1.0000000000 (fixed)
19 Orbital period (P)	$0.0566283127 \pm 0.0005528577$
20 Ephemeris timebase	2457016.0314749600 (fixed)
21 Limb darkening A2	0.0000000000 (fixed)
Limb darkening law for primary star:	quare-root
Limb darkening law for secondary star:	linear
Fractional primary radius:	0.0211248568
Fractional secondary radius:	0.1533352754

3.6.2 Binary Maker 3.0 software (BM3)

BM3 is a software using to get an accurate model of the light curve and the radial velocity curve for almost any type of binary stars system. The major display shows the light curves of theoretical and the observational data. This software can generate professional quality postscript output which can be created of all major display. Supplementary functions include the capability of generating cross-sectional diagram of the stars within their Roche surface. We can add the spot of stars, eccentric orbits and also, asynchronously rotating stars can be accurately modeled. Moreover, BM3 can calculate the difference between the analysis light, radial velocity values and the observational data.

To get the modeling of SDSS J2141 +0507, we need to obtain the stellar and binary parameters for this system. The initial stellar and binary parameters which we have to input in this software such as the mass ratio of system, the effective temperature, the radii of white dwarf and secondary stars etc. then the output of BM3 will be given the Roche model, radial velocity and also, the 3D model of eclipsing binary. The specific parameters used to model are: mass ratio, radii of WD and MS stars, effective temperature and effective wavelength of SDSS filter in angstroms, gravity brightening, limb darkening, reflection effect, inclination, and spot. Table 3.8 shows the initial stellar and binary parameters for BM3 in SDSS r' filter. r(1) back and r(2) back are the radii of WD and MS stars. Temperature 1 and Temperature 2 are the effective temperature of WD and MS stars. G1 and G2 are the gravity darkening of WD and MS stars. X1 and X2 are the limb darkening of WD and MS stars.

Figure 3.19 shows the display windows of BM3 software. We can input the initial parameters such as mass ratio, the effective temperature, the radii of white dwarf and secondary stars etc., then the output of BM3 will give the Roche model,

Table 3.8 The initial parameters for SDSS J2141 +0507 using BM3 in SDSS r'
filter.

Parameter(s)	
Mass Ratio	0.058
r(1) back	0.029
r(2) back	0.198
Wavelength	6261
Temperature 1	31500
Temperature 2	3750
G1	0.3
G2	0.3
X1	0.3
X2	0.3
Inclination	87

radial velocity and also, the 3D model of eclipsing binary. Table 3.9 shows the
table output from BM3.
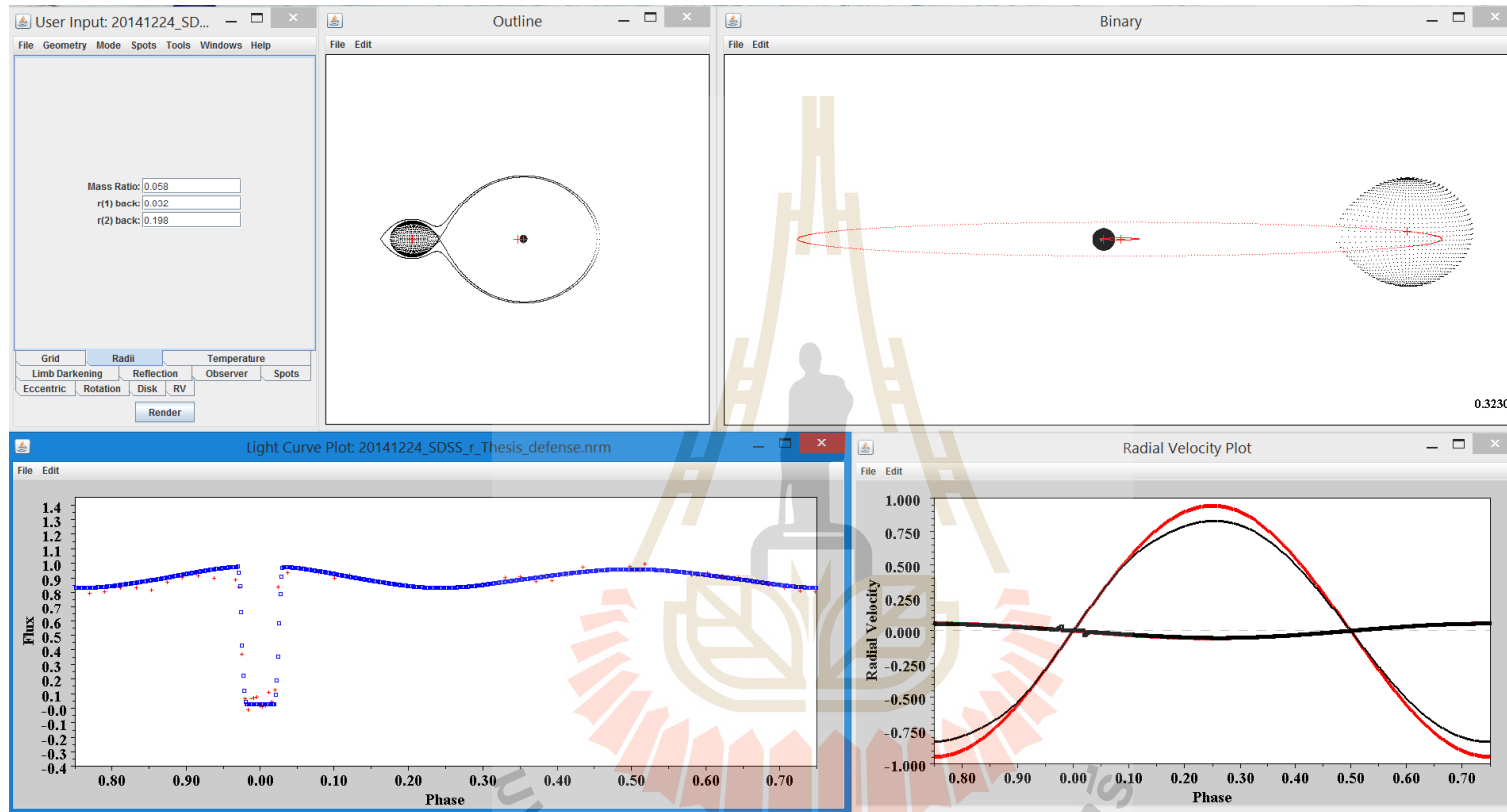
Figure 3.19 The result of SDSS J2141 +0507 which was obtained from the fitting of the observational data on 24th Dec 2014 in SDSS r' filter using BM3.

Table 3.9 The data output of SDSS J2141 +0507 which was obtained from the fitting of the observational data on 24th Dec 2014 in SDSS r' filter using BM3.

Output from Binary Maker	
mass ratio input = 0.058000	mass ratio < 1 = 0.058000
Omega 1 = 31.308599	Omega 2 = 1.817393
Omega inner = 1.818910	Omega outer = 1.780663
C 1 = 59.187503	C 2 = 3.438530
C inner = 3.441398	C outer = 3.369098
Fillout 1 = -0.941856	Fillout 2 = 0.039661
Lagrangian L1 = 0.758442	Lagrangian L2 = 1.287615
AG = r1(back) = 0.032000	AS = r2(back) = 0.198000
BG = r1(side) = 0.032000	BS = r2(side) = 0.167978
CG = r1(pole) = 0.031999	CS = r2(pole) = 0.161479
DG = r1(point) = 0.032000	DS = r2(point) = 0.241558
Surface area 1 = 0.012871	Surface area 2 = 0.392223
Volume 1 = 0.000136	Volume 2 = 0.022435
Mean radius 1 = 0.032000	Mean radius 2 = 0.175819
Mean radius 1 (vol) = 0.031922	Mean radius 2 (vol) = 0.174962
Eccentricity = 0.00000	Longitude of Periastron = 0.2500
Phase of periastron = 0.00000	Phase of conjunction = 0.0000
Angular Rotation F1 = 1.0000	Angular Rotation F2 = 1.0000
Normalization Phase = 0.32550	Normalization Factor = 0.87000
inclination = 87.000	wavelength = 6261.00

Continued on next page

Table 3.9 The data output of SDSS J2141 +0507 which was obtained from the fitting of the observational data on 24th Dec 2014 in SDSS r' filter using BM3. (Continued).

Output from Binary Maker	
temperature 1 = 31500.00	temperature 2 = 3570.00
luminosity 1 = 0.9550	luminosity 2 = 0.0450
gravity coefficient 1 = 0.150	gravity coefficient 2 = 0.150
limb darkening 1 = 0.150	limb darkening 2 = 0.330
reflection 1 = 0.000	reflection 2 = 1.300
Third light = 0.0000	Period = 0.054691

CHAPTER IV

STELLAR PARAMETERS OF SDSS J2141 +0507

4.1 The Modelling of SDSS J2141 +0507 using BM3

From Figure 4.1, the fitting model for SDSS J2141 +0507 using BM3 shows that the outside of eclipse for this model cannot be fitted. This phenomena is indicated that the pattern of the outside eclipse is not occur from the shape of the second star only. Normally, the outside of eclipse is occurs from the shape of the secondary star but when we input the radius of the secondary star then we cannot generate the sinusoidal pattern of the outside of eclipse. To correct the graph fitting, we need to input some bright spot on the secondary star which in this case means the hot spot on the primary star. The model can be fitted better after we input the bright spot on the primary star as shown in Figure 4.2.

From Figure 4.3 and 4.4, the Roche models of SDSS J2141 +0507 and the phase increment of this model are shown, respectively. The red dots represented the light curve from the observations while the blue dots represented the light curve from adjust initial parameters (Bradstreet et al., 2015). The stellar and binary parameters with without bright spot and included bright spot from the estimation are shown in Table 4.1 and 4.2.
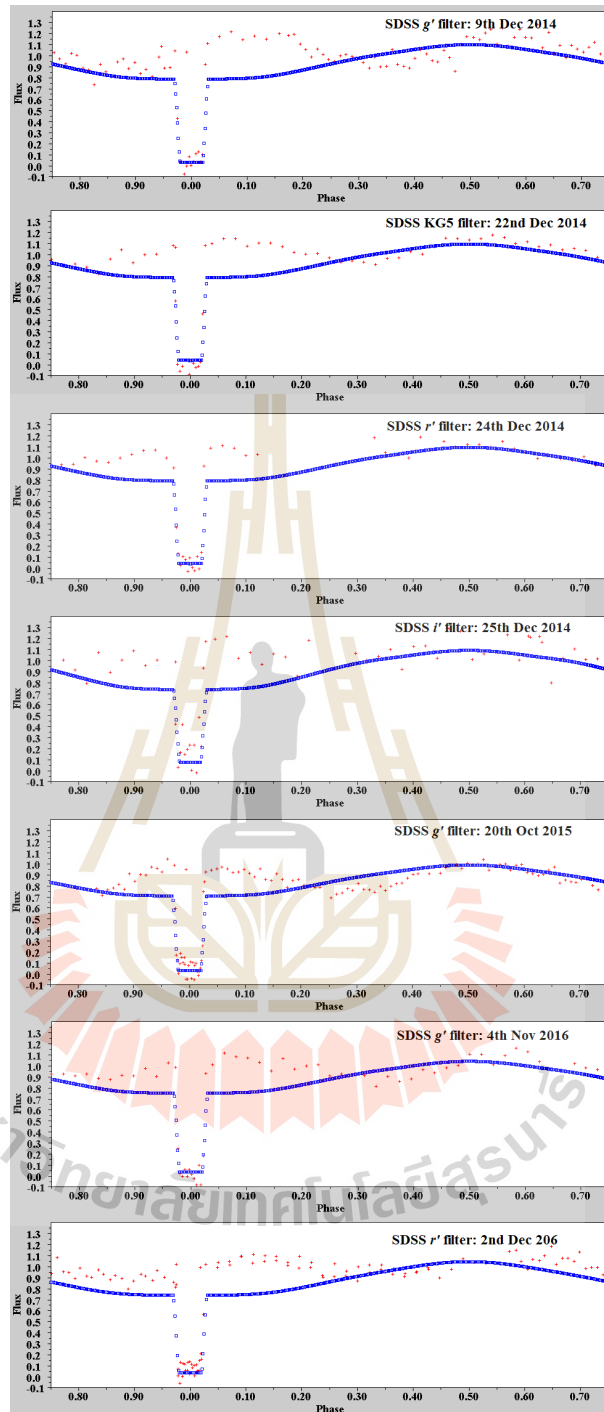
Figure 4.1 Light curves of SDSS J2141 +0507 with the best fitting without the bright spot on the white dwarf. From top to bottom: The light curve of SDSS J2141 +0507 in SDSS g', KG5, r', and i' filters which was observed on 9th Dec, 22nd Dec, 24th Dec, 25th Dec 2014, 20th Oct 2015, 4th Nov and 2nd Dec 2016.
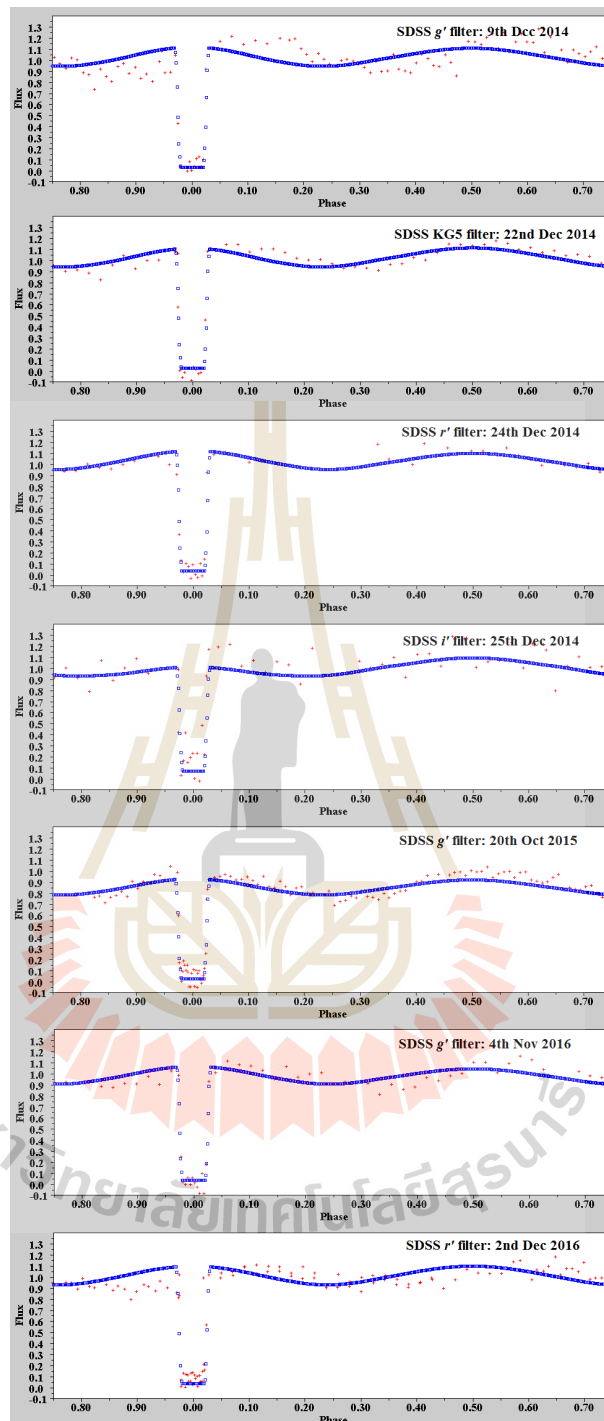
Figure 4.2 Light curves of SDSS J2141 +0507 with the best fitting included the bright spot on the white dwarf. From top to bottom: The light curve of SDSS J2141 +0507 in SDSS g', KG5, r', and i' filters which was observed on 9th Dec, 22nd Dec, 24th Dec, 25th Dec 2014, 20th Oct 2015, 4th Nov and 2nd Dec 2016.
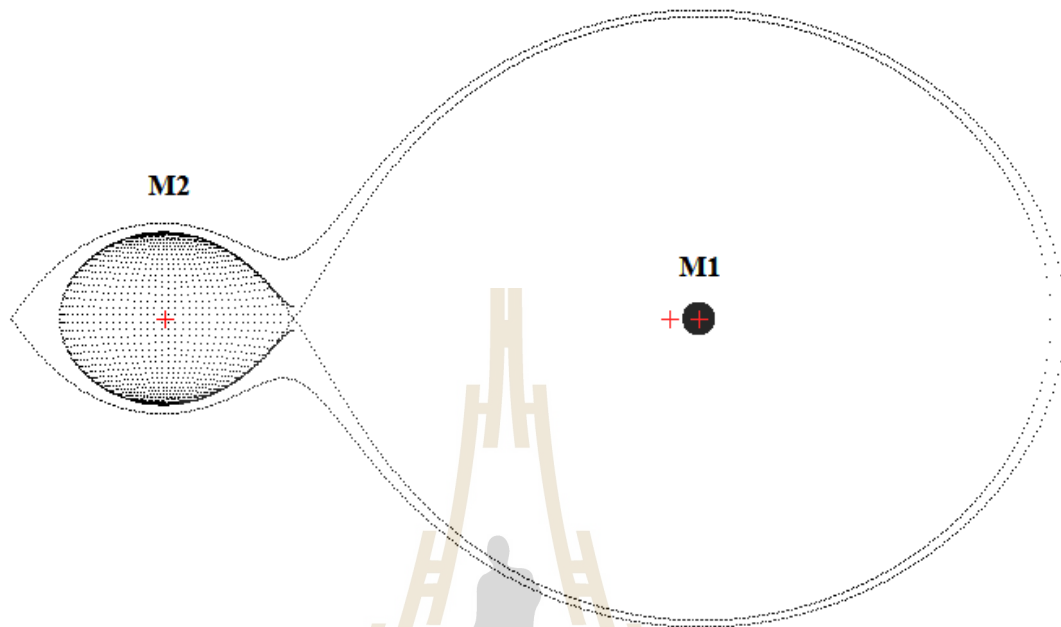
Figure 4.3 The Roche lobe model of SDSS J2141 +0507 is generated by Binary Maker 3.0 (BM3) software. In this case, the primary and secondary stars are white dwarf (WD) and main sequence (MS) stars, respectively.
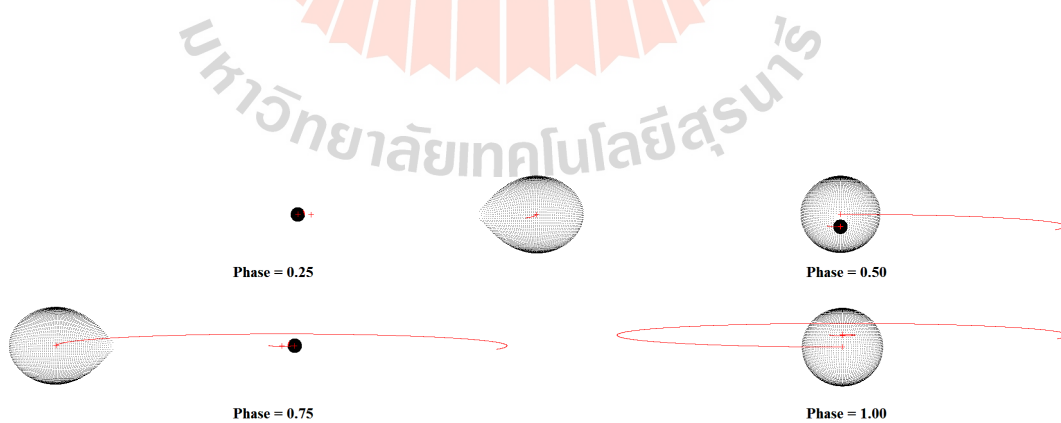
Figure 4.4 The phase increment of SDSS J2141 +0507 made using Binary Maker 3.0 (BM3) software.

Table 4.1 The stellar and binary parameters of SDSS J2141 +0507 without the bright spot on the white dwarf using BM3. G1, G2, X1 and X2 are the gravity darkening and the limb darkening of primary and secondary stars, respectively.

Parameter(s)	9th Dec 2014	22nd Dec 2014	24th Dec 2014	25th Dec 2014
Mass Ratio	0.058	0.058	0.058	0.058
WD Radius ($R_\odot$)	0.032	0.031	0.026	0.032
MS Radius ($R_\odot$)	0.198	0.198	0.198	0.200
Filter (SDSS)	g'	KG5	r'	i'
WD T_{eff}(K)	31000	31500	31500	31000
MS T_{eff}(K)	3500	3550	3570	3570
G1	0.3	0.3	0.3	0.3
G2	0.3	0.3	0.3	0.3
X1	0.3	0.3	0.3	0.3
X2	0.3	0.3	0.3	0.3
WD Reflection	0	0	0	0

Continued on next page

Table 4.1 The stellar and binary parameters of SDSS J2141 +0507 without the bright spot on the white dwarf using BM3. G1, G2, X1 and X2 are the gravity darkening and the limb darkening of primary and secondary stars, respectively. (Continued).

Parameter(s)	20th Oct 2015	4th Dec 2016	2nd Dec 2016
Mass Ratio	0.058	0.058	0.058
WD Radius (R$_\odot$)	0.032	0.032	0.026
MS Radius (R$_\odot$)	0.198	0.198	0.198
Filter (SDSS)	g'	g'	r'
WD T$_{eff}$(K)	31000	31000	31000
MS T$_{eff}$(K)	3500	3500	3570
X1	0.3	0.3	0.3
X2	0.3	0.3	0.3
WD Reflection	0	0	0

Table 4.2 The stellar and binary parameters of SDSS J2141 +0507 included the bright spot on the white dwarf using BM3. G1, G2, X1 and X2 are the gravity darkening and the limb darkening of primary and secondary stars, respectively.

Parameter(s)	9th Dec 2014	22nd Dec 2014	24th Dec 2014	25th Dec 2014
Mass Ratio	0.058	0.058	0.058	0.058
WD Radius (R$_\odot$)	0.032	0.031	0.026	0.032
MS Radius (R$_\odot$)	0.198	0.198	0.198	0.200
Filter (SDSS)	g'	KG5	r'	i'
WD T$_{eff}$(K)	31000	31500	31500	31000
MS T$_{eff}$(K)	3500	3550	3570	3570
G1	0.3	0.3	0.3	0.3
G2	0.3	0.3	0.3	0.3
X1	0.3	0.3	0.3	0.3
X2	0.3	0.3	0.3	0.3
WD Reflection	0	0	0	0
MS Reflection	1.3	1.3	1.3	1.3

Table 4.2 The stellar and binary parameters of SDSS J2141 +0507 included the bright spot on the white dwarf using BM3. G1, G2, X1 and X2 are the gravity darkening and the limb darkening of primary and secondary stars, respectively. (Continued).

Parameter(s)	9th Dec 2014	22nd Dec 2014	24th Dec 2014	25th Dec 2014
Inclination	87°	87°	86°	86°
WD Spot				
Colatitude	75	75	75	75
Longitude	0	0	0	0
Spot Radius	25	25	25	25
Temperature Factor	2.7	2.7	2.7	2.7
Period (days)	0.05469 ± 0.00004	0.05469 ± 0.00004	0.05469 ± 0.00004	0.05469 ± 0.00004
χ^2	1.14	0.66	0.08	0.50

Continued on next page

Table 4.2 The stellar and binary parameters of SDSS J2141 +0507 included the bright spot on the white dwarf using BM3. G1, G2, X1 and X2 are the gravity darkening and the limb darkening of primary and secondary stars, respectively. (Continued).

Parameter(s)	20$^{\text{th}}$ Oct 2015	4$^{\text{th}}$ Dec 2016	2$^{\text{nd}}$ Dec 2016
Mass Ratio	0.058	0.058	0.058
WD Radius (R$_\odot$)	0.032	0.032	0.026
MS Radius (R$_\odot$)	0.198	0.198	0.198
Filter (SDSS)	g'	g'	r'
WD T$_{\text{eff}}$(K)	31000	31000	31000
MS T$_{\text{eff}}$(K)	3500	3500	3570
G1	0.3	0.3	0.3
G2	0.3	0.3	0.3
X1	0.3	0.3	0.3
X2	0.3	0.3	0.3
WD Reflection	0	0	0
MS Reflection	1.3	1.3	1.3

Continued on next page

Table 4.2 The stellar and binary parameters of SDSS J2141 +0507 included the bright spot on the white dwarf using BM3. G1, G2, X1 and X2 are the gravity darkening and the limb darkening of primary and secondary stars, respectively. (Continued).

Parameter(s)	20$^{\text{th}}$ Oct 2015	4$^{\text{th}}$ Dec 2016	2$^{\text{nd}}$ Dec 2016
Inclination	87°	87°	86°
WD Spot			
Colatitude	75	75	75
Longitude	0	0	0
Spot Radius	25	25	25
Temperature Factor	2.7	2.7	2.7
Period (days)	0.05469 ± 0.00004	0.05469 ± 0.00004	0.05469 ± 0.00004
χ^2	0.24	0.21	0.27

Referring chapter III, we can report a new ephemeris of SDSS J2141 +0507 with T0 (HJD) as 2456215.45338 ± 0.00005 and an orbital period is 0.05469 ± 0.00004 days. We used the new ephemeris of SDSS J2141 +0507 to model and determine the stellar and parameters for this system.

The schematic of a CV which consists of a low mass main sequence secondary star (MS) and a white dwarf primary star (WD) with accretion disc have been shown in Figure 4.5. In this work, BM3 is used for obtaining the stellar and binary parameters of SDSS J2141 +0507. However, BM3 cannot be used for model directly in case of the CV because this software cannot generate the gas stream. The sinusoidal pattern of this system is occurred from the shape of the secondary star, however we input the accurate of the radius of secondary stay but then we cannot fit the profile of outside eclipse. We need to input bright spot on the white dwarf then we got the result as shown in Figure 4.2
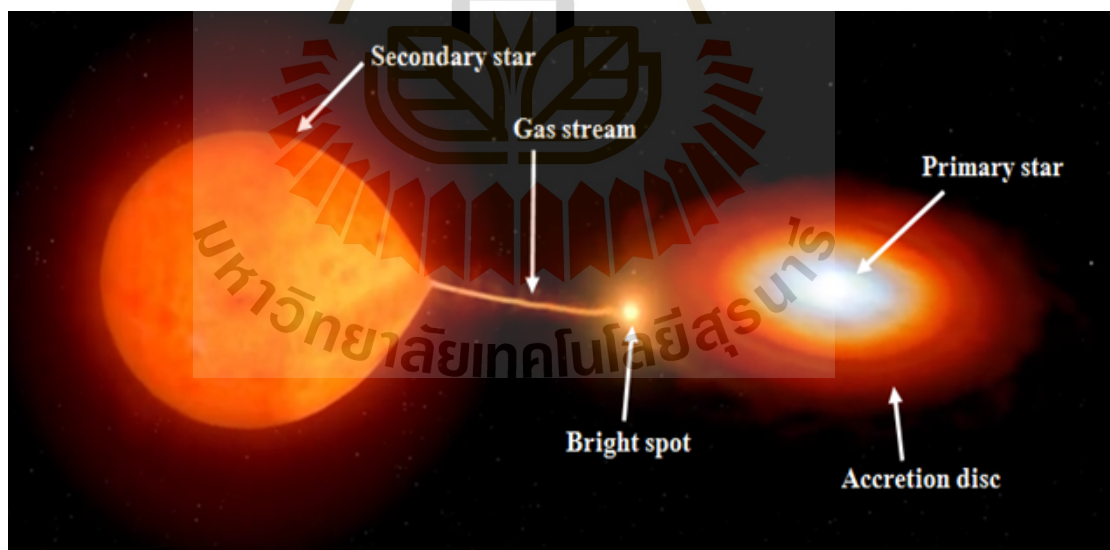
Figure 4.5 The schematic of Cataclysmic Variable (CV), with the primary and secondary stars, gas stream, bright spot and accretion disc (Garlick, 2011).

4.2 The Modeling of SDSS J2141 +0507 using JKTEBOP Code

JKTEBOP code is similar to the BM3 because JKTEBOP code cannot generate the gas steam of CV directly. The light curve of SDSS J2141 +0507 can be generated by changing the initial parameters such as the mass ratio, sum of the radii and ratio of the radii etc. The final of the stellar and binary parameters is quite similar to BM3. The stellar and binary parameters from the estimation are shown in Table 4.3. The light curves of SDSS J2141 +0507 with the best fitting and the residual of model from JKTEBOP code are shown in Figure 4.6 to 4.12. The top panel of Figure 4.6 to 4.12 are the light curve of the observational data (red dots with error bars) and the modeling (blue dots) where this graph is plotted between the delta magnitude versus the orbital phase.

Figure 4.6 Left: Full light curve of SDSS J2141 +0507 with the best fitting and the residual of model. Right: light curve of SDSS J2141 +0507 with only the out of eclipse region. The observational data was obtained on 9th Dec 2014 in SDSS g' filter.

Figure 4.7 Left: Full light curve of SDSS J2141 +0507 with the best fitting and the residual of model. Right: light curve of SDSS J2141 +0507 with only the out of eclipse region. The observational data was obtained on 22nd Dec 2014 in SDSS KG5 filter.
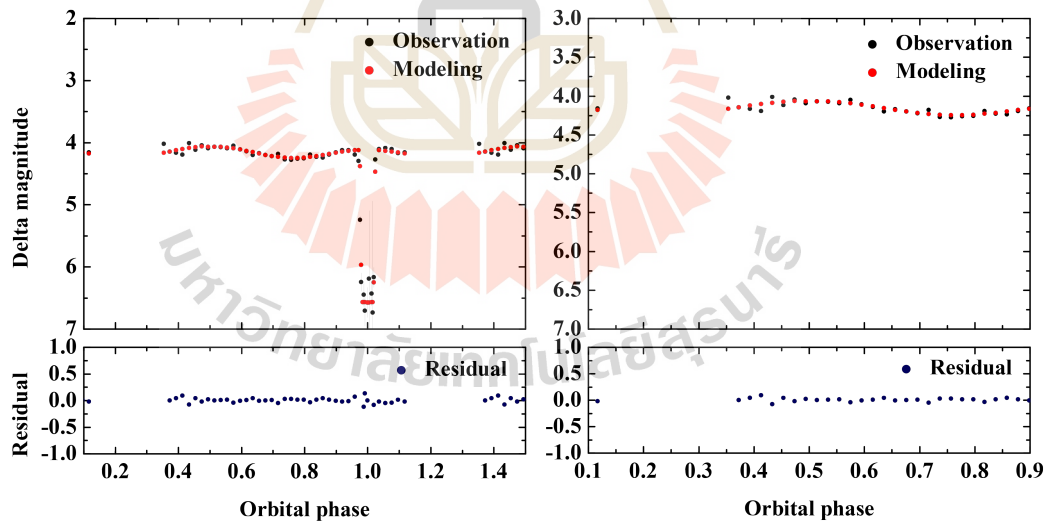
Figure 4.8 Left: Full light curve of SDSS J2141 +0507 with the best fitting and the residual of model. Right: light curve of SDSS J2141 +0507 with only the out of eclipse region. The observational data was obtained on 24th Dec 2014 in SDSS r' filter.
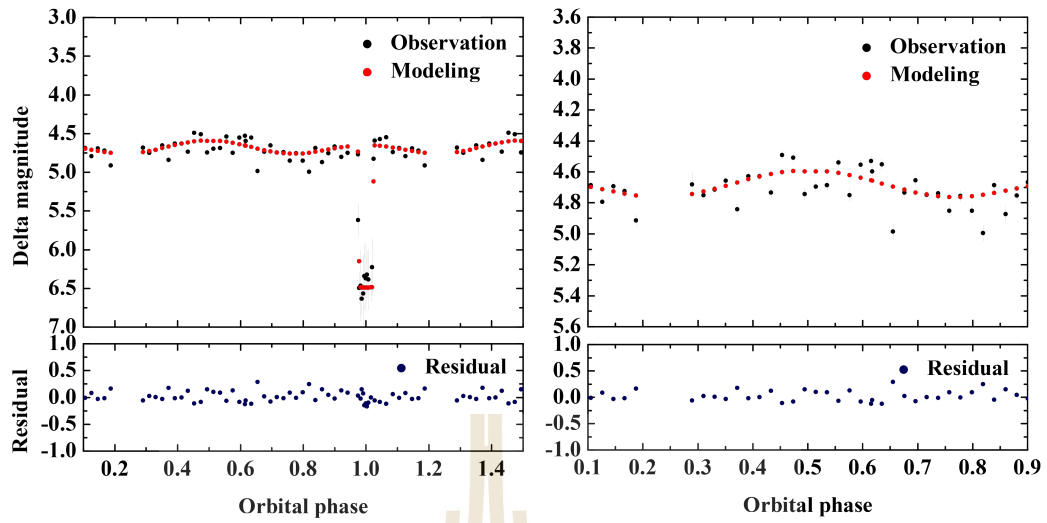
Figure 4.9 Left: Full light curve of SDSS J2141 +0507 with the best fitting and the residual of model. Right: light curve of SDSS J2141 +0507 with only the out of eclipse region. The observational data was obtained on 25th Dec 2014 in SDSS i' filter.
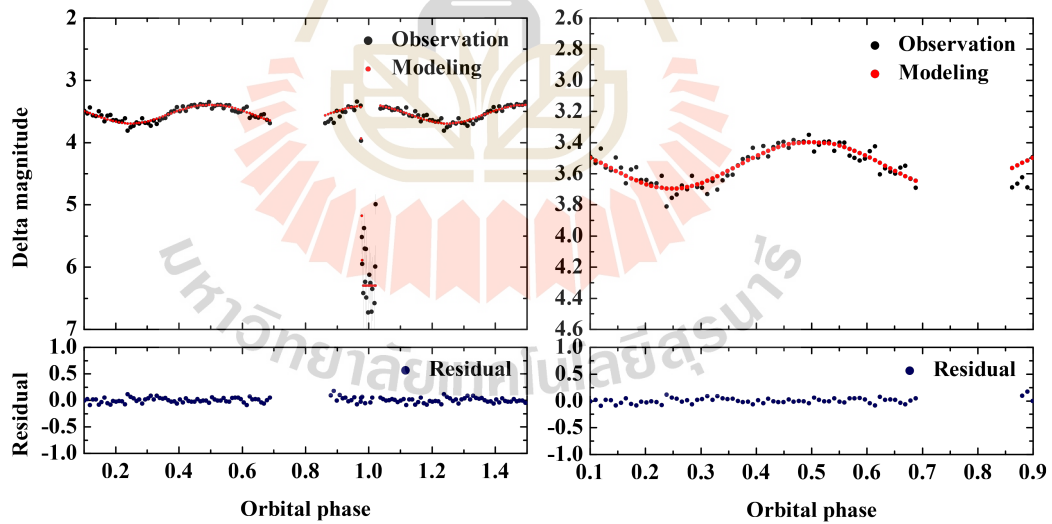
Figure 4.10 Left: Full light curve of SDSS J2141 +0507 with the best fitting and the residual of model. Right: light curve of SDSS J2141 +0507 with only the out of eclipse region. The observational data was obtained on 20th Oct 2015 in SDSS g' filter.
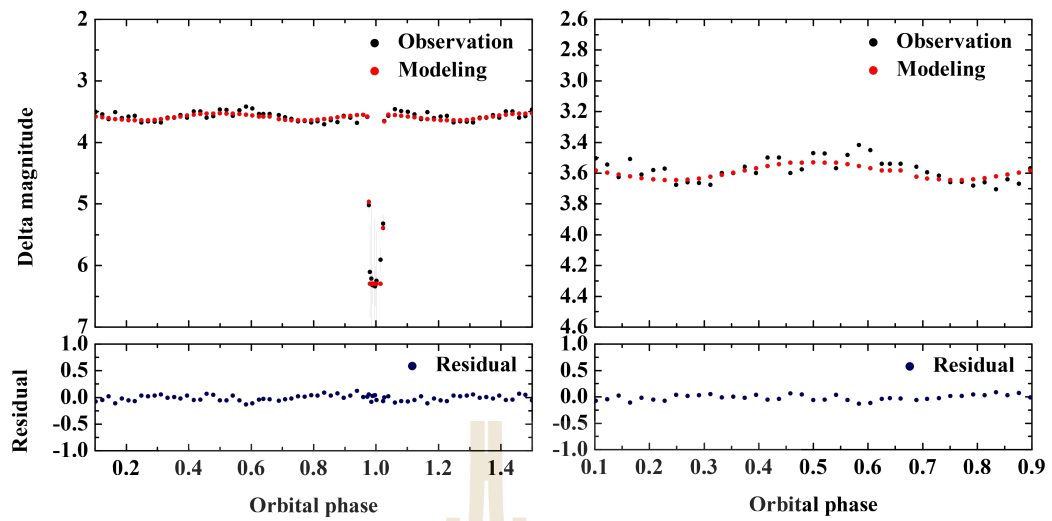
Figure 4.11 Left: Full light curve of SDSS J2141 +0507 with the best fitting and the residual of model. Right: light curve of SDSS J2141 +0507 with only the out of eclipse region. The observational data was obtained on 4th Nov 2016 in SDSS g' filter.

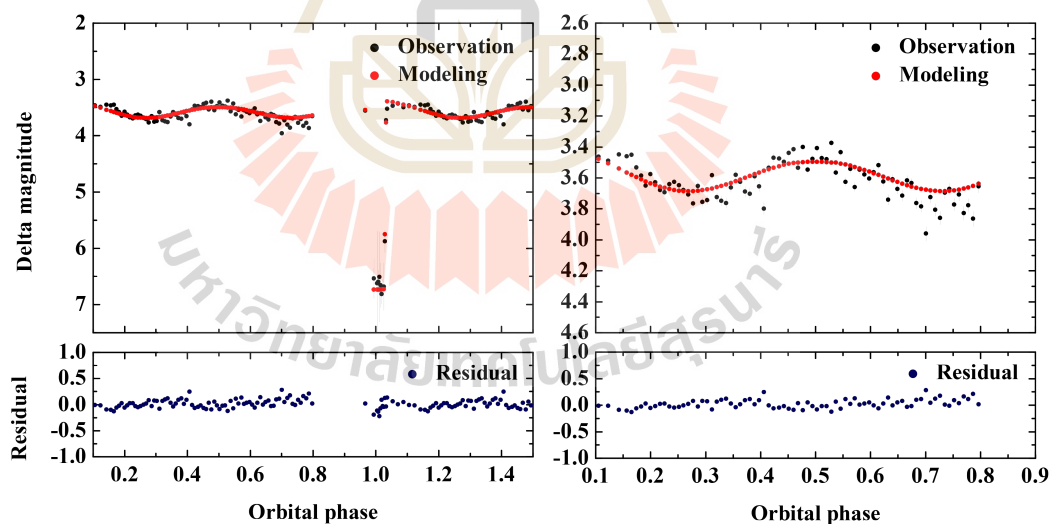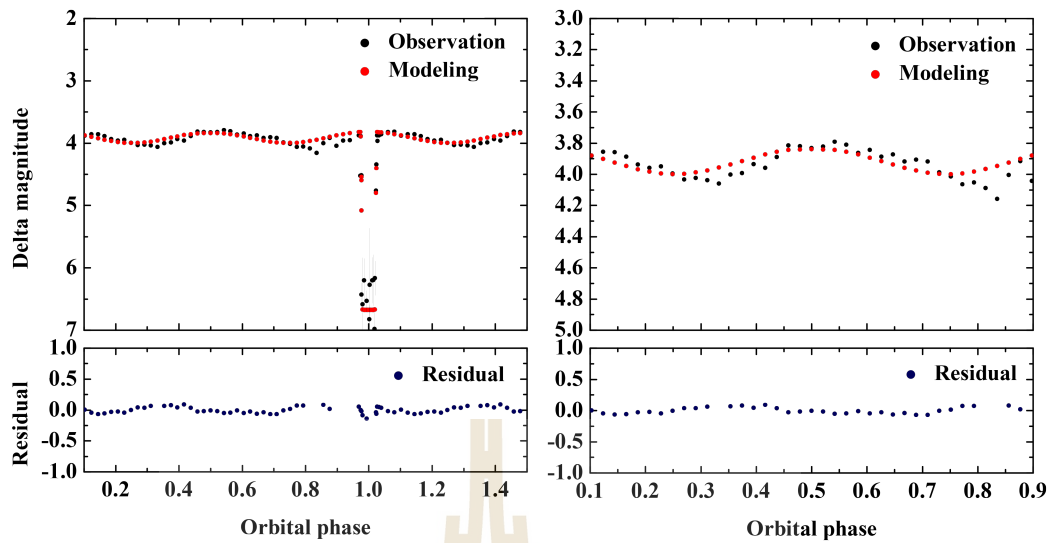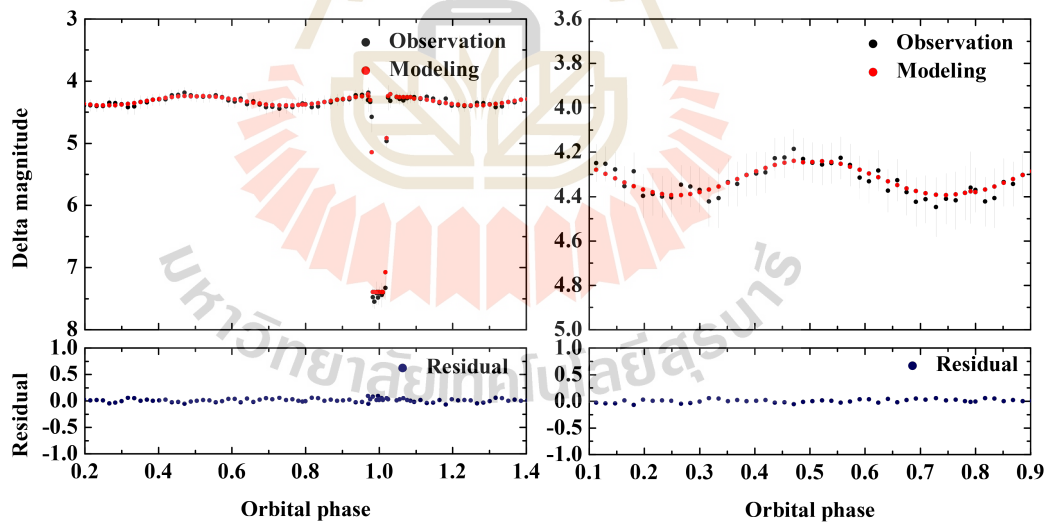**Figure 4.12** Left: Full light curve of SDSS J2141 +0507 with the best fitting and the residual of model. Right: light curve of SDSS J2141 +0507 with only the out of eclipse region. The observational data was obtained on 2nd Dec 2016 in SDSS r' filter.

Table 4.3 The stellar and binary parameters of SDSS J2141 +0507 from JKTEBOP Code.

Parameter(s)	9th Dec 2014	22nd Dec 2014	24th Dec 2014	25th Dec 2014
Surface brightness ratio	0.0009 ± 0.0001	0.0015 ± 0.0002	0.0033 ± 0.0004	0.0041 ± 0.0010
Sum of fractional radii	0.2223 ± 0.0018	0.1734 ± 0.010	0.1744 ± 0.0020	0.1724 ± 0.0046
Ratio of the radii	10.1734 ± 0.4988	9.0184 ± 0.5450	7.2585 ± 0.4059	9.1914 ± 1.1660
Limb darkening A1	0.3	0.3	0.3	0.3
Limb darkening B1	0.3	0.3	0.3	0.3
Orbital inclination	87	87	87	87
Gravity darkening A	0.3	0.3	0.3	0.3
Gravity darkening B	0.3	0.3	0.3	0.3
Reflected light A	0.4247 ± 0.1853	0.2320 ± 0.0075	0.1931 ± 0.0167	0.1814 ± 0.0312
Reflected light B	0.3371 ± 0.1609	0.2228 ± 0.0072	0.2284 ± 0.0108	0.2202 ± 0.0300
Phot mass ratio	0.058	0.058	0.058	0.058
Orbital period (P)	0.06554 ± 0.00050	0.05469 ± 0.00006	0.05662 ± 0.00055	0.05597 ± 0.00140

Continued on next page

Table 4.3 The stellar and binary parameters of SDSS J2141 +0507 from JKTEBOP Code. (Continued).

Parameter(s)	9th Dec 2014	22nd Dec 2014	24th Dec 2014	25th Dec 2014
Ephemeris timebase	2457001.04518	2457014.00788	2457016.03147	2457017.01592
	$\pm$ 0.00001	$\pm$ 0.00001	$\pm$ 0.00001	$\pm$ 0.00002
Fractional primary radius	0.020	0.020	0.021	0.020
Fractional secondary radius	0.204	0.156	0.153	0.155
Total number of datapoints	93	68	48	61
Total number of fitted parameters	8	8	8	8
χ^2	0.28	0.57	0.11	0.52

Continued on next page

Table 4.3 The stellar and binary parameters of SDSS J2141 +0507 from JKTEBOP Code. (Continued).

Parameter(s)	20th Oct 2015	4th Nov 2016	2nd Dec 2016
Surface brightness ratio	0.0020 ± 0.0004	0.0017 ± 0.0002	0.0060 ± 0.0010
Sum of fractional radii	0.1704 ± 0.0016	0.1824 ± 0.0012	0.1886 ± 0.0025
Ratio of the radii	11.3724 ± 0.9386	8.9624 ± 0.4538	5.8996 ± 0.4767
Limb darkening A1	0.3	0.3	0.3
Limb darkening B1	0.3	0.3	0.3
Orbital inclination	87	87	85
Gravity darkening A	0.3	0.3	0.3
Gravity darkening B	0.3	0.3	0.3
Reflected light A	0.5002 ± 0.0160	0.1334 ± 0.0082	0.1478 ± 0.0013
Reflected light B	0.5095 ± 0.0519	0.1456 ± 0.0985	0.1074 ± 0.0114
Phot mass ratio	0.058	0.058	0.058
Orbital period (P)	0.05825 ± 0.00018	0.05471 ± 0.00003	0.05477 ± 0.00001

Table 4.3 The stellar and binary parameters of SDSS J2141 +0507 from JKTEBOP Code. (Continued).

Parameter(s)	20th Oct 2015	22th Nov 2016	2nd Dec 2016
Ephemeris timebase	$2457316.07051 \pm 0.00001$	$2457697.05332 \pm 0.00002$	$2457725.00079 \pm 0.00003$
Fractional primary radius	0.014	0.019	0.027
Fractional secondary radius	0.156	0.164	0.161
Total number of datapoints	102	54	48
Total number of fitted parameters	8	8	8
χ^2	0.36	0.29	0.15

CHAPTER V

DISCUSSION AND CONCLUSIONS

5.1 Discussion and Conclusions

In this chapter, we summarize the result of SDSS J2141 +0507 from the observational data and fitting model. To obtain the observational data, we used the 2.4 meter Thai National Telescope (TNT) with ULTRASPEC instrument in SDSS g', KG5, r' and i' filters at the Thai National Observatory (TNO), Doi inthanon National Park, Chiang Mai, Thailand. The observational data was obtained on 9th Dec, 22nd Dec, 24th Dec, 25th Dec 2014, 20th Oct 2015, 4th Nov and 2nd Dec 2016, respectively. We used Binary Maker 3.0 (Bradstreet et al., 2015) and JKTEBOP code (Southworth et al., 2009) to determine the stellar and binary parameters of this system. A new ephemeris for SDSS J2141 +0507 with the mid-eclipse timing (in HJD) as 2456215.45338 $\pm$ 0.00005 and the orbital period of 0.05469 $\pm$ 0.00004 days. From the estimation of stellar and binary parameters of SDSS J2141 +0507 using BM3 and JKTEBOP code, then we can report that the orbital inclination of $(86 \pm 1)°$. The radii of white dwarf and main sequence stars are $(0.030 \pm 0.003)R\odot$ and $(0.20 \pm 0.01)R\odot$, with the mass ratio (M2/M1) of this system is 0.058. The effective temperature of white dwarf (WD) and main sequence (MS) are 31200 $\pm$ 300 K and 3540 $\pm$ 40 K, respectively. Table 5.1 shows the stellar and binary parameters of SDSS J2141 +0507 which was determined using Binary Maker 3.0 and JKTEBOP code.

The ephemeris for SDSS J2141 +0507 can be written as $T_0(\text{HJD}) = 2456215.45338 + 0.05469 \times E$. From the light curve of SDSS J2141 +0507 with

the best fitting and the residual of this system, we will see that there was a discrepancy with the observational data. When we consider the light curve of SDSS J2141 +0507 in only the out of eclipse region, we cannot fit the sinusoidal pattern. For example, we analyze the light curve in KG5 filter which was obtained on 22nd Dec 2014 then our model cannot fit the sinusoidal pattern in the light curve. Normally, the outside of eclipse pattern was occurred by the shape of the secondary star but after we input the radius of the secondary then we cannot fit the sinusoidal pattern of the outside of eclipse. This phenomena was indicated that SDSS J2141 +0507 should have the mass transfer and also, the accretion disc. According to SDSS spectral for SDSS J2141 +0507 was taken by Szkody et. al (2014) can be confirmed that this system is the new cataclysmic variable with the low mass transfer rate. The absorption and the emission lines of SDSS J2141 +0507 was occurred by white dwarf and accretion disc, respectively. To explain the stellar and binary parameters for SDSS J2141 +0507, we used the light curve with the best fitting from the observational data which was obtained on 24th Dec 2014 in SDSS r' filter. The discrepancy between the observational data and our model is the smallest when we compared to other filters then we can derive the stellar and parameters using this filters. The chi-square fitting of this model using JKTEBOP code is 0.11. The stellar and binary parameters of this system can be obtained by using Binary Maker 3.0 and JKTEBOP code. The 3D model of SDSS J2141 +0507 can be constructed using Binary Maker 3.0 and JKTEBOP code was determined to confirm the type of a new eclipsing binary by analyzing the outside eclipse of light curve region. From the analysis light curve of SDSS J2141 +0507, we can fit the sinusoidal pattern, especially in SDSS r' filter. The stellar and binary parameter was obtained using Binary Maker 3.0 which was yield as same as the values of the stellar and binary parameters using JKTEBOP code.

We are showing the results both of these program in Table 5.1

Table 5.1 The stellar and binary parameters were obtained by using BM3 and JKTEBOP code in SDSS r' filter.

| Parameter(s)	BM3	JKTEBOP code
Mass Ratio(M2/M1)	0.058	0.058
The binary separation (a)	0.00282 AU	0.00282 AU
The radius of WD	$(0.030 \pm 0.003)R\odot$	$0.021R\odot$
The radius of MS	$(0.20 \pm 0.01)R\odot$	$0.20R\odot$
The effective temperature of WD	31200 ± 300 K	-
The effective temperature of MS	3540 ± 40 K	-
The gravity darkening of WD (G1)	0.3	0.3
The gravity darkening of MS (G2)	0.3	0.3
The limb darkening of WD (X1)	0.3	0.3
The limb darkening of MS (X2)	0.3	0.3
The reflection of WD	0	0.1931 ± 0.0167
The reflection of MS	1.3	0.2284 ± 0.0108
Inclination	$(86\pm 1)°$	87°
The spot of WD		
Colatitude	75	-
Longitude	0	-
Spot radius	25	-
Temperature factor	2.7	-
Orbital period	0.05469 ± 0.00004 days	-
χ^2	0.10	0.11

5.2 Future Work

For the future work, we will study the physical properties and construct the model of other Cataclysmic Variable (CV) other system. From the follow-up photometry of SDSS J2141 +0507 can be used as the first example to investigate the evolution of others CV if the light curve pattern from the observation is similar to this system. More photometric observations on SDSS J2141 +0507, leading to study the evolution of CV. From observation, we can calculate the O-C diagram to predict the chance of the orbital period. The mass transfer of SDSS J2141 +0507 will be studied using the O-C diagram as well. Spectroscopic observation is very important to study the spectral type on SDSS J2141 +0507. The radial velocity will be determined using spectroscopic observation leading to calculation of the stellar and binary parameters. For example, we can directly obtain the radii of the primary and secondary stars. From the spectral type of SDSS J2141 +0507 can be measured the effective temperature of primary and secondary stars, respectively.

Moreover, we can obtain the orbital inclination and the masses for the system. Therefore, both of photometric and spectroscopic observation are important to study SDSS J2141 +0507 which the stellar and binary parameters of system will be more accurate if we can get more observational data. The modeling of SDSS J2141 +0507 is absolutely important to describe the evolution of system, especially we can see the chance model of binary system when we use the original observational data until the latest observational data. Therefore, the evolution of the binary system such as the mass transfer will be obtained. We prefer Binary Maker 3 (BM3) and JKTEBOP code to construct the model and obtain the stellar and binary parameters and study more software in order to compare the result.

In finally, we hope that if we can observe to get more the observational data then we can determine the precise of the stellar and binary parameters which

is very important to analyze in deep part, especially the variation of the outside eclipse.
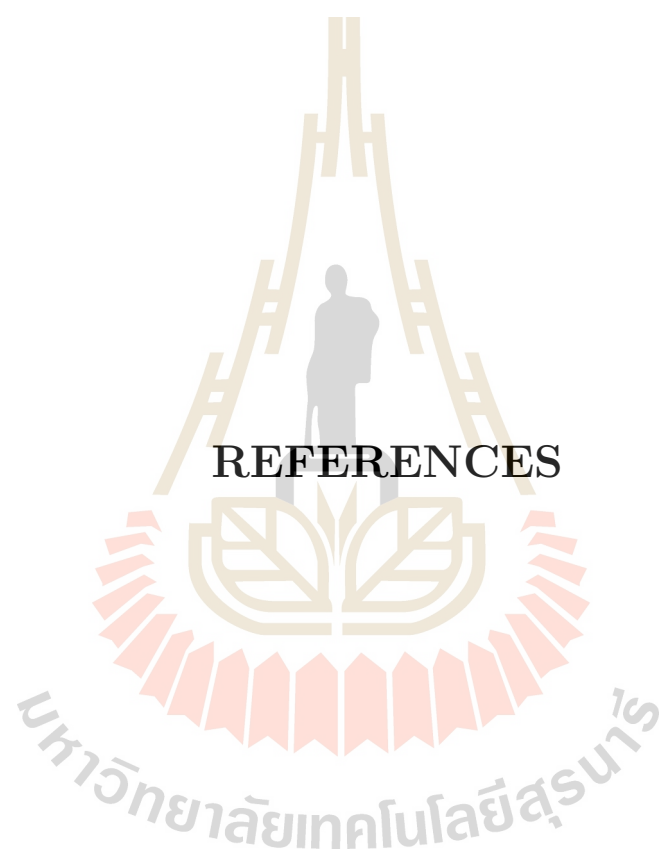
REFERENCES

REFERENCES

Aungwerojwit, A. (2007). The properties of a spectroscopically selected sample of cataclysmic variables. **Ph.D. Thesis**. The university of Warwick.

Bogan, L. (1997). Astronomy 2 - Lecture Notes. (online) Available: from http://plato.acadiau.ca/courses/phys/1523/jan18/JAN18.HTML.

Bours, M. C. P. (2015). Detailed studies of white dwarf binaries and their orbital periods. **Ph.D. Thesis**. The university of Warwick.

Bradstreet, D. H. (2011). Heliocentric Julian Date. (online) Available: from http://www.physics.sfasu.edu/astro/javascript/hjd.html.

Bradstreet, D. H. (2015). Fundamentals of Solving Eclipsing Binary Light Curves Using Binary Maker 3. The Society for Astronomical Sciences 24th Annual Symposium on Telescope Science. **Society for Astronomical Sciences**. 4:23.

Carroll, B. W. and Ostlie, D. A. (2007). An Introduction to Modern Astrophysics. **Pearson**. 2.

Dhillon, V. S., Marsh, T. R., Atkinson, D. C., Bezawada, N., Bours, M. C. P., Copperwheat, C. M., Gamble, T., Hardy, L. K., Hickman, R. D. H., Irawati, P., Ives, D. J., Kerry, P., Leckngam, A., Littlefair, S. P., McLay, S. A., O'Brien, K., Peacocke, P. T., Poshyachinda, S., Richichi, A., Soonthornthum, B., and Vick, A. (2014). ULTRASPEC: a high-speed imaging photometer on the 2.4-m Thai National Telescope. **Monthly Notices of the Royal Astronomical Society**. 444: 3504–3516.

Digital-Drew-Space-Art's-Photostream (2013). Example of PCEB WD 0137-349. (online) Available: from https://trkendall.wordpress.com/2013/01/14/post-common-envelope-binary-wd-0137-349/.

Garlick, M. A. (2011). Animation of Cataclysmic binary. (online) Available: from http://www.space-art.co.uk/.

Herschel, W. (1802). Catalogue of 500 New Nebulae, Nebulous Stars, Planetary Nebulae, and Clusters of Stars; With Remarks on the Construction of the Heavens. **Philosophical Transactions of the Royal Society of London**. 92: 477–528.

Hilditch, R. W. (2001). An Introduction to Close Binary Stars. **THE PRESS SYNDICATE OF THE UNIVERSITY OF CAMBRIDGE**.

Howell, S. B. (2006). Handbook of CCD Astronomy. **Cambridge University Press**. 2.

Izzard, R. G., Hall, P. D., Tauris, T. M., and Tout, C. A. (2012). Common envelope evolution. **Proceedings of the International Astronomical Union**. 7: 95–102.

Kepler, S. O., Kleinman, S. J., Nitta, A., Koester, D., Castanheira, B. G., Giovannini, O., Costa, A. F. M., and Althaus, L. (2007). White Dwarf Mass Distribution in the SDSS. **Monthly Notices of the Royal Astronomical Society**. 375: 1315–1324.

Lucy, L. B. (1976). Gravity-Darkening for Stars with Convective Envelopes. **Zeitschrift für Astrophysik**. 65: 89-92.

McCarthy, D. D. (1998). The Julian and Modified Julian Dates. **Journal for the History of Astronomy**. 327.

NOAO (2015). IRAF project homepage. (online) Available: from http://iraf.noao.edu/.

Paczynski, B. (1976). Common Envelope Binaries. **Structure and Evolution of Close Binary Systems; Proceedings of the Symposium**. 73: 75-80.

Parsons, S. G., Gaensicke, B. T., Boris, T., Marsh, T. R., Drake, A. J., Dhillon, V. S., Littlefair, S. P., Pyrzas, S., Rebassa-Mansergas, A., and Schreiber, M. R. (2013). Eclipsing Post Common Envelope Binaries from the Catalina Surveys. **Monthly Notices of the Royal Astronomical Society**. 429: 256–268.

Pringle, J. E. and Wade, R. A. (1985). Book-Review - Interacting Binary Stars. **Astronomy Express**. 1: 159.

Ray, R. (2000). Modified Julian Dates. (online) Available: from http://bowie.gsfc.nasa.gov/time/.

Rebassa-Mansergas, A. (2008). Post-Common-Envelope Binaries from the Sloan Digital Sky Survey. **Ph.D. Thesis**. The University of Warwick.

Rebassa-Mansergas, A., Gaensicke, B. T., Schreiber, M. R., Koester, D., and Rodriguez-Gil, P. (2009). Post-common envelope binaries from SDSS - VII: A catalogue of white dwarf-main sequence binaries. **Monthly Notices of the Royal Astronomical Society**. 419: 806–816.

Smale, K. (2004). Cataclysmic Variables (CVs). (online) Available: from NASA's HEASARC: Education Public Information, website: https://heasarc.gsfc.nasa.gov/docs/objects/cvs/cvs.html.

Southworth, J. (2013). JKTLD - for calculating limb darkening coefficients. (online) Available: from http://www.astro.keele.ac.uk/jkt/codes/jktld.html.

Southworth, J. (2014). JKTEBOP - for analysing light curves of detached eclipsing binaries and transiting planets. (online) Available: from http://www.astro.keele.ac.uk/jkt/codes/jktebop.html.

Szkody, P., Everett, M. E., Howell, S. B., Landolt, A. U., Bond, H. E., Silva, D. R., and Vasquez-Soltero, S. (2014). Followup Observations of SDSS and CRTS Candidate Cataclysmic Variables. **The Astronomical Journal**. 148: 63–97.

Van der Sluys, M. (2006). Roche lobe. (online) Available: from https://en.wikipedia.org/wiki/File:RochePotential.jpg.

White, H. E. and Thomas W. Baumgarte, S. L. S. (2012). GRAVITY DARKENING AND BRIGHTENING IN BINARIES. **The Astrophysical Journal**. 752:122.

Zeipel, V. (1924). Radiative Equilibrium of a Double-Star System with nearly Spherical Components. **Monthly Notices of the Royal Astronomical Society**. 84: 702-720.
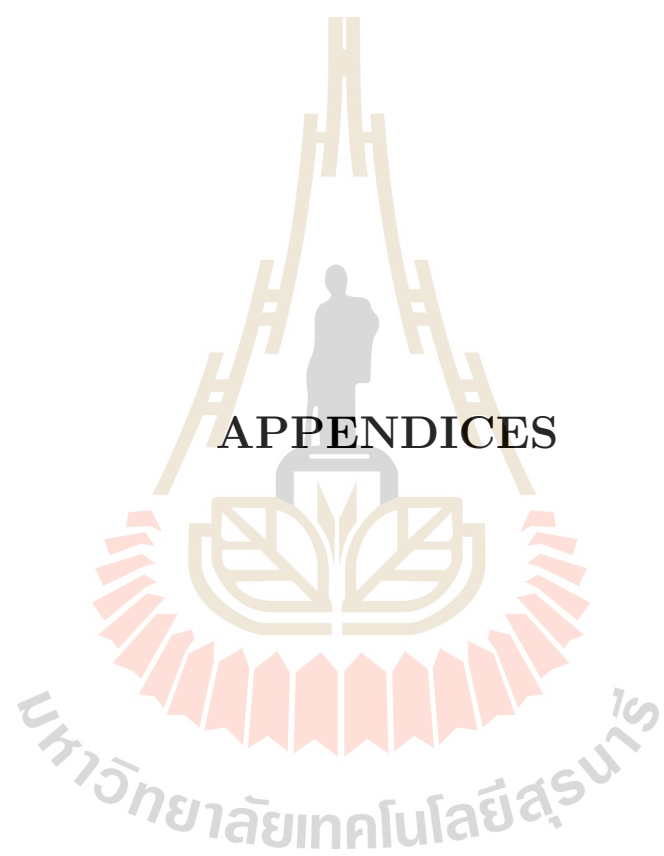
APPENDICES

APPENDIX A

A   CHARGE–COUPLED DEVICES

Charge-Coupled Devices (CCDs) is a device for the movement of electrical charge which have been used in astronomy since their development in the early 1970s. The device is consists of an input element for injecting a controlled charge into the main part. An array of MIS capacitors is used in the dynamic operation mode and also a sensor device registering the charge arriving at the end of the array (Howell, 2006).
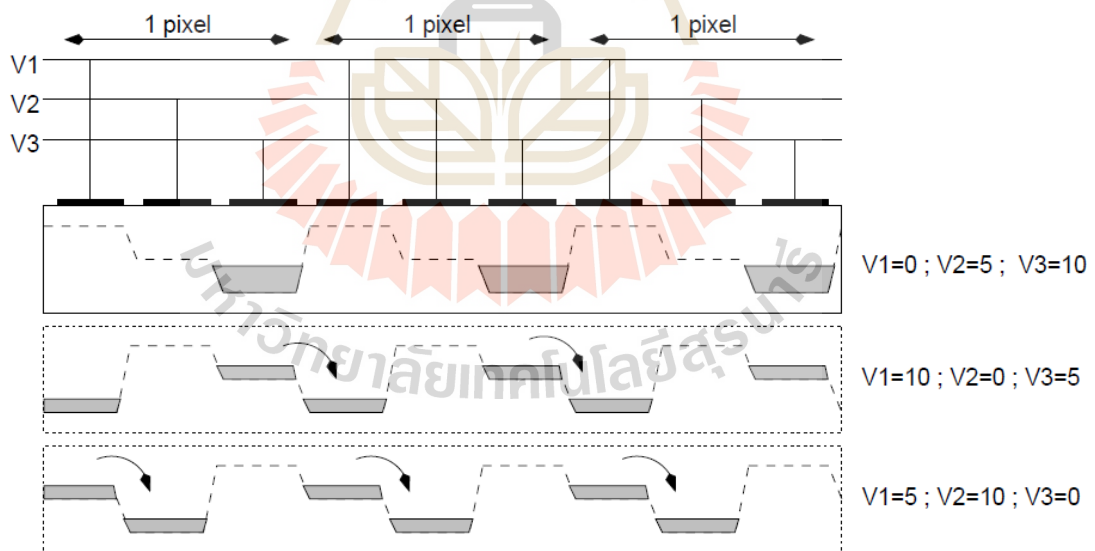
Figure A.1 The schematic of charge transfer in a CCD operating in a three-phase mode (Bours, 2015).

Figure A.1 shows the schematic of charge transfer in a CCD operating in a three-phase mode. After one full cycle, the charge in a pixel has been transferred

to a neighboring pixel. In this research, we use the Electron-Multiplying CCDs (EMCCDs) which are another subset of CCDs. The EMCCDs is core of the ULTRASPEC which have the option to read out data in avalanche mode.

APPENDIX B

B ULTRASPEC AT THE 2.4 METER THAI NATIONAL TELESCOPE

ULTRASPEC is a high-speed imaging photometer with the field of view of 7.7′ x 7.7′ with a pixel scale of 0.45″ / pixel (Dhillon et al., 2014). In November 2013, ULTRASPEC was installed at the 2.4 meter Thai National Telescope (TNT) on Doi Inthanon, Chiang Mai, Thailand. A selection of 14 difference broad band and narrow band can be facilitated in 6-position filters wheel which is covering the wavelength range between 300 - 1000 nm. The core of ULTRASPEC is the Electron Multiplying Charged Couple Device (EMCCD) detector (Dhillon et al., 2014). The design of ULTRASPEC includes a frame-transfer EMCCD rather than a standard CCD in order to maximize the signal to noise ratio. The detector is cooled down with liquid nitrogen to operate at a temperature of 160 K, to provide dark current less than 10 e^-/pixel/hr. The filters of ULTRASPEC consist of several SDSS filter such as u', g', r', i', z' and Schott KG5 filter. The details of available filters and the transmission of the ULTRASPEC filters are given in Table B.2. Figure B.2 shows the Thai National Telescope (TNT) and Thai National Observatory (TNO), Chiang Mai, Thailand. The mechanism drawing of the ULTRASPEC and the final ULTRASPEC optical design is shown in Figure B.3

Figure B.4 shows the scale ray trace through the ULTRASPEC optics, with the telescope focal plane on the left and the EMCCD in its cryostat on the right and the details of ULTRASPEC optical. Both of ROC and TFP are Radius of

Figure B.2 Left: The mirror of Thai National Telescope (TNT) covers are open and the 2.4 m f/1.5 primary mirror can be seen towards the bottom. Right: Outside of the TNT is shown the tower on which the telescope sits and the adjacent control room building (Dhillon et al., 2014).
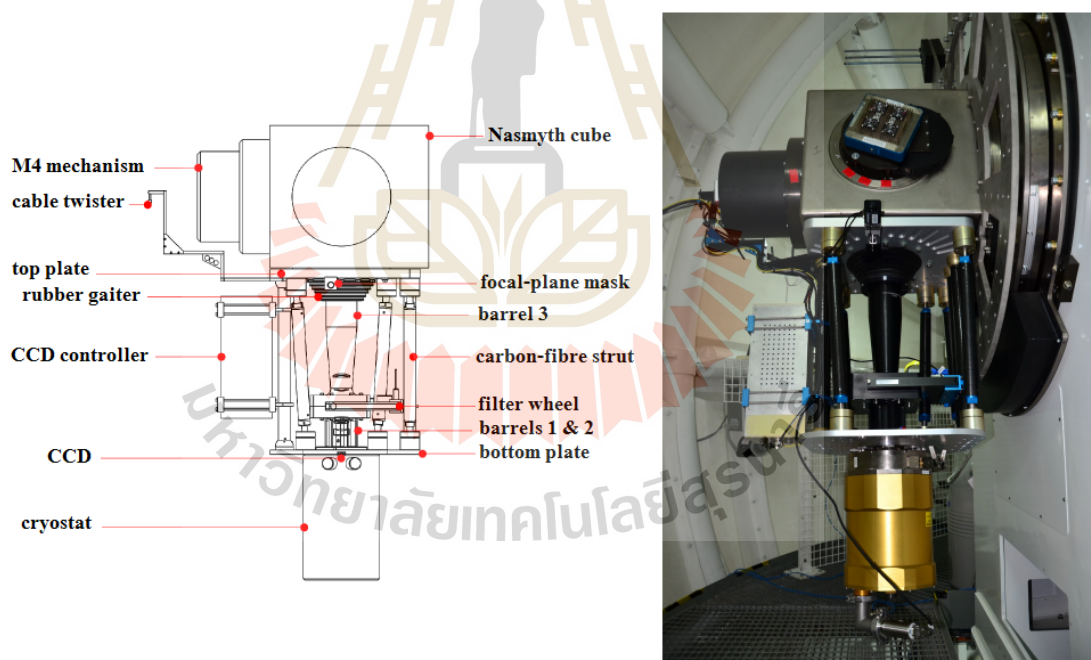

Figure B.3 Left: Mechanism drawing of the ULTRASPEC. Right: Photograph of ULTRASPEC on the Nasmyth focus of the 2.4 m Thai National Telescope (TNT), Thai National Observatory, Thailand (Dhillon et al., 2014).

Curvature and Telescope Focal Plane is shown in Table B.1 (Dhillon et al., 2014).
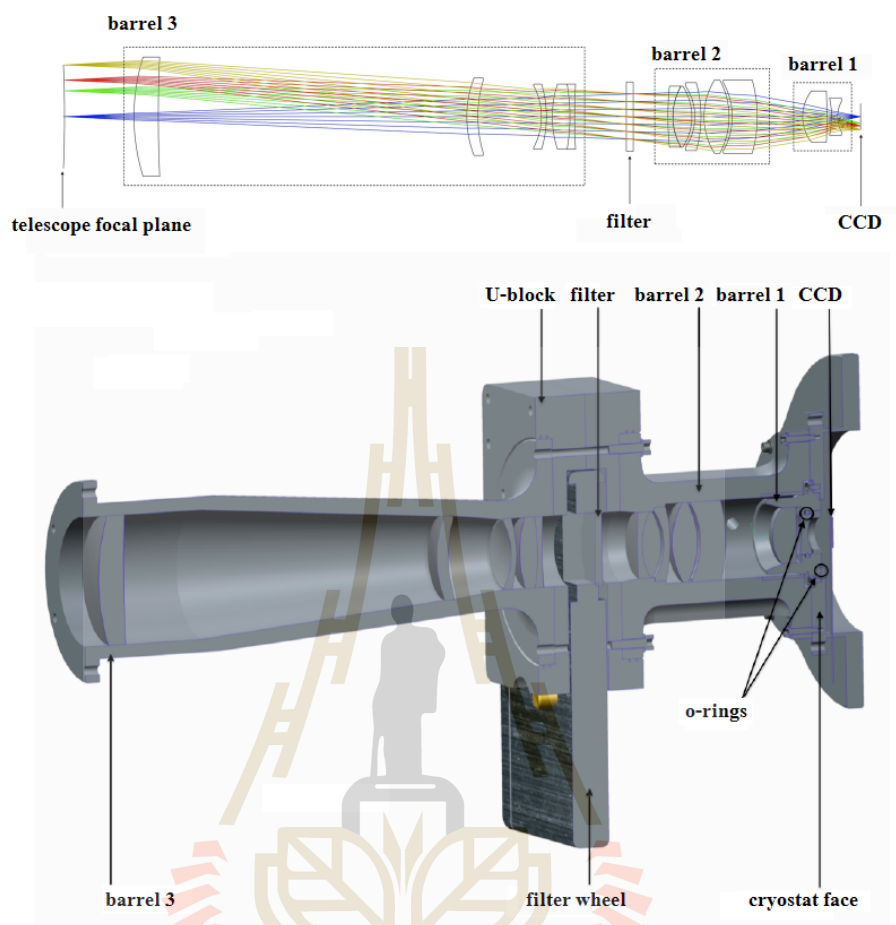

Figure B.4 Top: Scale ray trace through the ULTRASPEC optics, with the telescope focal plane on the left and the EMCCD in its cryostat on the right. Bottom: Cross-section through the optics barrels, highlighting some of the components described in the text (Dhillon et al., 2014).

The Sloan Digital Sky Survey (SDSS) photometric system is applied as the primary filter set for ULTRASPEC which is shown in Figure B.5. The SDSS filter is consists of u', g', r', i', and z'. ULTRASPEC has an extensive set of broadband and narrow-band filter and also only 6 filters can be mounted at any one time in the wheel. All ULTRASPEC filters are 50 x 50 mm^2 and thickness of 5 mm approximately. Hence, ULTRASPEC filters have been designed to have iden-

tical optical thickness so that their differing refractive indices are compensated by slightly different physical thickness, making the filters interchangeable without having to refocus the telescope. The filters have also been designed taking the ULTRASPEC optical design into account to ensure that the required central wavelength and FWHM are achieved. All of the filters used in ULTRASPEC were designed and manufactured by Asahi Spectra Company, Japan (Dhillon et al., 2014). The transmission profile of the ULTRASPEC SDSS filters is shown in Figure B.5 and Table B.2 is the central wavelength and the FWHM of ULTRASPEC filters.
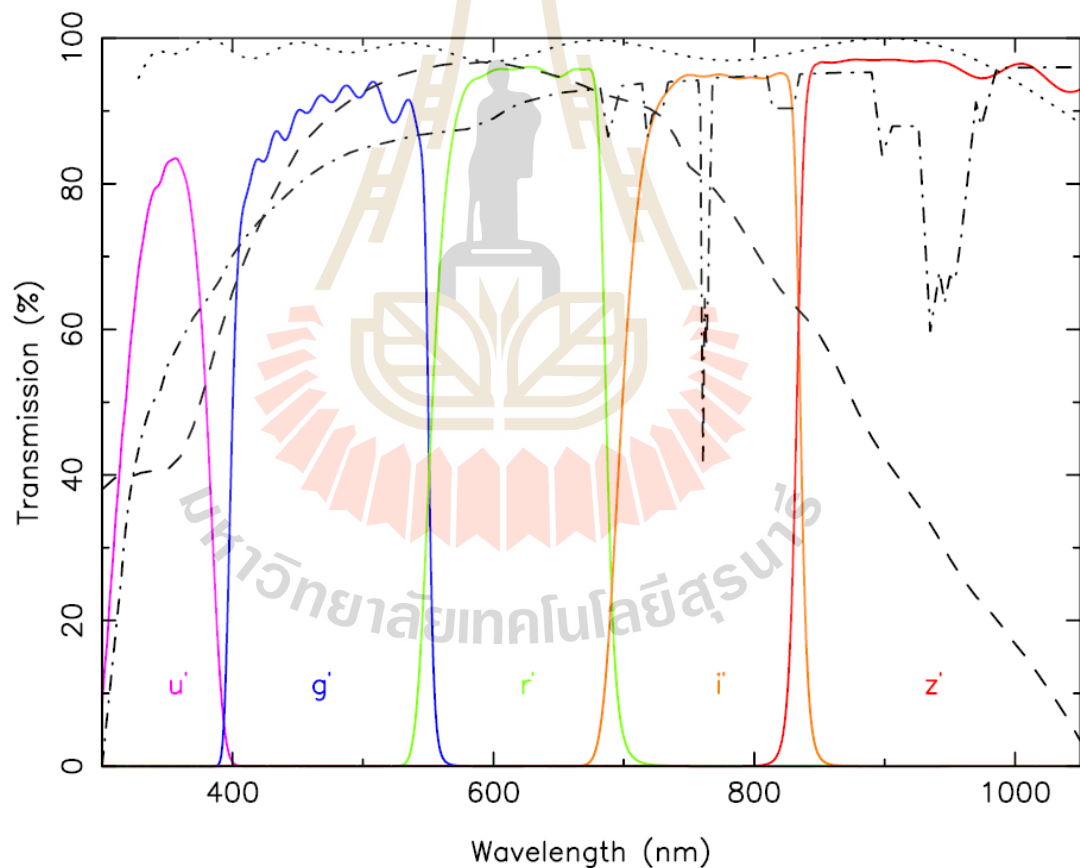

Figure B.5 Transmission profiles of the ULTRASPEC SDSS filter set (purple, blue, green, orange and red solid lines correspond to u', g', r', i', and z', respectively (Dhillon et al., 2014).

Table B.2 The details of ULTRASPEC optical. Both of ROC and TFP are Radius of Curvature and Telescope Focal Plane, respectively (Dhillon et al., 2014).

Surface	ROC(mm)	Thickness(mm)	Glass
TPF		50.046	
Lens 1	144.930	17.970	N-FK51A
	931.800	220.924	
Lens 2	77.885	8.000	N-BK7
	90.995	43.511	
Lens 3	-47.345	3.730	N-PSK53A
	-81.505	2.351	
Lens 4	75.800	12.740	N-BK7
	-134.940	3.500	N-LAK21
	412.675	38.684	
Filter	Infinity	5.000	SILICA
	Infinity	25.000	
Lens 5	223.375	3.500	N-SK14
	44.605	12.570	CAF2
	-40.600	2.194	
Lens 6	-39.460	4.460	N-LAK21
	-90.995	1.911	
Lens 7	50.065	18.000	CAF2
	-55.690	2.315	
Lens 8	-50.065	18.000	N-BK7
	-96.860	33.544	

Continued on next page

Table B.2 The details of ULTRASPEC optical. Both of ROC and TFP are Radius of Curvature and Telescope Focal Plane, respectively (Dhillon et al., 2014). (Continued).

Surface	ROC(mm)	Thickness(mm)	Glass
Lens 9	30.255	17.450	N-LAK21
	-475.220	3.358	
Lens 10	-62.415	4.150	N-LAK21
	23.070	16.244	D
CCD	Infinity		

Table B.3 The ULTRASPEC SDSS filter. λ_C is the central wavelength and $\Delta\lambda$ is the FWHM.

SDSS filter	λ_C(nm)	$\Delta\lambda$(nm)
u'	355.7	59.9
g'	482.5	137.9
r'	626.1	138.2
i'	767.2	153.5
z'	909.7	137.0
Schott KG5	507.5	360.5

CURRICULUM VITAE

NAME: Kittipong Wangnok   **GENDER**: Male

NATIONALITY: Thai   **DATE OF BIRTH**: December 13, 1990

EDUCATIONS:

- 9 June 2012 Bachelor Degree of Science in Physics (Second Class Honours)

PUBLICATIONS:

- The conference on the 12th Asia-Pacific Reginal IAU Meeting (APRIM 2014) in the topic of "FOLLOW-UP PHOTOMETRY OF TWO NEW ECLIPSING PCEBs FROM THE SLOAN DIGITAL SKY SURVEY" during 18-22 August 2014 at Daejoen Convention Center (DCC), Korea.

- The conference on Siam Physics Congress 2015 (SPC 2015) in the topic of "Follow-up Photometry of New Eclipsing PCEB from the Sloan Digital Sky Survey: SDSS J214140.43+050730.0" during 20-22 May 2015 at Sofitel Krabi Phokeethra Golf and Spa Resort, Krabi

AWARDS:

-

GRANTS AND FELLOWSHIPS:

- Received the scholarship of The Development and Promotion of Science and Technology Talents project (DPST Scholarship), Ministry of Science and Technology, since 2012-2020

POSITION AND PLACE OF WORK:

-